Aalto University
School of Chemical
Engineering

Tino Koponen

ELECTROSPUN SCAFFOLDS IN A RWV BIOREACTOR

Master´s Programme in Chemical, Biochemical and Materials Engineering
Major in Biotechnology

Master's thesis for the degree of Master of Science in Technology submitted for inspection, Espoo, 2 June, 2017.

Supervisor Professor Katrina Nordström

Instructor PhD Ari Ora

Aalto-yliopisto
Kemian tekniikan
korkeakoulu

Aalto-yliopisto, PL 11000
00076, AALTO
www.aalto.fi

Diplomityön tiivistelmä

Tekijä Tino Koponen

Työn nimi Jännitekehrättyjen tukirakenteiden käyttö pyöriväseinäisessä bioreaktorissa

Koulutusohjelma Master's Programme in Chemical, Biochemical and Materials Engineering

Pääaine Biotekniikka

Työn valvoja Professori Katrina Nordström

Työn ohjaaja Tohtori Ari Ora

Päivämäärä 02.06.2017 **Sivumäärä** 96+9 **Kieli** Englanti

Tiivistelmä

Kudosteknologisten verisuonten kehitystä tutkitaan laajalti sekä perustutkimuksen että soveltavan tutkimuksen lähtökohdista. Kudosteknologisia verisuonia voidaan hyödyntää lääkeaineiden kuljetusjärjestelminä ja vaikutusaineseulonnassa. Niiden kasvattamiseen tarvittavat tukirakenteet, eli scaffoldit, voidaan valmistaa keinotekoisesti eri valmistusmenetelmillä, joista eniten käytettyjä ovat jännitekehräys (eli elektrospinnaus) ja pyöriväseinäiset bioreaktorit (eli Rotary Wall Vessel (RWV) -bioreaktorit). Tämän diplomityön tavoitteena oli tutkia näiden mainittujen menetelmien soveltuvuutta scaffoldin tuottamiseksi ja niiden kykyä tukea solujen kasvattamista, pidemmällä tähtäimellä verisuonten kasvattamista.

Jännitekehrääminen on menetelmä, jossa tuotetaan ohuista mikro- tai nanokokoisista langoista koostuva verkkorakenne ilman säännönmukaista kudontaa. Keruualustan ja polymeeriliuosta sisältävän ruiskun neulan väliin tuotettavalla korkeajännitteellä näitä ohuita lankoja voidaan kehrätä. Jännitekehräämisen jälkeen materiaalia voidaan hyödyntää kudoksista luonnollisesti löytyvää soluväliainetta jäljittelevänä kudosteknologisena tukiverkkona (eli scaffoldina). Gelatiinia, poly-ε-kaprolaktonia (PCL) ja polyetyleenioksidia (PEO) jännitekehrättiin itsekootulla LEVIOSA! laitteistolla. Glutaraldehydillä ristisidostettua gelatiinia sekä PCL:a hyödynnettiin sekä staattisissa että bioreaktorikasvatuksissa.

Pyöriväseinäinen bioreaktori hyödyntää vaakatasossa pyöritettävän kasvatusastian liikettä mikropainovoiman luomiseksi. Seinän liike saa kasvatusnesteen liikkumaan ja nesteen noste sentrifugaalivoimaan yhdistettynä kumoaa hetkellisesti painovoiman. Näin soluja tai pieniä tukiverkkopohjaisia kudoksia voidaan kasvattaa kolmiulotteisesti. Tähän diplomityöhön liittyvän opiskelijaprojektin puitteissa rakennettua pyöriväseinäistä bioreaktoria nimeltään BIOHOVER käytettiin tässä diplomityössä jännitekehrättyjen putkilomaisten tukiverkkojen kasvattamiseen.

Putkilomaisten 72 tuntia ristisidostetun gelatiinin ja PCL:n keskimääräinen lankapaksuus oli 500 ± 100 ja 2200 ± 700 nm, ja huokoskoko 800 ± 300 ja 13900 ± 4600 nm. Ihmiskeuhkojen karsinoomasoluja (A549) kasvatettiin kolme päivää edellä mainituilla putkilomaisilla tukiverkoilla BIOHOVER bioreaktorissa verisuonen kasvatusedellytysten tutkimiseksi. Työssä käytetyt menetelmät osoittautuivat pääsääntöisesti toimiviksi, ja jatkotoimenpiteinä työssä esitetään niihin liittyviä kehittämisehdotuksia, joiden avulla jatkossa olisi myös mahdollista tuottaa kudosteknologista verisuonta, johon ei vielä tämän työn puitteissa päästy. Lisäksi diplomityössä käytetyt metodit todettiin soveltuviksi opetukseen ja niitä hyödynnettiin DI-tason kudosteknologian kurssilla, joka oli osa Aalto Online Learning (A!OLE) opetuksenkehittämisohjelmaa.

Avainsanat Kudosteknologia, jännitekehräys, elektrospinnaus, gelatiini, PCL, PEO, pyöriväseinäinen bioreaktori, Rotary Wall Vessel (RWV) -bioreaktori, verisuoni

Aalto University
School of Chemical
Engineering

Aalto University, P.O. BOX 11000
00076, AALTO
www.aalto.fi

Abstract of Master's Thesis

Author Tino Koponen

Title of Thesis Electrospun Scaffolds in a RWV Bioreactor

Degree Programme Master´s Programme in Chemical, Biochemical and Materials Engineering

Major Biotechnology

Thesis Supervisor Professor Katrina Nordström

Thesis Advisor PhD Ari Ora

Date 06/02/2017 **Number of Pages** 96+9 **Language** English

Abstract

Tissue-engineered blood vessels (TEBVs) are among tissues that are under active research worldwide. They can be used for drug delivery systems and drug screening. Methods to produce scaffolds for the growth of cells for a TEBV include electrospinning and a Rotary Wall Vessel bioreactor, which both were also used in this thesis. Namely, the aim of the thesis was to test the suitability of these methods for the production of scaffolds that could support the growth of cells and the subsequent generation of a tissue-engineered blood vessel.

Electrospinning is a method for the production of nonwoven mesh of fibers, which varies from micro- to nanometerscale. By applying a high voltage between a collector plate and a syringe filled with solvent-dissolved polymer thin fibers may form and be collected. Later on the fibers can be used for the cell scaffolds which mimic the natural extracellular matrix (ECM). Gelatin, poly-ε-caprolactone (PCL) and poly(ethylene oxide) (PEO) were electrospun with a self-assembled electrospinning set-up LEVIOSA!. Glutaraldehyde-cross-linked gelatin and PCL were used in static and bioreactor cultivation tests.

Rotary Wall Vessel (RWV) bioreactor utilizes a horizontally-laid and rotated cultivation vessel to produce microgravity-like conditions. Rotating walls rotate the cultivation medium, which creates a lift and centrifugal force that balances out the effect of gravity. In this way cells or small cell-scaffold constructs can be cultivated and three-dimensional structures may formed. As part of an adjoining student project, a student-built RWV bioreactor called BIOHOVER was used in this thesis to cultivate electrospun tubular scaffolds.

Tubular-scaffold-polymers, 72-hours cross-linked gelatin and PCL, had an average fiber diameter of 500 ± 100 and 2200 ± 700 nm, and an average pore size of 800 ± 300 and 13900 ± 4600 nm, respectively. Human lung carcinoma cells (A549) were grown along these materials for 3 days in the BIOHOVER bioreactor in order to study how a TEBV could be created. The methods were found to be successful, whilst needing further development, which could later also facilitate the production of a TEBV. Moreover, the methods developed and used in this thesis were found to be suitable for teaching cell and tissue engineering in a M.Sc. level course as a part of the Aalto Online Learning (A!OLE) Biology Meets Mechatronics concept.

Keywords Tissue engineering, electrospinning, gelatin, PCL, PEO, Rotary Wall Vessel (RWV) bioreactor, blood vessel

Preface

Although my name solely takes the credit for this Master's Thesis on the cover page, I was not the only one whose effort made this possible. First of all, I would like to thank the instructor of this thesis, PhD Ari Ora, who gave me great advice and helped me to brainstorm Plan B's when the unexpected happened. Also, I would like to thank the thesis supervisor, professor Katrina Nordström for helping me with practical issues and giving me the opportunity to work on this topic.

Teaching and the collaboration with the School of Engineering at Aalto University were big parts of the thesis project. Thus, I would like to thank D.Sc. (Tech.) Panu Kiviluoma and M.Sc. (Tech.) Tommi Lintilä – the BIOMEETSMEX collaboration would not have succeeded without you. Also, I would like to thank B.Sc. (Tech.) Catarina Brites, B.Sc. (Tech.) Jesse Isokangas, B.Sc. (Tech.) Tomi Kankaanoja and B.Sc. (Tech.) Ville Majuri for designing and building the BIOHOVER bioreactor, all of the bioreactor-project students on the CHEM-E3225 Cell and Tissue Engineering course, B.Sc. (Tech.) Ara Taalas and B.Sc. (Tech.) Anton Vanamo.

As all of the work within this thesis was done in the premises of the School of Chemical Engineering at Aalto University, I would like to thank every staff member who helped me along the way – especially D.Sc. Heli Viskari and the employees at the School's workshop were invaluable. In addition, a special thanks to the School's janitors, who were there to lend me some duct tape just when I needed it the most.

This project has been funded by the Aalto University A!OLE – initiative.

In Espoo, Finland
06/02/2017

Tino Koponen

Table of Contents

Abbreviations

1-D/2-D/3-D = one-, two- or three dimensional

A549 = human lung carcinoma cell line

AC / DC = alternating current / direct current

CHEM = School of Chemical Engineering at Aalto University

CHO (cells) = Chinese hamster ovary (cells)

DMEM = Dulbecco's Modified Eagles Medium

DMSO = dimethylsulfoxide

EC = endothelial cell

ECM = extracellular matrix

ENG = School of Engineering at Aalto University

Etax A = Altia Oyj's brand name for ethanol (>94% (w/v), >96,1% (v/v))

F_g, F_c, F_d = force (gravitational, centrifugal, (hydrodynamic) drag)

GAG = glycosaminoglycan

GTA = glutaraldehyde

HARV = High Aspect Rotary Vessel

HF (bioreactor) = Hollow Fiber (bioreactor)

HFIP = 1,1,1,3,3,3-hexafluoroisopropanol, also known as HFP

in vitro / in vivo = in the glass / within the living

kV = kilovoltage

(LS)CM = (Laser Scanning) Confocal Microscope

MSC = mesenchymal stem cell

NASA = National Aeronautics and Space Administration

PBS = phosphate buffered saline

PCL = poly-ε-caprolactone

PFA = paraformaldehyde

PEO = poly(ethylene oxide)

RCCS = Rotary Cell Culturing System

RGD (sequence) = arginine, glycine and aspartic acid tripeptide sequence

PHP = periodic hydrostatic pressure

PLCL = poly(L-lactide-co- ε-caprolactone)

rpm = rotations per minute

RSB = Rotating Shaft Bioreactor

RT = room temperature

RWV(B) = Rotary Wall Vessel (Bioreactor)

SMC = smooth muscle cell

SE = Secondary Electron (detector), in SEM

SEM = Scanning Electron Microscope

STLV = Slow Turning Lateral Vessel

SMC = smooth muscle cell

TE = Tissue engineering

TEBV = Tissue-engineered Blood Vessel

TFE = 2,2,2-trifluoroethanol

tunica intima/media/externa = inner, middle and outer layer of a blood vessel

UV = ultraviolet

WFM = Widefield Microscope

1. Introduction

Although engineering is commonly comprehended merely as a term of creating and designing larger mechanical objects, the underlying scientific methods and innovative mindset do not exclude the use of smaller parts such as cells, biomaterials and biologically active molecules. Tissue engineering (TE) combines these small biological components in order to repair, reform, create or improve tissues and organs that may be directly used as spare parts in our bodies. (Martin, Wendt and Heberer, 2004, Moffat et al., 2014)

Tissue engineering serves as a natural next step in the continuum of human health care improvements. Compatibility problems and poor availability of both allogeneic and xenogeneic organ and tissue transplants may be avoided by growing the patient's own cells into functioning tissues and organs. Biological spare parts also outperform artificial grafts such as synthetic-fiber-based bypass surgery grafts by enabling the body's own repair systems to merge the graft into the surrounding tissues. Eventually, there are no borderlines between implanted tissue-engineered and pre-existed tissues. Hence, there is no need for further surgical interventions since the body may self-maintain these structures. In addition to organ transplants, engineered tissues also enable better *in vitro* research on cell functions, on the progression of diseases and the effects of new drugs. This paves the way towards animal-test-free research and development. (Martin, Wendt and Heberer, 2004, Moffat et al., 2014)

Currently, the main problem with tissue engineering is how to grow human cells in the three dimensional structures that is necessary for achieving tissue functionality. Traditionally, human cells have been cultivated in rather small scale in static conditions in which only thin cell layers are able to grow with low stress levels and sufficient oxygen supply. In their native form *in vivo*, however, tissue thickness varies and they are complex by nature. Therefore, cultivation methods should be improved to allow tissue formation *in vitro*, that would bear close resemblance to the complexity and structure of tissues *in vivo*. These methods include new types of bioreactors such as Rotary Wall Vessel (RWV) bioreactors that combine low shear forces with the efficient diffusion of

nutrients and gases. This type of bioreactor set-ups allow thicker cell clusters to thrive. On the other hand, as they fail to trigger the formation of complex tissue structures, tissue engineering relies on cultivation with scaffolds. These scaffolds have nano- and microfiber-based structures, which mimic the *in vivo* extracellular matrix (ECM). There are many ways to produce the scaffolds, one being a method called electrospinning. By seeding multiple cell types onto a suitable scaffold and cultivating it in a bioreactor, a close resemblance to human tissues may be created. (Martin, Wendt and Heberer, 2004, Moffat et al., 2014)

The aim of this Master's Thesis is to utilize these new methods in order to study how a functional, natural-mimicking blood vessel could be created. This aim may be divided into two goals: 1) production of a suitable scaffold by electrospinning and 2) utilization of a student-assembled RWV bioreactor in tissue cultivation. Once a cell-scaffold construct is created it may be used as a drug delivery system or as a model tissue in drug discovery research, however, the implementation of these are beyond the scope of this thesis. On the other hand, the methods presented in this Master's thesis have been used in teaching of the CHEM-E3225 Cell and Tissue Engineering course at Aalto University form spring 2017 onwards as the Biology Meets Mechatronics (BIOMEESTMEX) concept of the Aalto University A!OLE learning initiative. A!OLE strives to offer new multidisciplinary education concepts, which combine both hands-on learning and digitalized learning tools.

2. Literature review

The emphasis of this literature review is to introduce key aspects that are needed for composing a fully functional tissue such as a blood vessel since traditional static human cell culturing methods do not give rise to histologically-correct multilayered structures. The first part will cover the basics of cell and tissue biology from cell-to-cell and cell-to-ECM communications to the structural composition of blood vessels and the demands these aspects pose. The second and third part will cover the different solutions for these problems that have been presented in the literature. Electrospinning will be introduced as a convenient method to generate artificial ECM-resembling scaffolds for cells to grow along and the Rotary Wall Vessel (RWV) bioreactor will be introduced as a method that enables cells to thrive and grow in truly three-dimensional shapes as they naturally do in tissues *in vivo*. The last part of this literature review will cover tissue-engineered blood vessel examples from the literature that utilize some of these methods.

2.1 From individual cells to tissues

Complex and highly interacting human tissues are formed by the growth and differentiation of individual cells. Thus when growing tissues *in vitro* the complexity of cell-to-cell and cell-to-ECM connections need to be taken into account. Also, the histological properties, functionality and specialties of the target tissue are key issues in the process of tissue engineering.

2.1.1 Human cell adhesion

Although the detailed information of cell biology is not the main focus of this thesis or literature review, some important facts that affect the production of tissue-engineered blood vessels (TEBV) or tissues in general need to be taken into consideration. Multicellular organisms in the form of animals started to evolve about 600 million years ago and the multicellularity did and still does require cells to be in close contact with, adhere to and communicate with each other and their surroundings. The animal cell membrane is composed of a lipid bilayer, which is embedded with proteins with different functions. For example,

receptors transmit chemical or physical messages in or out of the cell in response to the chemical stimulus of surrounding cells, cell membranes or extracellular matrix (ECM). (Alberts et al., 2008, Hynes 2009, Geiger and Yamada, 2011, Hynes and Naba, 2012)

The cadherin and integrin superfamilies constitute the most important membrane receptors for tissue adhesion. In humans, cadherins include about 180 different transmembrane proteins that connect animal cell membranes to each other – especially in epithelial tissue. The cadherins form adherens and desmosome junctions by linking cadherin receptors of different cells together. Since cadherins are linked to actin and intermediate filaments, a signal may be transmitted between neighboring cells. (Alberts et al., 2008, Hynes 2009, Geiger and Yamada, 2011, Hynes and Naba, 2012)

The integrins link cytoskeleton filaments to extracellular matrix instead of neighboring cells by binding to specific amino acid sequences such as Arg-Gly-Asp (RGD) along ECM proteins (Ruoslahti, 1991). In humans, the integrins are a group of 24 different heterodimers with non-covalently bound α and β chains. As the large extracellular N-terminal part interacts with ECM proteins, intracellular C-terminal ends of α and β chains separate. This enables the binding of an intracellular anchorage protein talin, an adhesion plaque protein, to the β chains. In turn, talin binds to actin filaments, which also may bidirectionally transmit nucleus-originated cellular signals out of the cell through the same pathway. The cytoskeleton channels cadherin- and integrin-conveyed signals further inside the cell. These signaling cascades regulate cell, leading to differentiation in cell growth, proliferation, survival, fate, shape, polarity and migration. (Alberts et al., 2008, Hynes 2009, Geiger and Yamada, 2011, Hynes and Naba, 2012)

2.1.2 The matrisome and the extracellular matrix (ECM)

Extracellular matrix consists of polymers that cells have secreted to their surroundings. Cells attach to these protein polymers via integrins and sometimes via cadherins to form a functioning tissue with optimal conditions

for cells to thrive. In addition to the ECM polymers, there are many ECM-associated proteins and molecules near cells such as growth factors and proteases, which affect the functions and fate of the tissue. In general, this multicellularity-enabling system is called the matrisome and in mammals the core of it consists of some 300 proteins (Hynes, Naba 2012). The main ECM polymers have a diameter ranging from 50 to 1000 nm and they fall into three main categories: fiber-forming proteins such as collagens and elastin, proteoglycans, and other proteins such as glycoproteins laminin and fibronectin. The exact ECM composition, however, varies between cell and tissue types. These polymers give the ECM different properties that support tissue functionality. A schematic picture of the ECM is presented in Figure 1. (Alberts et al., 2008, Geiger and Yamada, 2011, Hynes and Naba, 2012)

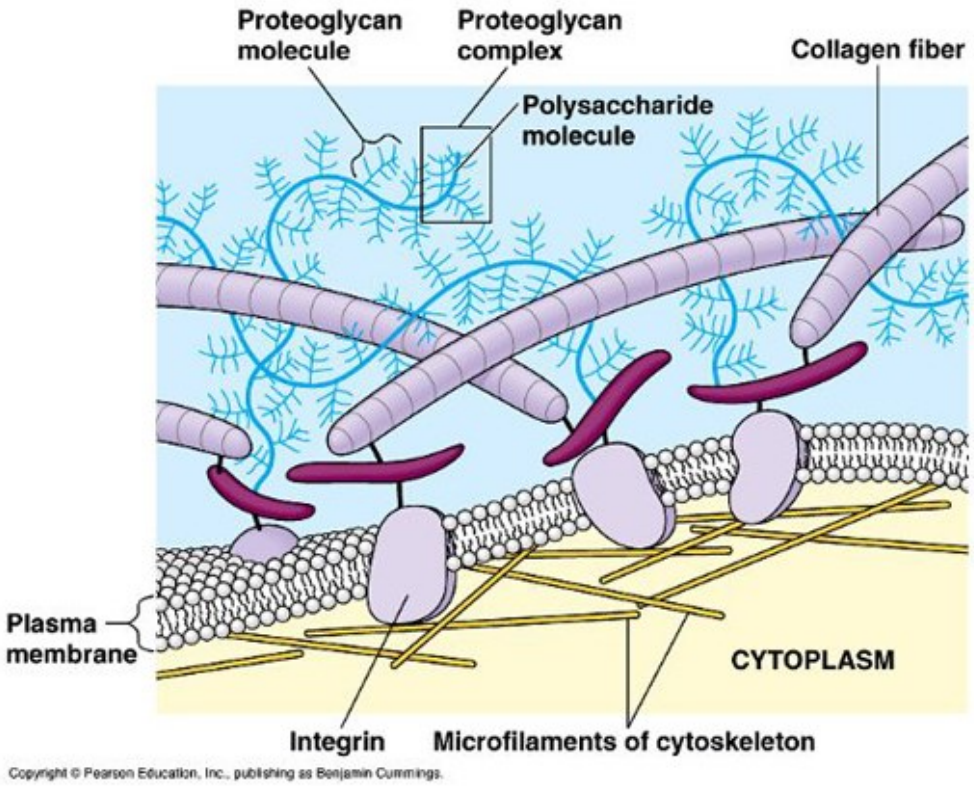

Figure 1. A generalized overview of the ECM and its main components. Integrins convey messages in and out of cytoplasm where the cytoskeleton interacts with the nucleus. The main components of the ECM are collagen fibers, fibronectins and proteoglycans but also other components such as

elastin fibers may be present depending on the tissue type. (Sigma-Aldrich, 2017)

Collagens are the major ECM protein group and they are the most abundant proteins in mammals by constituting about 25% of the total amount of proteins in an individual. There are 28 different collagen types in vertebrates named according to Roman numerals (I-XXVIII). All collagens share a common structure of a triple-helical domain, which forms when three polypeptide chains, called α chains, intertwine as a hydrogen bonded superhelix. The content of triple-helical structure dictates the rigidity and causes the formation of fibrillary structures. These fibers give the ECM resistance against tensile forces. Individual collagen α chains are usually composed of repetitive triplets of Glycine-X-Y. X and Y may be any amino acids though usually they are proline, hydroxyproline, lysine or hydroxylysine depending on the type of collagen. Type I collagen is the most common in human ECM. Superhelices tend to form bigger fibrils (10 - 300 nm), which further form collagen fibers with a diameter exceeding even 1 µm. Some collagen types, such as IX, IV and VII are fibril-associated, network-forming or anchoring collagens, respectively, which primarily link fibrils and fibers together and also with other ECM components. (Alberts et al., 2008, Ricard-Blum, 2011)

As collagens give tissue stiffness, elastin, on the other hand, is responsible for elasticity in the regions where it is needed for example in blood vessels. Elastin is proline- and glycine-rich, about 750 amino acids long chain with alternating hydrophobic elasticity-giving segments and α-helical cross-linkage-enabling segments. Like collagens, elastin polypeptides form bigger fibrils by binding together. These fibrils form around glycoprotein cores called microfibrils. Fibrils intertwine into even bigger elastic fibers. (Alberts et al., 2008)

Proteoglycans apart from hyaluronan consists of a small core protein with covalently bound glycosaminoglycans (GAGs). GAGs are unbranched polysaccharide chains with a repetitive unit of an amino-sugar-containing disaccharide. Usually the sulfated N-acetylglucosamine or N-acetylgalactosamine is the amino sugar while uronic acid such as glucuronic

or iduronic acid is the second sugar of the disaccharide. These sugar units are highly anionic and by attracting cations they also osmotically retain major amounts of water in the ECM. This leads to swelling pressure, also known as turgor, in the tissue. Turgor helps tissue to withstand compressive forces, which is also one of ECM's main physical functions. GAGs are stiff and they stay linear in the ECM. Thus, spatially they take a lot of space although out of the total mass of the ECM their contribution is not massive. GAGs are divided into four main groups: hyaluronan, chondroitin and dermatan sulfate, heparan sulfate and keratin sulfate. Although proteoglycans are an active part of the ECM, they may also be co-receptors in the cell membrane. (Alberts et al, 2008)

The glycoproteins are polypeptide chains that are glycosylated with oligosaccharide chains. These side chains provide binding sites for the matriosome's macromolecules such as growth factors, and they also link the ECM to cell membrane receptors. The most important ECM glycoproteins include fibronectin, fibrinogen and laminin. Fibronectins contain two large disulfide bonded subunits, which have integrin-binding type III fibronectin repeat (RGD sequence). Fibronectins may also bind to collagen fibers, and thus they act as important cell-ECM-mediators. The laminins also help cells to bind to ECM and they are mainly found in the basal lamina, which connects epithelial layers to connective tissue. The fibrinogens play a crucial role in wound healing by clotting blood. The glycoproteins are abundant in cell membranes where they for example anchor the matrix metalloproteases and serine proteases near the cell. Once released and activated these enzymes cleave fibers in the ECM. In this way, the ECM may be partially degraded when tissue needs to reform. This also helps cells to migrate through the fiber mesh of the ECM. (Alberts et al. 2008)

2.1.3 Histology of blood vessels

Although the ECM is composed of somewhat the same components throughout the human body, the specific ratios vary between tissues. This is why knowledge about the histology and composition of the target tissue is essential for producing well-functioning artificial tissue such as blood vessels.

In Figure 2, cross-sectional overviews of the two main blood vessel types are presented. The third blood vessel type, the capillary, resembles arteries and veins but only consists of single cell layers that enable efficient substance exchange between tissue and blood vessels. Blood vessel diameters range from 8 µm to 25 mm (Blakemore and Jennett, 2001) and burst strength from 200 mmHg to over 4000 mmHg for small capillaries and larger arteries, respectively (L'Heureux et al., 2006, Jung et al., 2015)

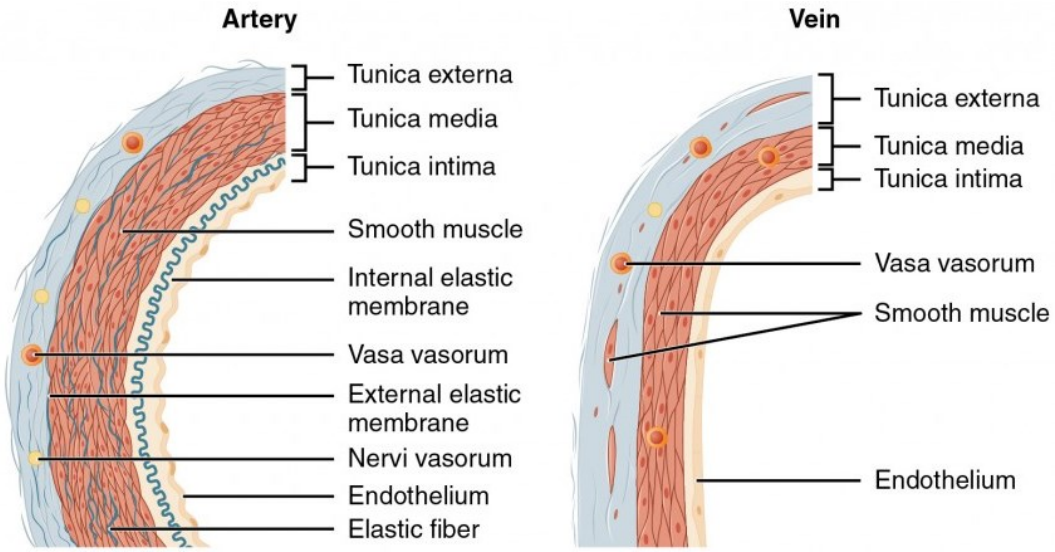

Figure 2. The F-section of arteries and veins. Three different tunicae are presented in addition to other histologically important blood vessel parts. (OpenStax, 2016)

Three different layers may be distinguished when scrutinizing blood vessels. These layers are referred as *tunicae – intima, media* and *externa* from inside out. The blood flows in a hollow space called lumen and it is surrounded by a thin *tunica intima*, which is composed of a sheet of endothelial cells. This endothelium does not contain much ECM since endothelial cells adhere to each other directly. Endothelial cells form a smooth surface that eases the blood flow. *Tunica intima* is separated from *tunica media* by basal lamina, which contains laminin, type IV collagen and nidogen, and proteoglycan perlecan. Laminin is the main component of basal lamina, of which the main task is to provide mechanical strength and serve as an attachment surface for

the endothelium. *Tunica media* contains connective tissue with smooth muscle cells, fibroblasts and sheets of elastic fibers. The elasticity and smooth muscle cells of *tunica media* enable vasodilation and vasocontraction. The fibroblasts secrete ECM polymers and they are also present in the outermost layer of blood vessels. *Tunica externa* anchors blood vessels to the surrounding tissue by mainly being composed of collagen fibers. Veins and arteries differ histologically by the thickness of *tunicae* but they share the same principle in their structure. The small capillaries also have the same histological structure but in smaller scale and without the *tunica externa*. (Blakemore and Jennett, 2001, Alberts et al., 2008)

2.2 Electrospinning ECM-mimicking scaffolds

Electrospinning is an over hundred-year-old method and it was first patented by John F. Cooley in 1902 to electrically disperse fluids in order to produce fibers (Cooley, 1902). The same year William J. Morton also patented a similar device (Morton, 1902). In 1934, Anton Formhals patented a way to produce artificial filaments by spinning dissolved polymers with the help of an electric field (Anton, 1934). During the last two decades, electrospinning has gained interest as a method to produce nanoscale ECM-mimicking scaffolds for tissue engineering (Khorshidi et al., 2016). This chapter reviews electrospinning as a method and the properties of produced scaffolds with regards to the properties of natural ECM. By optimizing solution, process and ambient parameters different scaffold properties may be gained, which aid cells to grow into functional tissues.

2.2 1 Electrospinning as a method

A basic electrospinning set-up is illustrated in Figure 3 and it contains three major components. The syringe pump acts as a spinneret pumping polymer solution towards a grounded collector. These two are coupled with an electric field formed by a high voltage DC power supply, which enables the electrospinning process to occur. When a like charge between the polymer solution and the power supply is conducted to the metallic needle of the

syringe pump, repulsive interactions start to affect the polymer solution. When the electric field strength is increased to about 10 – 30 kV, liquid surface tension is balanced out and individual polymer fibers start to move towards the oppositely charged metallic grounded collector. (Pham, Sharma and Mikos, 2006, Sill and von Recum, 2008, Sell et al. 2010, Khorshidi et al. 2016, Ercolani, Del Gaudio and Bianco, 2015)

While travelling through air fibers bend chaotically, causing the excess polymer solvent to evaporate. Thus when fibers reach the collector they are solid polymers that depending on the collector shape form sheets, hollow cylinders or other 3-D shapes made out of nonwoven polymer mesh. The individual fibers are from nano to micron scale ranging from 50 nm to 10 µm in diameter, depending on the electrospinning variables such as the polymer concentration or applied voltage. In addition to the electrospinning with dissolved polymers, which is sometimes referred as a wet spinning, a method called melt spinning can be used. There melted polymers are electrospun into fibers under vacuum without any solvents (Muerza-Cascante et al., 2015). If the collector is cylindrical and the electrospun material is biocompatible, the electrospun scaffold may be used as an artificial surgery graft *in vivo* as such. In addition, if the scaffold is further developed *in vitro* by cultivating cells on it, a functioning tissue-engineered blood vessel may be created. (Pham, Sharma and Mikos, 2006, Sill and von Recum, 2008, Sell et al. 2010, Khorshidi et al. 2016, Ercolani, Del Gaudio and Bianco, 2015)

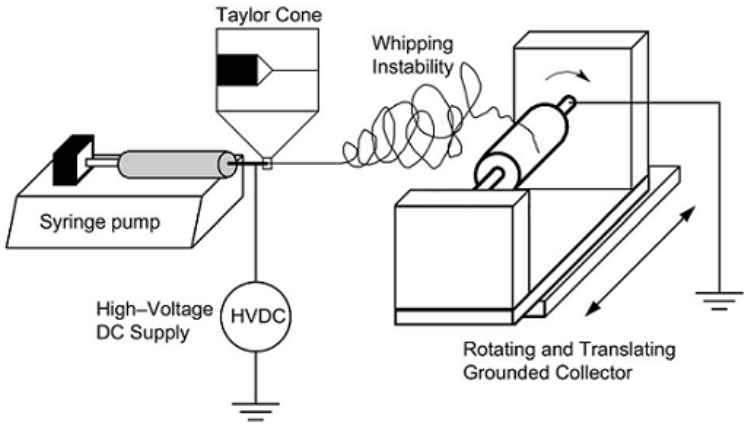

Figure 3. A basic set-up for electrospinning. The syringe pump pumps polymer-containing liquid through a metallic blunt-ended needle. When a charge is greater than the surface tension in the liquid, the needle tip's liquid bubble transforms into a Taylor cone, which ejects polymer fibers towards the opposite-charged grounded collector. The grounded collector may be for example a rotating mandrel onto which the polymer is spun. (Sill and von Recum, 2008)

In the next chapter different electrospinnable natural, synthetic and composite polymers and their solvents are reviewed as potential ECM-mimicking materials when blood vessels are created *in vitro.* The optimization of solution, process and ambient parameters are then discussed in the terms of scaffold durability, fiber size and orientation, pore size and surface area, and scaffold cross-linking since these variables affect the cell viability and motility in the scaffold.

2.2.2 Electrospinnable polymers and solvents

Over 200 polymers have been successfully electrospun so far and they may be categorized into natural, synthetic and composite polymers (Bhardwaj and Kundu, 2010). Since the goal is to produce a scaffold that resembles natural ECM found in tissues the polymers that either are the same ones or that induce the formation of natural ECM and its functions are regarded as most suitable. Also, biodegradability, non-thrombogenicity and non-cytotoxicity are important factors. (Sill and von Recum, 2008, Ercolani, del Gaudio and Bianco, 2015)

Natural polymers include those that are found in the animal ECM: collagens, elastin, fibronectin, fibrinogen, proteoglycans such as hyaluronan and combinations of them. These polymers are mostly from animal origin and thus they pose for example the risk of non-human-compatibility and zoonotic transmission. Also, non-human-ECM polymers such as silk fibroin, chitosan, starch, alginate and gelatin may be used, although they might induce different cellular mechanisms that may or may not be advantageous for cell growth and tissue formation. They also might have zoonotic risks depending on the origin. Collagen types I and III are considered to be ideal scaffold materials since they are the main structural elements of the ECM and they provide support for tissue. Also, elastin is regarded as an important polymer especially in blood vessel engineering since it provides the much-needed elasticity. All of the natural polymers may also be produced with recombinant protein technology, which reduces some of their inherent risks. (Ercolani, del Gaudio and Bianco, 2015)

Synthetic polymers are human-produced and non-natural. The ones that are used in tissue engineering should eventually degrade so that natural ECM would replace the artificial scaffold. The synthetic polymers are mainly co-spun with natural polymers as strength-giving supportive fibers. However, some electrospun blood vessel scaffolds have been made only of synthetic polymers. Electrospun synthetic polymers may be for example polyethylenoxide (PEO), polydioxanone (PDS), polyglycolic acid (PGA), poly-L-lactic acid (PLLA), poly-DL-lactide acid (PDLLA), poly-ε-caprolactone (PCL) or (thermoplastic) polyurethane ((T)PU). Also co-polymers of the aforementioned polymers or other substances may be used such as poly-L-lactide-co-ε-caprolactone (P(LLA-CL)), polyethylene-co-vinyl alcohol (EVOH) or polyglycolide-co-dioxanone-co-trimethylene carbonate (Biosyn®). (Sill and von Recum, 2008, Ercolani, del Gaudio and Bianco, 2015)

Electrospinning solvents depend on the used polymers since they need to dissolve before use in wet-electrospinning. The most used solvents are 1,1,1,3,3,3-hexafluoro-2-propanol (HFIP), 2,2,2-trifluoroethanol (TFE),

common organic liquids such as acetone, formic acid, acetic acid, ethyl acetate, chloroform, methanol and ethanol, and water. Since the natural ECM is not easily soluble in water, most electrospun natural polymers also do not dissolve in water. Solvent usually mostly evaporates during the electrospinning process but some residues might remain in the scaffold and causing cytotoxicity. (Sill and von Recum, 2008, Ercolani, del Gaudio and Bianco, 2015) Also, solvent might change the chemical composition of the polymer. For example, there is evidence that collagen denatures into gelatin when dissolved in HFIP (Zeugolis et al., 2008).

The multiple polymers can be dissolved to the same solvent and electrospun with one needle but if different solvents are used, the electrospinning set-up can be changed so that there are multiple syringes and needles that eject polymer towards the same collector – also the direction of ejection can be changed in order to alter the fiber orientation. Moreover, different types of nozzles may be used so that one polymer of even cell suspension will get trapped inside another polymer. This is accomplished by inserting one needle inside another to form a co-axial circular two-chamber nozzle. (Bhardwaj and Kundu, 2010, Ercolani, del Gaudio and Bianco, 2015)

2.2.3 Scaffold durability

The durability of electrospun scaffold is a two-edged sword. The scaffold should endure handling and the increasing weight of cell mass when cultivation proceeds but on the other hand it should degrade in a controlled manner so that cells would eventually replace it with self-secreted natural ECM. The main problem with electrospinning with only natural polymers is that they are rather fragile and tend to degrade before cells have grown enough. Thus, synthetic polymers should be used as a supportive material. If the synthetic polymers are chosen, they should be biodegradable and the debris should not be cytotoxic or form any cloths in the tissue. The scaffold durability may be enhanced by spinning polymers into a thicker layer but this causes problems with the pore size. Also, cross-linking enhances the scaffold durability and this will be discussed later. (Bhardwaj and Kundu, 2010)

2.2.4 Fiber size and orientation

Fiber size of the electrospun scaffold may be altered by changing electrospinning variables. The fiber diameter will increase if the polymer concentration, needle diameter or flow rate is increased or the applied voltage is really high. Also, the fiber diameter will increase if electrospinning is performed under vacuum. The fiber diameter will decrease if the solution conductivity, needle-to-collector distance, temperature or applied voltage in the smaller scale of optimal voltages is increased. The polymer fibers will form beads if the flow rate is too high or polymer concentration is too low, and micropores on the fiber surface if solvent is highly volatile or humidity is high. Usually these are not desirable attributes but useful in some applications. Molecular weight of the polymer affects viscosity, conductivity and also surface tension and electrical properties of the polymer suspension – the bigger molecular weight the larger fiber diameter in general. There is an optimal range for all of these variables and by identifying them, an optimal-sized fiber may be produced. (Khorshidi et al. 2016)

The orientation of the fiber matt on the collector may be altered with different nozzle systems and by spinning the collector. If a rotating mandrel is used to gain a tubular scaffold, the speed of the rotation affects the fiber orientation. At low rotations (0 - 1000 rpm) fibers form a random mesh but if the rotation speed is increased (up to 6000 rpm) fibers become more aligned (Sill, von Recum 2008). Moreover, the different collector materials, for example aluminum foil, copper mesh, water, methanol or paper, may be used and they too have an effect on the fiber matt (Pham, Sharma and Mikos, 2006)

2.2.5 Pore size and scaffold's surface area

An appropriate pore size and the fibers' surface area are essential for a 3-D tissue to form. On average human cells have a diameter ranging from 10 to 30 µm. Cells migrate through the scaffold matrix so that the tissue can differentiate and has functionality. This is the reason why the electrospun scaffold should have an average pore size greater than 10 µm. This may be achieved by optimizing the spinning conditions or by using sacrificial polymers.

Sacrificial polymers are co-electrospun polymers that either are washed away after the electrospinning or that degrade faster than the structural fibers when cultivated. As an example, co-spun gelatin and synthetic polymers can be used in this manner, namely the synthetic polymer holds the tubular structure for a longer period of time as gelatin degrades faster while still providing attaching points for cells to grow along during the first days. (Khorshidi et al., 2016)

The diameter of the native ECM fibers vary from 50 to 1000 nm. This should also be the aim of electrospun scaffolds since too large fibers have a poor surface-area to diameter ratio. Cells have more places to attach along thinner fibers and this helps them to migrate through the scaffold. (Sill and von Recum, 2008)

2.2.6 Cross-linking

The scaffold cross-linking aims to generate more chemical interactions between individual chains, fibrils and fibers so that the overall scaffold durability increases. The most common chemical cross-linker with electrospun scaffolds is glutaraldehyde vapor but also glyceraldehyde, formaldehyde, epoxy, 1-ethyl-3-(3-dimethylaminopropyl)-carbodiimide, 1,6-diisocyanato-hexane and N-(3-dimethylaminopropyl)-N'-ethylcarbodiimide hydrochloride, citric acid, dissuccinimidyl suberate and genipin are used depending on the polymer. Also, proteins may be enzymatically cross-linked for example with transglutaminase. In addition, the chemical cross-linkers as well as physical factors such as UV or gamma radiation and elevated temperatures in vacuum (dehydrothermal treatment (DHT)) may cross-link polymers by breaking long chains and thus creating more possible cross-linkage sites. Physical cross-linking has no risk of cytotoxic effects in contrast to chemical cross-linking, which may leave compounds in the scaffold after treatment. These residues might cause calcification *in vivo* after implantation in addition to inhibiting cell growth. Even though cross-linking usually is beneficial for the scaffold durability and stiffness, it sometimes makes the scaffold brittle and thus deteriorates it. (Ercolani, del Gaudio and Bianco, 2015, Reddy, Reddy and Jiang, 2015)

2.2.7 Conclusions about electrospinning

As has been presented above, electrospinning appears to be an ideal method for producing a scaffold for tissue engineering since it enables ECM-mimicking constructs. Especially, cylindrical scaffolds could be suitable for tissue-engineered blood vessels if electrospinning conditions are optimized and the end-result is a durable, cell-friendly scaffold with large-enough pores and ideal fiber diameter. Some of the literature on tissue-engineered blood vessels will be further reviewed in Chapter 2.4. First, however, cultivation methods will be reviewed as the electrospun scaffold is not sufficient on its own to enable the growing of 3-D tissues.

2.3 Cultivation methods that enable 3-D structures

Although, the electrospun scaffold provides a large array of structural cues and durability, the cells in the tissue that is beginning to form require optimal cultivation conditions for growth such as ideal temperature, nutrients and oxygen-to-carbon-dioxide ratio. Traditionally, human cells with or without a scaffold have been grown in static conditions for example in T-flasks or in Petri dishes, however, in this set-up only thin layers of cells on the surface receive enough oxygen and nutrients. It has been estimated that a spheroid of cells with a diameter in excess of 1 mm will not receive sufficient flows of nutrients and other essential compounds and the cells in the middle will become necrotic, which means that the cells simply die out without apoptotic self-regulation (Unsworth and Lelkes, 1998). Thus, the amount of viable cells is restricted to the bottom area size of the flask, and it has been difficult to achieve the formation of cell layers and more complicated 3-D structures. Accordingly, in the following, bioreactor set-ups enabling 3-D-forms of tissues will be reviewed with a special emphasis on Rotary Wall Vessel (RWV) bioreactors that will be used in the experimental part of this thesis. The monitoring of bioreactor conditions will then be discussed in terms of optimizing tissue growth.

2.3.1 Cultivation methods for human cells

A bioreactor may be defined as an apparatus that influences biological phenomena by controlling the affecting physical and chemical variables such as temperature, pH, stirring and gas or liquid flows. In the simplest view, a flask may be referred as a bioreactor but usually set-ups that are more complex are used in order to better control cultivation parameters. Figure 4 shows some of the most common bioreactor set-ups that are used when human cells are cultivated *in vitro.* (Partap, Plunkett and O'Brien, 2010)

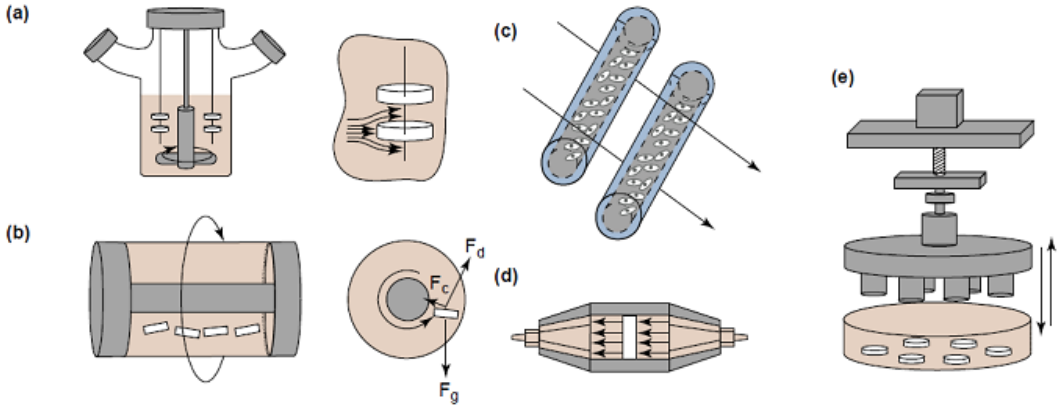

Figure 4. Different bioreactor types for cultivating human cells in vitro. (a) spinner flask, (b) rotating wall vessel (Slow Turning Lateral Vessel (STLV) shown here), (c) hollow-fiber, (d) perfusion and (e) compression bioreactor. (Martin, Wendt and Heberer, 2004, modified).

Static cultivation may be carried out for example in a Petri dish or a flask. Also so-called miniature bioreactors such as well plates or chips may be used for screening purposes. As these are the simplest systems for cell cultivation, they are also most commonly used. The downside in such systems is the poor circulation of oxygen, carbon dioxide, nutrients and metabolic products, which results in low cell yields. Accordingly, cells can be cultured in high-speed stirring in a "stirred tank bioreactor" (Figure 4a) to enhance the fluid movement and the mass transport of cell-essential compounds. Stirring causes heterogeneous shear forces in the liquid and this usually affects negatively cell growth and tissue formation although some CHO (Chinese hamster ovary) cell lines have adapted to these high shearing forces. The use of scaffolds,

microcarriers or cell encapsulation - for example hydrogels or cellulose microparticles – may help to endure stirring stress and the collisions. Even though an optimal balance between stirring speed and cell viability can be found, spinner flasks usually do not give the best end result. However, industrially they are appealing due to easy scale-up and simplicity of the set-up. (Chen and Hu, 2006, Liu et al. 2014, Kumar and Starly, 2015) Instead of a glass or plastic vessel, also eggshells may be used in small scale as a flask to enable more efficient gas exchange (Chen and Hu, 2006).

As an alternative, the spinner flask may be turned sideways. This so-called Rotating Shaft Bioreactor (RSB) is equipped with needles, which are attached to a rotating mandrel in a half-full vessel. The tissue constructs that are attached to needles slowly rotate between gas phase and medium, which enables nutrient and gas flows. (Chen and Hu, 2006) Another spinner-flask-resembling method is a wave bioreactor, which creates a steady flow of waves inside a cultivation vessel or bag by rocking it. This causes oxygen to dissolve better, which improves cell growth. Similar to RSBs and spinner flasks also wave bioreactors cause cell-growth-impacting shear forces. (Kumar and Starly, 2015)

Bioreactors, which facilitate the circulation of growth medium, are hollow-fiber (HF) bioreactors and perfusion bioreactors. In HF bioreactors the growth medium is slowly pumped into narrow semi-permeable capillaries. Cells that grow on intra- or extracapillary surfaces receive oxygen and nutrients from the medium and excrete wastes to the growth medium whilst enduring low shear forces. A special case of a HF bioreactor is a flow bioreactor for cardiovascular constructs. Instead of hollow fibers, the growth medium is pulsatile-pumped into a quasi-ready tissue-engineered blood vessel, which then further grows and develops when lumen-pumped medium nourishes the cells. Perfusion bioreactors are also based on medium flow but instead of tubular constructs or hollow fibers, the growth medium usually moves through a permeable mesh of scaffold and cells. In some cases, perfusion could be coupled with a flow bioreactor. Perfusion of growth medium couples low shear forces with

sufficient nutrient, waste and oxygen flows but the flow of medium can possibly cause directionality inside the tissue or poor cell attachment. (Martin, Wendt and Heberer, 2004, Liu et al., 2014, Kumar and Starly, 2015, Zhao et al., 2016)

Mechanical stress such as compression or pulling may be applied during static cultivation to induce tissue differentiation. These methods need special bioreactor set-ups and they are mainly used with tissues such as bone, cartilage, skin or muscle that need to be resilient when implanted *in vivo* and therefore may require conditioning by mechanical stimuli. To do so, conditioning stress is caused mechanically by applying a load, strain or hydrostatic pressure on the tissue or by using varying magnitude magnetic fields that cause an intratissular strain level when the cell-receptor-bound biosuitable magnetic nanoparticles cause physical movement of cells within the ECM. (Partap, Plunkett and O'Brien, 2010, Zhao et al., 2016)

2.3.2 Rotary Wall Vessel (RWV) bioreactors

As presented in the previous chapter on 3-D-structure-enabling bioreactor set-ups (2.3.1) there is one main dilemma, which is common to all, namely the efficient flow of nutrients, oxygen and wastes to and from cells has only been achieved by actions that cause shear stress, which in turn negatively affects the developing tissue. However, Rotary Wall Vessel (RWV) bioreactors are a type of bioreactors that cause minimal shear forces while still providing a sufficient flow of oxygen and nutrients to the tissue. Thus, RWV is a good choice for tissue engineering because tissue can develop freely in it. A cross-sectional view of High Aspect Rotary Vessel (HARV) is presented in Figure 5. HARV is one type of a RWV bioreactor. Another type (Slow Turning Lateral Vessel (STLV)) has been presented in Figure 4b (page 17)

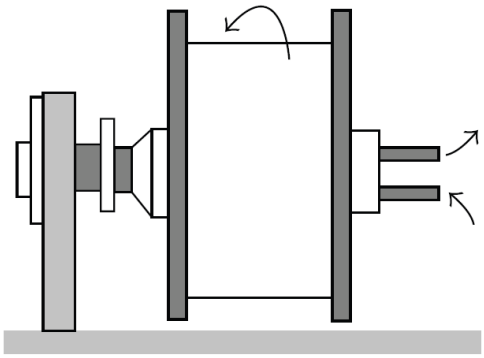

Figure 5. A cross-sectional view of High Aspect Ratio Vessel (HARV) bioreactor. The vessel is attached to a motor (on the left), which rotates the fully-liquid-filled vessel. Moving liquid and centrifugal forces balance out gravity and cause microgravity-like conditions inside the vessel. The media may be changed through the syringe ports (arrows on the right). The gas exchange occurs through the silicone membrane in the lid. (Salehi-Nik et al., 2013, modified)

RWVB was invented in 1987 by NASA (National Aeronautics and Space Administration, USA) researchers. It has since been used to culture cells in the microgravitational environment, however, applying a constant rotational movement to a horizontally growing organism has already been used since the 18th century when the first clinostats were invented. Clinostats may be used when gravitropism is studied in plants and actually, a RWV bioreactor is just a more specialized version of a clinostat. Figure 4b (page 17) illustrates the physical theory behind RWV bioreactors: unidirectional force of gravity (F_g) on Earth may be time-averaged to near zero when centrifugal force (F_c) and hydrodynamic drag force (F_d) act upon the particle. These two latter forces are caused when the walls of the horizontally-laid vessel rotate and friction between the wall and the liquid cause the movement of the medium. (Martin, Wendt, and Heberer, 2004, Korossis et al., 2005, Klaus, 2007, Ayyaswamy and Mukundakrishnan, 2007)

There are two types of RWV bioreactors: STLV and HARV that are shown in Figures 4b and 5, respectively. RWV bioreactors are also known by the name

RCCS (Rotary Cell Culture System) but this name refers to a commercial RWV bioreactor system manufactured by Synthecon. Both RWV bioreactor types have the same working principle and are much alike. The main difference lies in the gas exchange. STLV has a horizontal gas-permeable exchange silicone membrane in the middle of the vessel where as HARV's gas exchange membrane is located in the lid of the vessel. This enables more efficient oxygen and carbon dioxide flows, and also slower rotational movement allowing the medium to move in the middle part of the vessel. Both RWV bioreactor types may be coupled with a flow of medium. The RWV bioreactor vessel is usually made of sterilization-enduring plastic such as polypropylene, it has a volume of about 100 ml, medium change may be done through syringe ports and the vessel should rotate about 10 - 40 rpm to ensure that the cell constructs stay suspended. Careful monitoring is necessary when the vessel is filled, because any bubbles inside the vessel lead to shear stress and changes in the liquid flow, which cancels out the benefits of RWV bioreactors in comparison to other bioreactor types. (Unsworth and Lelkes, 1998, Richardson, 2003, Martin, Wendt and Heberer, 2004, Martin and Vermette, 2005, Korossis et al., 2005, Chen and Hu, 2006, Klaus, 2007, El Haj and Cartmell, 2010, Partap, Plunkett and O'Brien, 2010)

Another bioreactor type that utilizes the same concept of rotating wall in a horizontally laid vessel is called miniPerm by Sarstedt. The bioreactor vessel consists of two different modules, a medium tank and a cell-containing production module, that are connected via dialysis membrane. This allows the exchange of glucose and cell metabolism wastes between two modules hence keeping their levels optimal. The gas exchange occurs via the production module's silicone membrane and the vessel is laid over rotating mandrels without any attaching. Although miniPerm allows a good production yield per volume within the production module, it does not create microgravity-like environment. (Mihailova et al. 2006) There are also other types of bioreactors that utilize microgravity, such as 3-D Random Positioning Machine (RPM) and 2-D Fast-Rotating Clinostat (FRC), but they are not as effective (Grimm et al., 2014, Aleshcheva et al., 2016).

2.3.3 Monitoring the cultivation

Bioreactors provide ideal cultivation conditions that should also be measured throughout the cultivation process regardless on the bioreactor type to ensure good cell growth. Human cells grow at 36 - 37°C under humid conditions of 93 - 95% oxygen and 5 - 7% carbon dioxide. Dramatic changes in these parameters may affect cells and the developing tissue and thus they should be monitored within the cell incubator. Ideally, the oxygen and carbon dioxide levels should also be measured within the bioreactor vessel since they need to dissolve into the growth medium in order to reach and affect cells. The stirring speed or rotations per time unit should be noted if they are used in the bioreactor set-up. Other factors that affect cells within the growth medium are pH and the amounts of different nutrients and cell metabolites. In general, pH should be around pH 7.4. The nutrient and metabolite amounts affect cell growth, differentiation, movement and thus also the surrounding ECM and scaffold. (Partap, Plunkett and O'Brien, 2010, Rodrigues et al., 2011, Hasan et al., 2014)

The traditional large-scale bioreactors utilize measuring probes that are inserted beneath the growth medium. They are reliable and widely used but not ideal with small volume vessels. For example, they cannot be used with the RWV bioreactors since they would affect medium flow and thus the microgravity-like conditions that have been created. In addition, it is rather simple to take a sample out of a larger bioreactor and analyze it, but as the volumes with human cell cultivations are usually small, even taking one sample might significantly affect the cultivation volume. Recently new types of non-invasive nanotechnology-utilizing monitoring systems for measuring pH, oxygen and carbon dioxide levels, and viable cell amount have been created. These monitoring methods are usually based on spectroscopically or electrochemically measured changes in a small dot-like sensor that may be glued inside the vessel and measured through the clear vessel wall. In addition to pH, oxygen and carbon dioxide also other cell-essential compounds such as the concentration of glucose, nucleic acids, ions or enzymes may be

detected with proper probes. This would enable the estimation of the cell growth phases and the stage of tissue differentiation, improve cultivation conditions and automate the whole cell cultivation process, which would reduce the risk of contamination and lower the costs in larger scale. (Beutel and Henkel, 2011, Hasan et al., 2014)

2.4 Tissue-engineered blood vessels (TEBVs)

So far, the cell and ECM biology, electrospinning and cultivation methods have been reviewed above in the context of highlighting the main points that are important for understanding tissue engineering for functional blood vessels. The fate of a human cell is tightly linked to the physical and chemical signals, and tissues may only form if the adherent cells produce ECM and differentiate properly. These tissue-inducing factors are the key when tissues are engineered *in vitro*. This is why scaffolds should have the right attributes and the bioreactor must create the right milieu that directs cells towards functioning correctly – only with a correct mix of these cell-affecting signals a tissue-engineered blood vessel may be created. As this maze of different methods is rather complex, previous work from the literature will be reviewed next in order to give an overview of the state-of-the-art at the present time. The emphasis will be on scaffold attributes, cultivation methods and how well the end product resembles native blood vessels with reference to burst pressures given for human blood vessels (from 200 mmHg to over 4000 mmHg (L'Heureux et al., 2006, Jung et al., 2015)). Burst refers to the maximum pressure that the blood vessel withstands without rupturing. Articles that do not aim to produce blood vessels and only describe electrospinning have been excluded from this review since an abundance of research on electrospinning is published every year.

2.4.1 TEBVs without electrospun scaffold

The first attempt to create a tissue-engineered blood vessel (TEBV) was by Weinberg and Bell in the 1980's (Weinberg and Bell, 1986). They were able to produce a multilayered artery-resembling structure by casting collagen with

bovine smooth muscle cells (SMCs) and adventitial fibroblasts and using a Dacron mesh sleeve as a supportive material. Once this construct was statically grown long enough the central mandrel was removed and endothelial cells (EC) were seeded into the lumen. The highest burst pressure obtained was 323 ± 31 mmHg. (Weinberg and Bell, 1986) Other researchers have also tried to produce TEBVs by similar techniques. L'Heureux and his colleagues cultured human SMCs and fibroblasts statically, peeled of these cells as sheets and wrapped them around a mandrel. After maturation, ECs were seeded into the lumen and finally a burst pressure of 2594 ± 501 mmHg was reached (L'Heureux et al., 1998). Jung and her colleagues also used similar peeling technique and wrapped cultured human mesenchymal stem cell (MSC) sheets around a mandrel, cultured them in a STLV bioreactor and seeded human endothelial progenitor cells (EPCs) to the lumen after which a perfusion flow bioreactor was utilized. They reached a burst pressure of 342 ± 101 mmHg. (Jung et al., 2015)

Yokoyama and her colleagues also did not use any external scaffold when they produced a TEBV. By statically cultivating rat aortic SMCs for 24 hours, exposing the cultivation for periodic hydrostatic pressure (PHP) the next 24 hours, seeding a new layer of SMCs onto the existing one and repeating the PHP-seeding cycle for ten times a layer of *tunica-media*-resembling vascular structure was created. This cell sheet was then wrapped around a glass rod and matured for 14 days in static conditions. Burst pressure was not reported. (Yokoyama et al., 2017) In addition, Laura Buttafoco reported in her Doctoral thesis that by casting acetic-acid-dissolved type I collagen and elastin into a tubular mold, cross-linking them to form scaffolds, filtration seeding human umbilical vein SMCs in them and cultivating these cell-scaffold constructs in a pulsatile flow bioreactor a TEBV was created. Burst pressure was not noted (Buttafoco, 2005). TEBVs may also be created by 3-D printing hydrogel-cell suspensions but these techniques are reviewed elsewhere (Hoch, Tovar and Borchers, 2014).

2.4.2 TEBVs with electrospun scaffold

Most attempts to produce a TEBV involve the use of electrospinning since it is an easy method to produce tubular scaffolds with nanoscale fibers that support blood vessel formation (Chapter 2.2). Usually tubular shape is formed by directly electrospinning on a rotating mandrel hence wrapping is not necessary. Publications on TEBV-electrospinning may be divided into two categories: those that focus only on the scaffold and to those that also aim to further mature the tubular cell-scaffold construct.

Although usually researchers tend to mix both natural and synthetic polymers in the electrospinning process, sometimes only natural (for example HFIP-dissolved collagen, elastin and gelatin (Heydarkhan-Hagvall et al., 2008) or synthetic polymers (for example HFIP-dissolved poly(L-lactide-co-ε-caprolatone) (PLCL) (Inoguchi et al., 2006)) are used. Mixing two polymers within the same solvent is achieved usually with fluorinated alcohols (HFIP or TFE). Such combinations as PCL and gelatin (Jiang et al., 2017), PCL, gelatin and elastin (McClure et al., 2010), PLCL and collagen (He et al., 2005), PLCL and gelatin (Lee et al., 2008a), and poly(D,L-lactide-co-glycolide) (PLGA), collagen and elastin (Stizel et al., 2006) have been used. None of the aforementioned studies matured the scaffold as a tubular vessel further after electrospinning. Therefore, even though the burst strength was tested in some of the studies, the values obtained did not take into account the influence of cells and are therefore they are not discussed here in more detail.

Several studies have taken a step further and cultivated the scaffold with appropriate cells. Boland and his colleagues electrospun a collagen-elastin scaffold and seeded human fibroblasts, SMCs and human umbilical vein endothelial cells (HUVECs) on to it to create different blood vessel layers. A STLV bioreactor was used for cultivation and HFIP for dissolving polymers in electrospinning. Burst pressure was not noted. (Boland et al., 2004) Ju and his colleagues electrospun HFIP-dissolved PCL and type I collagen to achieve a bilayered structure. The inner layer with smaller fiber diameter was inoculated with human aortic endothelial cells (HAEC) and the outer layer with larger fiber

size with human aortic smooth muscle cells (HASMC). The cultivation was carried out statically and burst strength was not mentioned. (Ju et al., 2010) Previously the same group had studied the same polymers as a monolayer and did some scaffold stability tests with a perfusion bioreactor but these were done without cells (Lee et al., 2008b). Duan and colleagues also used HFIP-dissolved PCL and collagen but they used coaxial electrospinning technique with PCL inside and collagen outside of the fiber, and coated the scaffold with heparin. Statically cultivating SMCs on the scaffold showed cell filtration inside the scaffold but the burst pressure was not noted for the cell-scaffold construct. (Duan et al., 2016) Mun and colleagues electrospun HFIP-dissolved PLCL as a sheet, coated it with type I collagen, seeded SMCs on both sides and rolled this sheet into a tubular shape. After statically cultivating the cell-PLCL cylinder for four weeks a burst pressure of 933 ± 22 mmHg was measured. (Mun et al., 2012) Strobel and her colleagues combined electrospun TFE-dissolved PCL-gelatin scaffold sleeves with non-scaffold-grown SMC tissue rings. By statically cultivating these on a silicone mandrel a TEBV was created. Burst pressure was not recorded. (Strobel et al., 2017)

2.4.3 Tissue-engineered blood vessel in the present thesis

The aim of this thesis is to use both collagen and PCL for producing the electrospun scaffold. Collagen gives the seeded cells an ECM-like environment whereas PCL gives the scaffold resilience. This mixed-polymer scaffold has also been popular amongst other previously reported studies. As reviewed earlier, most of the TEBV-producing scaffolds use fluorinated alcohols (HFIP and TFE) in the electrospinning process. However, these solvents have several drawbacks: they are highly toxic, expensive to scale up and degrade collagen into gelatin (Zeugolis et al., 2008). Thus, the aim is to use safer and non-collagen-denaturing solvents, which are referred to as benign solvents in literature. Benign means harmless or gentle, and these solvents include water-based solutions of different salts, alcohols and acids. (Arnoult, 2010)

Acetic acid has been used to dissolve type I collagen either as a 90% solution in distilled water while co-dissolving PCL (Dippold et al., 2017) or as a 93:7 mixture of glacial acetic acid and dimethylsulfoxide (DMSO) (Punnoose, Elamparithi and Kuruvilla, 2015). The first use of ethanol and phosphate-buffered saline (PBS) to dissolve type I collagen in the electrospinning process was in 2009 (Dong et al., 2009). A water-based 1:1 (v/v) mixture of ethanol and 20X PBS (pH 7) was shown to dissolve collagen in room temperature without damaging its triple helical structure while enabling electrospinning. The same group also tested other PBS concentrations (Dong et al. 2009) and other alcohols such as methanol, propanol and butanol (Arnoult, 2010) but the 1:1 ethanol: 20X PBS solvent was proven the most suitable. In addition, other ethanol-to-PBS ratios such as 1.3:1 and 1.5:1 with type I collagen (Bak et al., 2016) and 2:3 and 3:2 with gelatin (Zha et al., 2012) have been tested. 1:1 (v/v) 20X PBS and ethanol solvent is able to dissolve collagen by disrupting the interchain hydrogen bonds although the dissolution mechanism is not fully understood (Fullana, 2015). Ethanol has also been used without PBS as a 50% w/w solution in distilled water. In this case pH was adjusted with 1 M hydrochloric acid to pH 2,30 and an electrospinning temperature of 45°C was applied (Jiang et al., 2013). However, none of the aforementioned studies aimed at production of a TEBV.

Since benign-solvent electrospinning on its own does not generate a tubular cell-scaffold construct, further maturation in a bioreactor must be carried out. In this thesis, a student-assembled RWV bioreactor (HARV) will be used. As has been presented above, most previous studies have mainly employed static conditions to cultivate electrospun-scaffold TEBVs. The only exception being Boland and his colleagues (Boland et al., 2004) who used a STLV bioreactor, which represents a different type of RWV bioreactor (more details may be found in Chapter 2.3.2). Jung and her colleagues (Jung et al., 2015) also used a STLV but they did not use an electrospun scaffold. Instead of TEBVs, RWV bioreactors have mainly been used to cultivate for example stem cells with and without microcarriers (human umbilical cord blood stem cells (CBSC) with Cytodex-3 microcarrier beads (MVB) in a HARV (Chiu et al.,

2005); human mesenchymal stem cells (hMSCs) in a STLV (Saleh et al., 2012); respectively), normal mammalian cells with microcarriers (human osteoblasts (hOSTs) with polycarbonate cell culture inserts in a HARV (Mazzoleni et al., 2011)) and cancer cells with or without cell-spheroid-scaffold (mouse melanoma cells (B16.F10) alone or on human keratinocytes (HaCaT) in a HARV (Marrero et al., 2009)). In addition to RWV bioreactors, TEBVs have been matured in flow bioreactors (Buttafoco, 2005, Jung et al., 2015). Although flow bioreactors provide a blood-vessel-like environment by circulating the medium inside the TEBV lumen, they should be used only after the TEBV has matured some time as the flowing medium causes shear forces that easily tear the vessel wall. Thus as the present thesis focused on the early steps of TEBV production, a flow bioreactor was not used and cell-scaffold constructs were cultivated in a student-built RWV bioreactor. However, similar to the work by Jung and her colleagues (Jung et al., 2015), it is evident that a flow bioreactor can be used in the future as a next step when maturing the produced TEBV.

3. Materials and methods

This chapter is divided into two subchapters for reader's convenience to emphasize especially the electrospinning set-up and the RWV bioreactor. Collagen was the primary natural polymer choice for electrospinning and its use is discussed under Chapter 3.1.1 Collagen and gelatin, where gelatin is introduced as a replacement polymer for collagen. This is followed by the description of the used synthetic polymers under Chapter 3.1.2 Electrospun synthetic polymers. Since the electrospinning set-up and RWV bioreactor were produced and built during this thesis and they are thus among the main outcomes of this thesis, their design, production and building are described in detail in Chapter 3.2 under methods. Different microscopy techniques are also shortly presented.

3.1 Materials

Different electrospun polymers, solvents and the used cell line are described and their choice is justified in this chapter. The electrospinning and cultivation conditions are presented in the following chapter (Chapter 3.2).

3.1.1 Collagen and gelatin

Initially collagen was chosen as the natural polymer for electrospinning since it is the most abundant ECM-polymer within human tissues (see Chapter 2.1.2 for more details). Type I collagen (collagen from calf skin, Bornstein and Traub Type I, Sigma Aldrich) was used and electrospinning was carried out first according to the protocol by Jiang et al. (2012), and then by Dong et al. (2009). Shortly, collagen was dissolved without stirring overnight either in a solution of 50% (v/v) ethanol and ultrapurified water (pH 2,30, adjusted with 1 M HCl) in 45°C to achieve a 15% (w/v) solution or in a 1:1 (v/v) solution of 20X PBS and ethanol at room temperature to achieve 7, 12,5 or 15% (w/v) solutions, respectively. However, both of the protocols led to a gel-like, non-running solution that was not electrospinnable, the reasons for which will be elaborated on in the Results and Discussion (Chapter 5) part of this thesis. Due to the problems encountered with collagen, it was replaced by gelatin, which was

electrospun successfully with the 1:1 (v/v) 20X PBS and ethanol solvent. Gelatin is a collagen-derived protein in which the triple-helical structure has been denaturated into single polypeptide chains. Similar work has also been reported in the literature (Zha et al., 2012, Erencia et al., 2016).

Gelatin (gelatin from porcine skin, Type A, Sigma-Aldrich) was dissolved in 1:1 (v/v) 20X PBS + Etax A solution to achieve the gelatin concentration of 13% (w/v). 20X PBS (phosphate-buffered saline) solution was prepared by weighting 0,20 g of KCl (potassium chloride, 100,1%, VWR International BVBA), 1,15 g of Na_2HPO_4 (*di*-sodium hydrogen phosphate, R. G., buffer substance, ≥99%, Riedel-de Haën), 8,00 g of KH_2PO_4 (potassium dihydrogen phosphate, ≥99,5%, for analysis, Merck KGaA) and 0,20 g of NaCl (sodium chloride, GR for analysis, ≥99,5%, Merck KGaA) on weighting boats and transferred into a 100 ml Schott bottle. 50 ml of ultrapurified water (<0,05 μS/cm, Direct-Q Water Purification System, Merck Millipore) was measured with a measuring glass and poured into the Schott bottle. The solution was shaken and incubated in room temperature until the salts had dissolved. The pH was adjusted from pH 6,66 to 7,31 with 5 M NaOH (sodium hydroxide). 2,60 g of gelatin was weighed (Precisa ES 2200C) into a 50 ml Falcon tube (50 ml Centrifuge Tubes with Printed Graduations and Flat Caps, VWR), 10 ml of 20X PBS was pipetted into the tube after which 10 ml of Etax A (94,0% (w/v), 96,1% (v/v), Altia Oyj) was pipetted to fulfill the total volume of 20 ml. In similar manner, solutions with concentrations of 10% (w/v) and 16% (w/v) were produced by weighing 1,00 and 1,60 g of gelatin into a 50 ml Falcon tube, respectively, and pipetting 5 ml of 20X PBS and 5 ml of Etax A to fulfill the total volume of 10 ml. Gelatin samples were shaken horizontally overnight 100 rpm (Certomat R Shaker) in room temperature before electrospinning. Also, 13% (w/v) samples with solvent ratios of 2:3 (4 ml of 20X PBS and 6 ml of Etax A) and 3:2 (6 ml of 20X PBS and 4 ml of Etax A) were made in a similar manner.

As electrospun gelatin samples easily dissolved in water, they needed to be cross-linked prior cell seeding. Cross-linking was done according to a protocol by Zhang et al. (2006) to achieve scaffolds that would not dissolve during the

lengthy cultivation time. This was achieved by exposing the scaffolds to glutaraldehyde (GTA) vapor. 10 ml of GTA (glutaraldehyde solution, Grade II, 25% in H_2O, Sigma-Aldrich) was pipetted onto a Petri dish, which was placed at the bottom of a desiccator. Gelatin scaffolds with the supporting aluminum foil or grid were placed on the ceramic shelf inside the desiccator, which was then closed. Scaffolds were cross-linked for 0, 24, 48 and 72 hours to compare how the cross-linking would proceed. Zhang et al. 2006 suggested that 3 days would be required to cross-link properly the gelatin scaffolds. (Zhang et al. 2006)

3.1.2 Synthetic polymers

As electrospun gelatin alone does not provide enough durability for growing tissue-engineered blood vessels a synthetic polymer poly-ε-caprolactone (PCL) was chosen to accompany gelatin. PCL (M_n = 80 000 g/mol, Sigma-Aldrich) is a biocompatible, naturally-dissolving, hydrophobic and cheap aliphatic linear polymer, which has been approved by for example the Food and Drug Administration (FDA) (Cipitria et al., 2011). PCL has also been popular among TEBV research (see Chapter 2.4.2) hence it is a good choice for an electrospun scaffold. PCL was electrospun according to a protocol by Bassi et al., 2011, by dissolving it into acetone (acetone Chromasolv for HPLC, ≥99,9%, Sigma-Aldrich) as a 15% (w/v) solution. PCL, 3,00 g, was weighed into a 50 ml Falcon tube and 30 ml of acetone was pipetted into the tube. Dissolving was done at +40°C incubation (Certomat HK Incubator) by shaking the tube horizontally 200 rpm overnight. Solutions with concentrations 5, 10, 12,5 and 17,5% (w/v) were done in a similar manner with the following amounts: 0,50, 1,00, 1,25 and 1,75 g of PCL in 10 ml of acetone, respectively.

Poly(ethylene oxide) (PEO) was chosen as another synthetic polymer of interest since it could be used either as a sacrificial component or as a electrospinning-aiding co-polymer. PEO is water-soluble, and therefore if it is electrospun alongside another polymer, the pore size can be increased by rinsing off PEO after electrospinning (Zander et al., 2013). Moreover, some researchers have used PEO to aid the electrospinning process of some

proteins, for example silk fibroin (Soffer et al., 2008). PEO (M_v = ca. 400 000 g/mol, Sigma-Aldrich) was dissolved overnight in purified water (reverse osmosis (RO) purified water; Elix Essential Water Purification System, Merck Millipore) at room temperature by shaking the tube 200 rpm. PEO, 0,50 g, was weighed in to a 50 ml Falcon tube and 10 ml of purified water was pipetted into the tube after that to achieve the concentration of 5% (w/v). Similarly, 0,30 and 0,70 g of PEO were weighed in order to achieve concentrations of 3 and 7% (w/v), respectively. As electrospun PEO is not naturally durable and it does not occur within the human ECM, there was no need to try to cross-link it nor use it in cell cultivations. However, the electrospinning of PEO is included in this thesis for future purposes as it could be used alongside PCL or gelatin as an aiding pore-size-increasing polymer.

3.1.3 Cell line A549 and cell passaging

Although native human blood vessels contain endothelial cells (ECs), smooth muscle cells (SMCs) and fibroblasts (see more in Chapter 2.1.3), these cells were not used in the experimental part of this thesis. Namely, since the Rotary Wall Vessel (RWV) bioreactor was student-built and it was not certain whether the culturing conditions would be ideal, a more resilient cell line was chosen. ECs, SMCs and fibroblasts do not tolerate fluctuating conditions, which might occur as the development work within the bioreactor was still in its early stages. Hence, A549, which is a human lung carcinoma epithelial cell line, was chosen (Giard et al., 1973). This cell line has been widely used in nanotoxicology tests (Chang et al., 2011) and thus it was considered a good choice for preliminary cell attachment tests on electrospun scaffolds. The A549 cells were kindly provided from the cell collection of the thesis instructor PhD Ari Ora at Aalto University.

Cell thawing, passaging and culturing were done according to guidelines presented in the Gibco Cell Culture Basics Handbook (Gibco, 2015) by the following protocol. Cryopreserved (N_2 tank) cell vial (2 ml, #430659, Corning Incorporation) with 1 ml of cells was placed into a 37°C water bath (Julabo TW20) and thawed until there was almost no ice left. The vial was wiped with

70% ethanol (Desinfektol, Berner Oy) and placed inside a laminar hood (Biowizard SilverLine, Kojair Blue Series Technology). Cells were pipetted (Eppendorf Easypet 3 pipettor with 5 (#4487), 10 (#4488) or 25 ml (#4489) Costar Stripette (Corning Incorporation) serological pipettes) on a 100 mm Petri dish (#430167, Corning Incorporation) after which 9 ml of preheated growth medium was added dropwise. Dulbecco's Modified Eagles Medium (DMEM) with High Glucose (4500 mg/l), L-glutamine (4,00 mM), sodium pyruvate and phenol red (SH30243.01, HyClone, GE Healthcare Life Sciences) was used as a growth medium. It was supplemented with 10% (v/v) Foetal Bovine Serum (FBS, 10270-106, Gibco) and 1% (v/v) Penicillin-streptomycin (10 000 U/ml penicillin and 10 000 µg/ml streptomycin). The cell dish was placed inside an incubator (37°C, 95% O_2 and 5% CO_2, Galaxy 170 R, New Brunswick). After cells had attached the medium was changed and cultivation continued for 3 to 5 days.

Before cells reached confluence, they were passaged. The medium was pipetted off and cells were rinsed once with 10 ml of preheated 1X PBS (Phosphate-buffered saline, 0,0067 M (PO_4) without Ca^{2+} and Mg^{2+}, BE17-516F, BioWhittaker, Lonza). After that 0,5 ml of trypsin-EDTA (0,5% Trypsin/EDTA solution without phenol red, # 15400-054 Gibco) was added and cells were incubated in the laminar hood for 5 to 15 minutes until cells had dissociated. Then 9,5 ml of DMEM medium was pipetted on the dish and cells were suspended by pipetting the solution up and down for five times. This 10 ml of cell suspension contained about 13 million cells. The cells were then ready for cultivation on scaffolds (see Chapters 3.2.1 and 3.2.2). 2 ml of this cell suspension and 8 ml of fresh DMEM medium were pipetted onto a new dish (1:5 dilution), which was then transferred into the incubator as cells were passaged several times during experiments.

3.2 Methods

The self-assembled electrospinning set-up, Rotary Wall Vessel (RWV) bioreactor and different microscopy techniques (light, scanning electron, confocal and widefield) are described in this chapter.

3.2.1 Electrospinning set-up LEVIOSA! and static cultivations

One of the main goals of the thesis was the setting up of the electrospinning of the scaffolds for the TEBV production. This set-up was placed in the same laboratory space with the cell culturing equipment, which proved to be a good choice since different scaffolds were easily and rapidly produced and cultivated in the same compact room. The electrospinning set-up is called LEVIOSA!. The overall set-up and different parts thereof are shown in Figure 6 and 7.

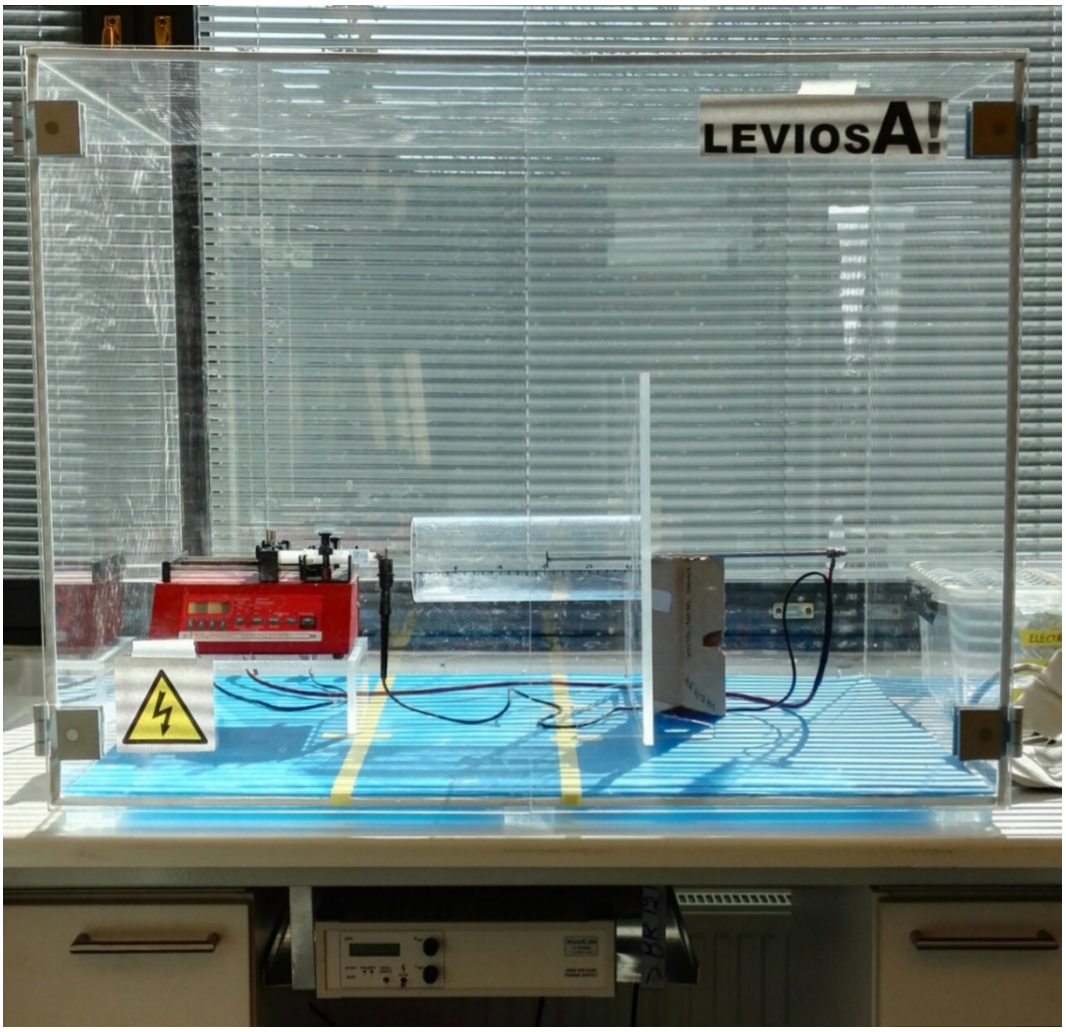

Figure 6. The self-assembled electrospinning set-up LEVIOSA!. LEVIOSA! consists of a polycarbonate cabinet, a syringe pump, a high-voltage source and a polycarbonate collector panel with hollow protective cylinder and a

metallic collector stick. The electrospinning set-up is placed on a normal laboratory bench where it easily operated.

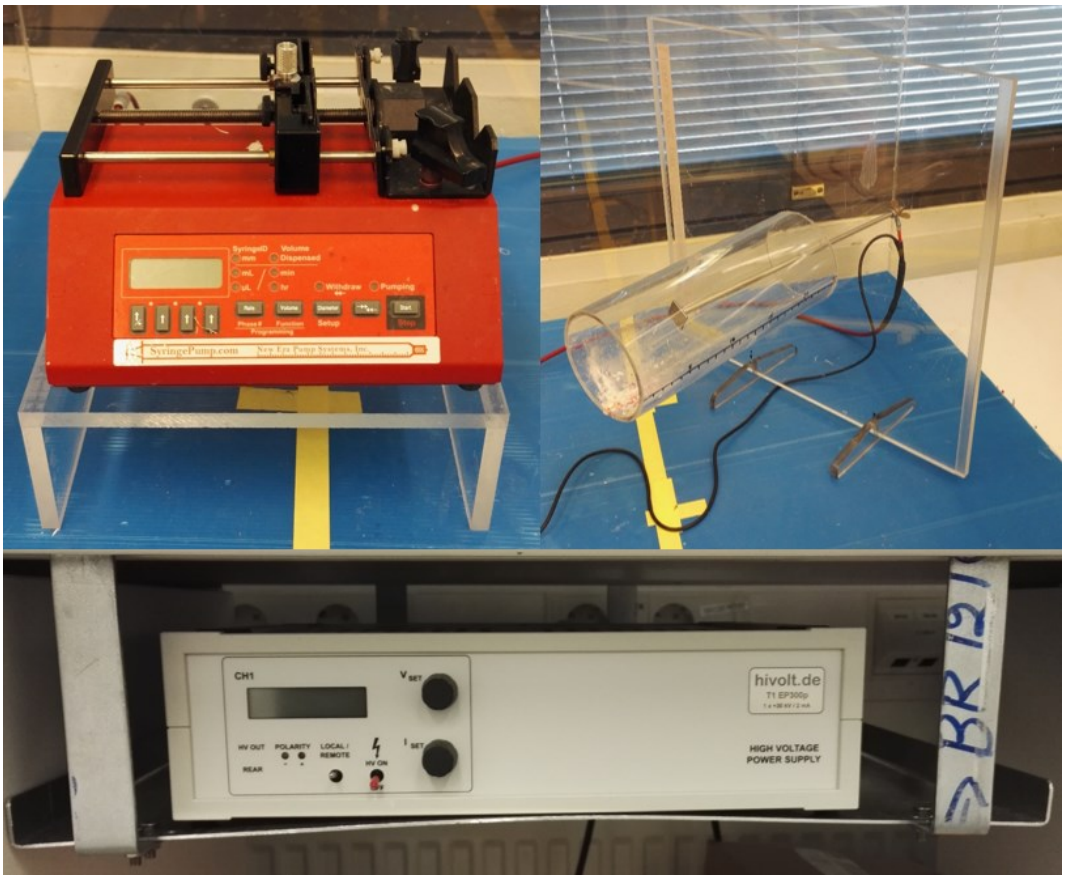

Figure 7. Different parts of the electrospinning set-up LEVIOSA!. The syringe pump on a polycarbonate podium can be seen in the upper left corner, the polycarbonate collector panel with hollow protective cylinder and a metallic collector stick in the upper right corner and the high voltage source on a beneath-bench-top metallic shelf is seen below. Equipment specifications can be found in the main text.

The LEVIOSA! electrospinning set-up consists of the following parts. A high voltage source T1 EP300p (1x 30 kV/ 2 mA, THQ Series, hivolt.de) with in-house-modified shielded HV cable (130660) was used. The main cable was connected to the collector plate's collector stick (positive charge) with a welded metallic loop, and a main-cable-welded side cable (negative charge) was connected to a metallic syringe needle with a crocodile clip. A syringe pump NE-4000 (Programmable 2 Channel Syringe Pump (New Era Pump Systems

Inc.), syringepump.com) was used and it was located on a polycarbonate podium so that the needle tip was on level with the collector stick's end plate. The self-designed collector panel was made out of 1 cm thick polycarbonate. There is a 6 mm hole in the middle of the panel's back board through which a collector stick is thread. Metallic collector sticks are about 35 cm in length, 6 mm in diameter and come in three different end plate versions (Figure 8.). The panel's back board is about 40 x 40 x 1 cm and the hollow protective cylinder is 25 cm in length, 10 cm in diameter and 0,5 cm in thickness. The cylinder prevents air flow from disrupting the electrospinning process although the cabinet itself also gives protection. The cabinet is 90 x 65 x 70 cm (width, depth and height, respectively) and it is also made out of 1 cm thick polycarbonate. Its main purpose is to isolate the high voltage field from surroundings.

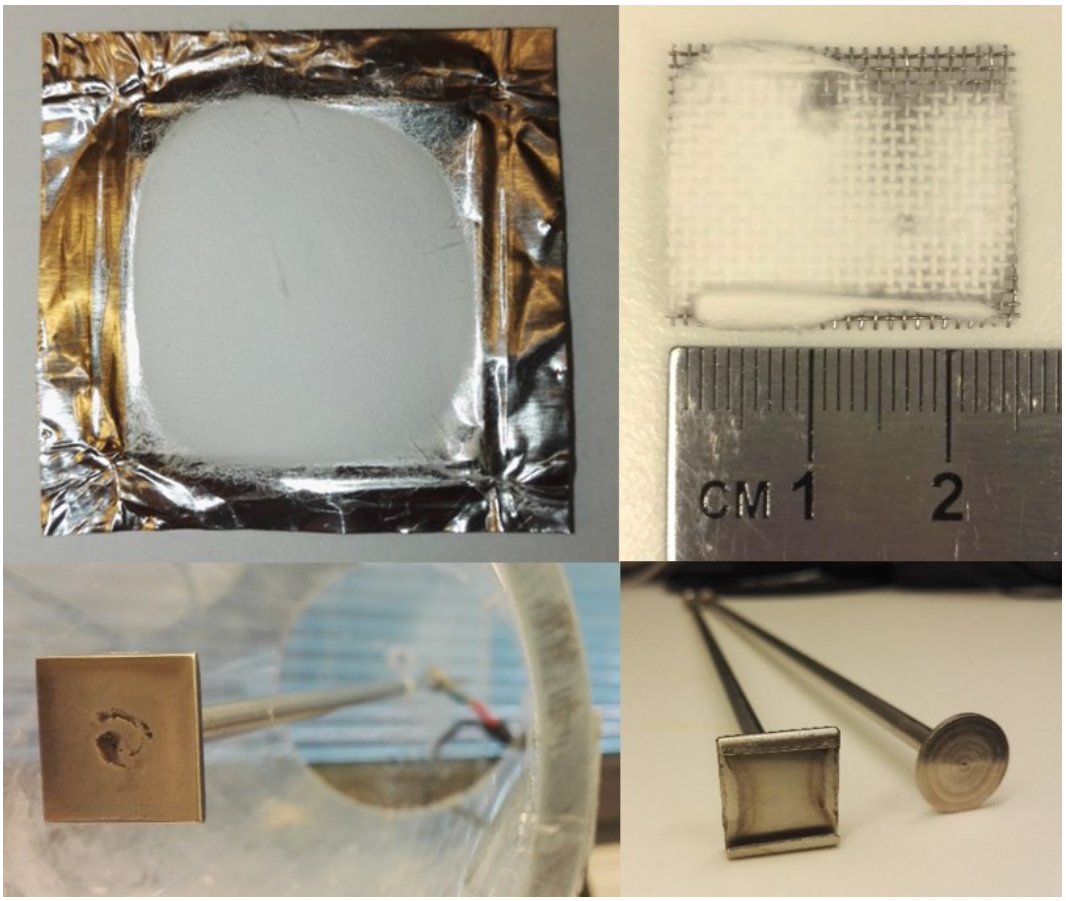

Figure 8. Collecting the electrospun material. Polymers were electrospun either on aluminum foil (up left) or on a metallic grid (up right). Aluminum foil (size about 3 x 3 cm) was wrapped around the collector stick's collector end

plate (size about 2 x 2 cm) before electrospinning and removed afterwards (down left). The stainless steel grid was slid into the collector stick's two-side-grooved collector end plate (down right; the collector stick on left) and removed afterwards. There was also a round collector stick's collector end plate (2 cm in diameter) but it was not used in the present studies.

The theoretical background behind electrospinning technique has been presented in Chapter 2.2 and the practical implementation by using the LEVIOSA! set-up was carried out according to the following protocol. Dissolved polymer solution (see Chapters 3.1.1 and 3.1.2 for more information) was drawn up into the syringe (plastic 10 ml Luer lock syringe, HSW (Thermo Fisher), diameter 15,9 mm) and a stainless steel Luer lock needle was attached to it. The gauge sizes of the available needles (*i.e.* the diameter) were 12, 16, 18, 20 and 25 (2,05, 1,29, 1,02, 0,81 and 0,46 mm, respectively). The amount that was drawn up the syringe depended on the electrospinning conditions but usually 3 - 8 ml was used and this aliquot was used for several consecutive samples. Air bubbles were removed from the syringe by tapping and pressing the plunger, and after that the syringe was attached to the syringe pump. After the appropriate pumping direction and speed (from µl/min to ml/h) had been chosen, the liquid amount inside the syringe and syringe diameter had been selected, and the crocodile clip had been attached to the needle, the syringe pump was ready for electrospinning.

Collector sticks with either a flat square (2 x 2 cm) collector end plate or a two-side-grooved collector end plate were used. Flat end plate was covered with aluminum foil (about 3 x 3 cm, Universal-Alufolie 30, thickness 0,030 mm) and a stainless grid (2,5 x 2 cm, 1 mm thread size, 1 x 1 mm pore size) was used with the grooved end plate. Electrospun material on the grid was used in the cell cultivation tests, and material on aluminum foil was used when determining the electrospinning conditions. After inserting either the aluminum foil or grid on the end plate, the collector stick was threaded through the back panel's hole and an appropriate electrospinning distance was determined with a measuring scale on the hollow protective cylinder (0 - 25 cm). The high voltage

cable's loop was tightened between two nuts at the screw thread end of the collector stick and the collector panel was positioned inside the cabinet so that the syringe needle's tip was centralized at the open end of the protective hollow cylinder. The syringe pump was turned on and the cabinet doors were closed. Once there was a drop of solution at the end of the needle, the high voltage was turned on and adjusted with the potentiometer until the desired voltage was achieved (0 - 30 kV). After a suitable electrospinning time (usually 5 minutes) the high voltage was turned off, cabine doors were opened, the syringe pump turned off and the sample collected by removing the aluminum foil or grid from the collector end plate. Electrospun material was not removed from the supporting foil or grid and these samples were stored on either 100 mm Petri dishes or 6-well plates (Corning Costar 3516, Corning Incorporation) until cultivation tests or microscopy (see Chapter 3.2.3).

Static cell cultivation tests were done directly on the grids, however, gelatin grids were cross-linked (Chapter 3.1.1) prior to cell seeding. PCL and cross-linked gelatin grids were evaporated in a fume hood overnight, UV-sterilized for 30 minutes (see Chapter 3.2.2), washed with 1X PBS for 30 minutes, transferred onto a new 6-well plate and then seeded with 0,135 ml of freshly trypsinized A549 cells (Chapter 3.1.3). DMEM medium, 3 ml, was added to the wells and grids were incubated for 3 days. After three days DMEM was removed and cells were fixed on the scaffolds with paraformaldehyde (see Chapter 3.2.2).

Table 1 presents the most suitable (so called "middle point") electrospinning conditions that were identified as the result of experimentation with polymer-solvent combinations (highlighted in grey in Table 1). The middle point was determined by visually comparing the shape of the Taylor cone and the smoothness and homogeneity of produced material with different parameter combinations. Varying parameters in electrospinning are voltage, distance, pumping speed, gauge size, solution concentration and solvent ratio (with the 1:1 (v/v) 20X PBS and Etax A solvent). Electrospinning time was kept the same with all of the samples (5 minutes) and ambient conditions were not altered

(room temperature and moisture, and the atmospheric gas composition). Also in Table 1 one high and one low limit for each parameter is listed. These were tested while keeping all of the other parameters similar to the middle point. This way the impact of each parameter could be evaluated, for which results are presented in Chapters 4.2, 4.3 and 4.4 (gelatin, PCL and PEO, respectively).

Table 1. Electrospinning conditions for each polymer. Gelatin was electrospun with the 20X PBS and Etax A solvent, PLC with acetone and PEO with purified water. The middle point conditions are highlighted in grey. Screening of the effect that different parameters have on electrospinning was carried out by changing one parameter to a higher or lower value and keeping all of the other parameters the same.

Polymer	Varying parameter	Voltage (kV)	Pumping speed (ml/h)	Distance (cm)	Gauge size	Concentration (% (w/v))	Solvent ratio
	High	20	0,4	20	25	16	3:2
Gelatin	Middle	17	0,3	7,5	20	13	1:1
	Low	15	0,2	5	18	10	2:3
	High	23	4	20	20	17,5	
PCL	Middle	20	3	15	18	15	
	Low	17	2	10	16	12,5*	
	High	27	0,7	20	20	7	
PEO	Middle	25	0,5	17,5	18	5	
	Low	23	0,3	15	16	3	

* = PCL was also electrospun with concentrations of 5 and 10% (w/v).

3.2.2 Rotary Wall Vessel bioreactor BIOHOVER and bioreactor cultivations

A Rotary Wall Vessel (RWV) bioreactor was built as a part of the Biology Meets Mechatronics (BIOMEETSMEX) project collaboration between Aalto University's School of Chemical Engineering (CHEM) and School Engineering (ENG). Namely, the BIOMEETSMEX project aims at developing of joint student activities between biotechnology and mechatronics students. At the time of the present thesis work, the School of Chemical Engineering M.Sc. program course CHEM-E3225 Cell and Tissue Engineering was used to implement this collaboration as a pilot between student groups from the School of Chemical Engineering (biotechnology) and the School of Engineering (mechatronics). The RWV bioreactor was used in the course for the first time simultaneous to the development work in the present thesis. After the completion of the CHEM-E3225 course in the spring of 2017, the RWV bioreactor was further tested and used for the purposes of the present thesis work. The theoretical background of RWV bioreactors has been presented in Chapter 2.3.2.

During the CHEM-E3225 course the RWV bioreactor was built and designed by students of the Aalto University School of Engineering (mechatronics), namely B.Sc. (Tech.) Catarina Brites, B.Sc. (Tech.) Jesse Isokangas, B.Sc. (Tech.) Tomi Kankaanoja and B.Sc. (Tech.) Ville Majuri. The mechanical design of the bioreactor was supervised by D. Sc. (Tech.) Panu Kiviluoma at Aalto University, and the usability and biological research suitability were commented by the author of this thesis, PhD Ari Ora and the CHEM-E3225 Cell and Tissue Engineering course participants. The RWV bioreactor was named as BIOHOVER (Figure 9).

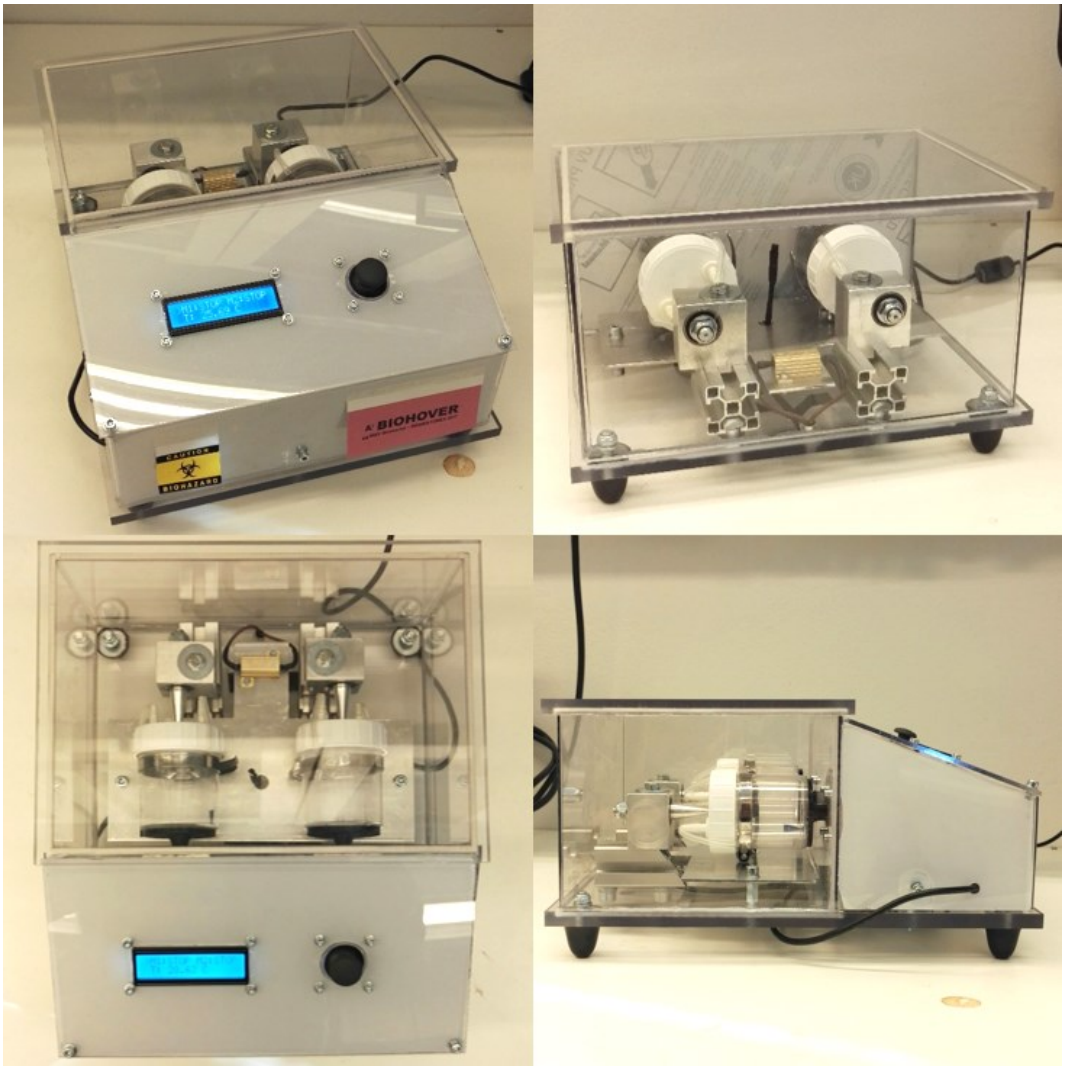

Figure 9. The BIOHOVER RWV bioreactor. BIOHOVER from the front (upper left corner), behind (upper right corner), above (lower left corner) and left side (lower right corner). The main components seen above are the LED display and the control joystick on the cover plate of the bioreactor, the transparent cultivation chamber and the two cultivation vessels (horizontally attached white-lid jars) inside the transparent chamber.

BIOHOVER consists of the operating module and the cell cultivation chamber. Two stepper motors inside the operating module are controlled by an Arduino Uno microcontroller, which also allows the control of temperature inside the cultivation chamber via a DS18B20 digital temperature sensor and a 25-watt heating element. The user may change the rotation speed (0 - 60 rpm) and turn on or off the heating by operating the microcontroller via the control

joystick on the cover plate. The cover plate's LED display shows the rotation speed for both of the stepper motors, which may be operated separately, as can also the temperature inside the cultivation chamber. When the temperature control is turned on, Arduino Uno automatically turns on heating when the temperature drops below 36,9°C and off above 37,1°C. Heat is dispersed evenly throughout the chamber by a thin aluminum plate, which is physically connected to the heating element. The polycarbonate walls and lid of the cultivation chamber keep the heat inside. A 3-D-printed poly(lactic acid) (PLA) flange is attached to the shafts of stepper motors. These shafts rotate and hold in place the cultivation vessels. The horizontal placement and attachment of the cultivation vessels is secured by tightening a slider-attached turned steel tailstock with ball bearing in the middle of the cultivation vessel's lid (specifically the round dent, which has been caused by the injection moulding of the lid (Figure 10)).

The cultivation vessel and an inner supportive structure for scaffolds are presented more closely in Figure 10. The transparent cultivation vessel is made out of polypropylene (PP) and it has a working volume of 100 ml and total volume of about 110 ml without air space. The white lid is made out of polyethylene (PE) and it has two injection valves (halved Fisherbrand PP tubing connectors, S50700B, Fisher Scientific) glued onto it (All Plastics Super Glue, Loctite). About 8 cm of silicone tubing (Silicone hose TRP, diameter 2 mm, wall thickness 1 mm, 10320004604, Etra Oy) was attached to each of the injection valves alongside a 10 ml syringe (Omnifix Luer Solo 10 ml syringe, 4616103V, B. Braun) in order to remove all of the air space from the vessel. The cultivation vessel was filled with medium (about 90 ml), syringes were also filled (about 8 ml) and then attached to the silicone tubes. By pressing the plunger of one of syringes while pulling the plunger of another one and repeating this several times all of the air was removed from the vessel. However, there were some problems, as the jar leaked when it was filled. The working ends of the silicone tubes were covered with 70%-ethanol-wiped Parafilm (Parafilm M, Bemis Company, Inc.) and closed by tightening the metallic choker around the vessel (see Figure 10). All of the parts within the

cultivation vessel were UV-sterilized (Puritech HNS 30W G13 germicidal ultraviolet lamp, dominant wavelength 254 nm, Osram GmbH) before use inside the laminar hood. Distance between the UV lamp and sterilized parts was about 40 cm and sterilization time at minimum 30 minutes although usually this was done either for longer time (up to 60 minutes) or several separate times as the UV light of the laminar hood was turned on automatically every night for 30 minutes.

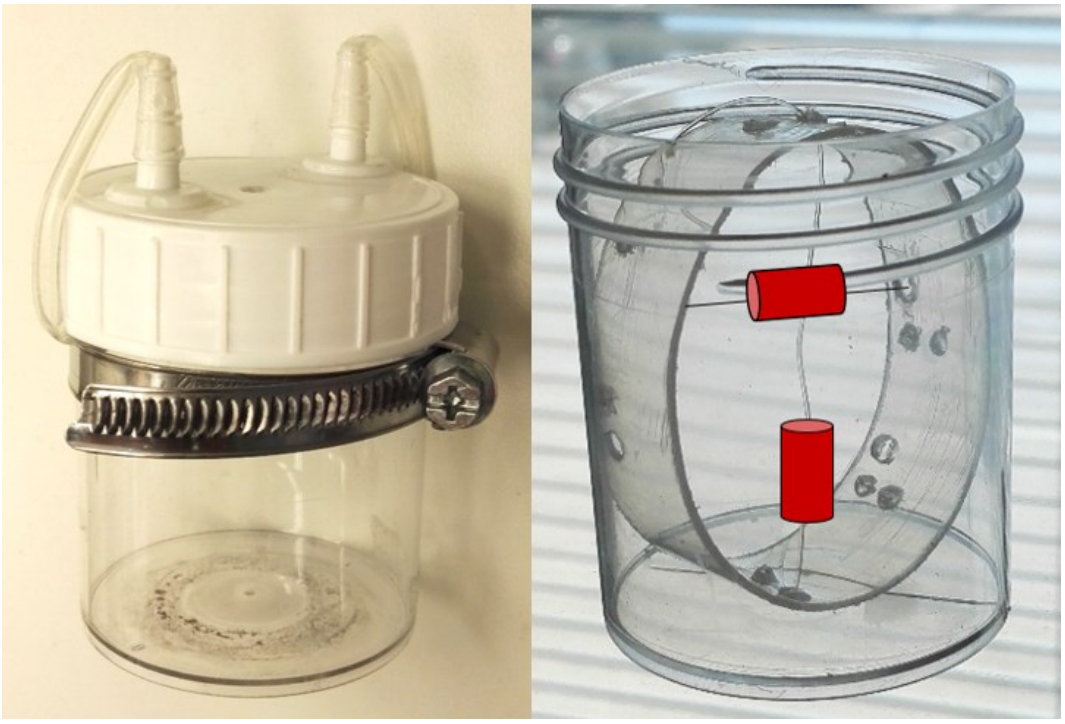

Figure 10. Cultivation vessel for the BIOHOVER bioreactor. Fully assembled cultivation vessel without inner structure on the left. Silicone tubes have been attached to the injection valves and closed with the metallic choker. Inner supportive structure inside a cultivation jar is presented on the right. It is made by cutting off a middle section of another cultivation vessel and drilling holes to it. By tying a transparent nylon thread (elastic nylon thread for jewelry, 0,5 mm) through the holes and stringing the tubular scaffold (red cylinders in the image) to the nylon thread, floating scaffolds were anchored in middle of the medium. Threads were bound so that the scaffold could be either in horizontal or vertical position in contrast to the horizontal axis of the bioreactor-attached cultivation vessel.

The cell-scaffold constructs were cultivated inside the vessels either with or without the inner supportive structure. Theoretically, cells or cell-scaffold constructs should stay approximately in the middle of the medium in the RWV bioreactor when it rotates. However, during the CHEM-E3225 Cell and Tissue Engineering course it was discovered that especially scaffolds made out of PCL tended to float because PCL is hydrophobic. Thus, experiments were also done with the inner supportive structure (Figure 10). It was made by cutting off a middle section of another cultivation vessel and drilling holes to it. When nylon threads were tied to the holes, scaffolds could be attached to them and floating prevented. The horizontal and vertical alignments of anchored scaffolds are presented in Figure 10.

Tubular gelatin and PCL scaffolds were electrospun according to the middle point conditions presented in Table 1. Three gelatin samples (2 x 2 cm) were electrospun and they were wrapped around an aluminum-foil-covered glass rod (diameter = 6 mm) to form one tubular scaffold (length = 2 cm). The glass rod was removed and tubular gelatin scaffolds were cross-linked for three days as described in Chapter 3.1.1. PCL was electrospun at a larger scale on a piece of aluminum to form a sheet of some 3 x 4 cm. This was then wrapped around an aluminum-foil-covered glass rod. The glass rod was then removed. After cross-linking the gelatin samples, all of the scaffolds were left in the fume hood overnight so that the remnants of the solvents would evaporate. Then they were UV sterilized in the laminar hood as described previously, moved to a 6-well plate, rinsed three times with 3 ml of 1X PBS for 5 minutes and stored in 1X PBS until use.

Bioreactor cultivations were performed in two vessels simultaneously. One vessel had the inner supportive structure so that one PCL and one gelatin scaffold was attached to the nylon thread, which was in alignment with the vessel's horizontal axis – one PCL and one gelatin scaffold was attached perpendicularly to the vertical threads. The other vessel did not have the inner supportive structure and two PCL and two gelatin scaffolds were allowed to move freely inside the vessel. Both of the vessels were filled as described previously and inoculated with 2 ml of freshly trypsinized A549 cells

(approximately 2,6 million cells, see Chapter 3.1.3 for trypsination details). However, both of the vessels leaked and not all of the air bubbles were successfully removed. Vessels were sealed with duct tape (Duct Tape Pro Strength 1210-A, Scotch) and cultivated for three days. Unfortunately, the stepper motor that was intended to rotate the supportive-structure-containing vessel broke down after 30 minutes, however, the cultivation was continued although the vessel rotated irregularly <30 rpm. The other vessel was rotated at 30 rpm without interruptions although none of the scaffolds continued to float as they were supposed to. The temperature inside the cultivation chamber fluctuated from 37 to 39°C during the cultivation. After three days, the scaffolds were removed from the vessels and inserted onto 6-well plates so that paraformaldehyde fixing could be done.

After both static and bioreactor cultivations cell-scaffold constructs were fixed according to the following protocol. Paraformaldehyde (PFA, 95%, 158127, Sigma-Aldrich) was diluted in 1X PBS to reach a 4% (w/v) solution. 3 ml of this PFA solution was pipetted into the 6-well plate wells, which contained statically cultivated scaffolds on grids or halved tubular scaffolds from the bioreactor cultivation. PFA was removed after 30 minutes and the samples were rinsed three times with 1X PBS. The fixed samples were left in 1X PBS and 6-well plates were stored in a refrigerator until phalloidin dyeing (see Chapter 3.2.3).

3.2.3 Optical, scanning electron and fluorescence microscopy

The majority of the results in the present thesis have been gathered based on visual assessment. Different microscopy techniques were used in order to determine for example how well the electrospinning succeeded or whether cells actually attached to and proliferated within the scaffolds. By microscopy with optical, scanning electron and fluorescence microscopes (confocal and widefield) information on different orders of magnitude was gained.

Leica DM IL LED Fluo (Leica Microsystems Ltd.) optical microscope with Hi Plan I Objectives (10X/0,25, 20X/0,30 and 40X/0,50) was used check cultivations and electrospun threads. The light optical microscope is a device that uses visible light and a set of focusing lenses to reveal microscopic details

such as mammalian cells or bacteria as visible light passes through the sample. Although optical microscopying of electrospun samples did not give highly focused images, the optical microscope was discovered to be a quick and easy method to determine whether electrospun samples contained unified fibers or not. When comparing these images to the electron microscope images (see Results) it was evident that optical microscopy actually gives a good estimation on the fiber quality of an electrospun sample. DF C3000 G (Leica Microsystems Ltd.) camera and LAS V4.5 program were utilized to capture images with maximal light and standard settings, and without further image enhancements. In addition to electrospun samples, also cell passaging and the medium of bioreactor cultivations were checked with the light microscope to determine if any visually identifiable contaminants were present. A size bar for the optical microscope images was determined with the 10X objective by measuring the length between two bars denoting 0,1 mm in a ruler and then scaling this size bar to images taken with 20X and 40X objectives. The actual magnification in the optical microscope images is 100X, 200X and 400X with 10X, 20X and 40X objectives, respectively.

Scanning electron microscope (SEM) uses a focused beam of electrons that reflects from the sample surface to produce a image (Carlton, 2011). SEM was used to scrutinize the electrospun samples and determine how different electrospinning parameters affect the resulting fibers. All the scanning electron microscopy was carried out in the Aalto University Nanomicroscopy Center (Aalto-NMC) premises. Leica EM ACE600 sputtering device was used to coat all of the samples with gold-palladium (Au-Pd). Sputtering was done without removing the aluminum foil and using carbon tape to attach the samples on sample stubs. The following sputtering conditions were used: 30 mA current, 0° tilt, 5,0 x 10^{-2} mbar pressure, coating thickness of 4,0 nm and sample height of 3 mm. The sputtering cycle lasted for about 9 minutes. Zeiss Sigma VP electron microscope with Schottky FEG emitter and in-column secondary electron (SE) detector was used to observe the coated electrospun samples. Acceleration voltage from 1,5 to 2,0 kV, brightness of 49,1%, contrast of 36,0%, linear average (LineAvg) noise reduction with a N-value of 50, tilt of 0°

and scanning speed of 4 were used during microscopy. SEM images with magnification from 100X to 10 000X were acquired.

Laser scanning confocal microscopy (LSCM, also known as confocal microscopy) is a technique that utilizes fluorescent materials or fluorophore staining and certain wavelengths to produce an image. With the help of pinholes that exclude stray light, an image with high resolution and contrast may be acquired. (Carlton, 2011) The confocal microscope was used to determine whether A549 cells actually attached to the scaffold material or not. As A549 cells are not fluorescent in nature, staining was done by using the following protocol.

1X PBS was removed and PFA-fixed cell-scaffold constructs were immersed in 3 ml of 0,1% Triton X-100 in 1X PBS (Triton X-100 BioXtra, Sigma-Aldrich) to make the cell membranes more permeable. The solution was removed after 20 minutes and the samples were washed three times with 3 ml of 1X PBS for 5 minutes. Then cells were stained with 1:400 phalloidin solution, which contained 0,25% of Alexa Fluor 568 (A12380, Invitrogen Molecular Probes) phalloidin, 5% of Foetal Bovine Serum (FBS), 0,1% of saponin (47036, Sigma-Aldrich) and the rest 1X PBS. 300 μl of this phalloidin solution was pipetted as a droplet on a clean sheet of Parafilm, which was inside a self-made wet chamber (water-soaked tissue paper inside a plastic box). Cell-scaffold construct either with or without grid were flipped cultivation side downwards and inserted on a staining droplet. The wet chamber's lid was closed, aluminum foil was wrapped around the chamber and samples were incubated at room temperature inside a laminar hood for 60 minutes. After staining samples were flipped and transferred back to 6-well plates. They were then washed three times with 3 ml of 1X PBS for 5 minutes. Samples on grids were detached from the grids. All of the samples were transferred on glass microscope slides and mounted with ProLong Gold Antifade Reagent (P36934, Invitrogen Molecular Probes) with cover slips.

After the mounting reagent had dried, the aim was to examine the samples with a confocal microscope at the School of Chemical Engineering at Aalto

University. However, initial tests showed that the scaffold material gave a great amount of autofluorescence and no cells were visible. In addition, the samples were thick and hence difficult to microscope. Thus, the mounted samples were also examined with Invitrogen EVOS FL Auto Cell Imaging System (Thermo Fisher Scientific) at the premises of Biomedicum Imaging Unit (BIU) at the University of Helsinki. DIBImage 1.0.0 program, objectives PlanFluor 4X, 10X, 20X and 40X, and light cubes RFP (excitation 531/44 nm, emission 593/40 nm) and TxRed (excitation 585/29 nm, emission 624/40 nm) with fluorescence filters were used. EVOS FL Auto Cell Imaging System is a widefield microscope (WFM) in which entire fluorescent samples may be viewed whereas a confocal microscope shows a section out of the sample. However, also WFM showed a great amount of autofluorescence, which is discussed in more detail in the Results section below.

4. Results

In the following, the results for the electrospun polymers (collagen, gelatin, PCL and PEO) are presented followed by data for experiments with cell cultivation. The results are elaborated on in the Discussion (Chapter 5).

4.1 Electrospun collagen

Type I collagen was used and electrospinning was first carried out according to the protocol by Jiang et al. (2012), and then by Dong et al. (2009). However, both of the protocols led to a gel-like, non-running solution that was not electrospinnable. According to the Jiang et al. (2012) protocol, electrospinning should be carried out at elevated temperature (45°C), however, in the present study this was not possible with the current equipment. The Dong et al. (2009) protocol was followed precisely according to instructions, the only difference being the collagen itself. Dong et al. (2009) used semed S, acid-soluble collagen from Kensey Nash Corporation. However, according to a Ph.D. dissertation by Matthew Fullana (2015) the semed S collagen differs from the Sigma-Aldrich collagen that was used in the present thesis due to the extraction procedure. The Sigma-Aldrich collagen has been extracted from calf skin by acidic treatment (pH 3,70 citrate buffer, protocol by Gallop and Seifter, 1963) and it has the chemical structure of tropocollagen, the native triple-helical collagen chain, which is able to form collagen fibrils. Semed S, however, has been extracted from the tissue with proteases such as pepsin, proctase, trypsin or pronase. These enzymes cleave non-helical telopeptide regions from the chain ends of tropocollagens and produce so called atelocollagen chains (*atelo-* prefix means incomplete). As telopeptides allow tropocollagen chains to form intermolecular cross-links and thus collagen fibrils, the enzymatically extracted collagen is more soluble as it lacks these cross-linking regions. (Fullana, 2015, Gallop and Steifter, 1963, Riemschneider and Abedin, 1979) Semed S collagen by Kensey Nash has been widely used within electrospinning studies that utilize benign solvents (Dong et al., 2009, Jiang et al., 2012, Arnoult, 2010, Fullana, 2015). Also pepsin-extracted collagen by self-extracting (Bak et al., 2016) or by Symatese

(Dippold et al., 2017) has been used with the 1:1 (v/v) 20X PBS and ethanol solvent. One option would have been to use enzymatically extracted collagen in the present thesis, however, due to delivery problems within the timeframe of the work, it was not tested.

Although the electrospinning of collagen with the 1:1 (v/v) 20X PBS and Etax A solvent did not succeed (see Chapter 3.1.1) the little material that was accumulated on the collector plate's aluminum foil was examined with SEM. No visible fibers were produced (Figure 11) and by using a higher magnification of 3000X, the accumulation of crystalized salts without electrospun collagen fibers could be seen (Figure 12).

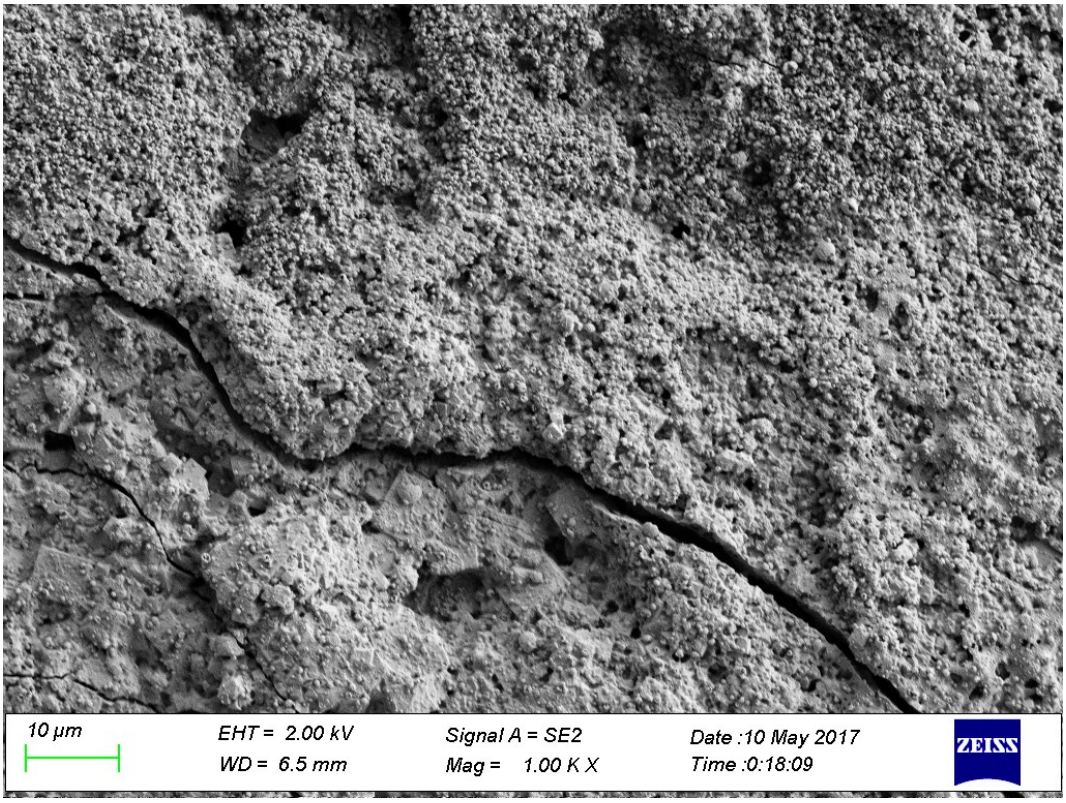

Figure 11. Electrospinning of 15% (w/v) collagen with 1:1 (v/v) 20X PBS and Etax A solvent. The experiment did not produce any visible fibers as can be seen from this SEM image with a 1000X magnification.

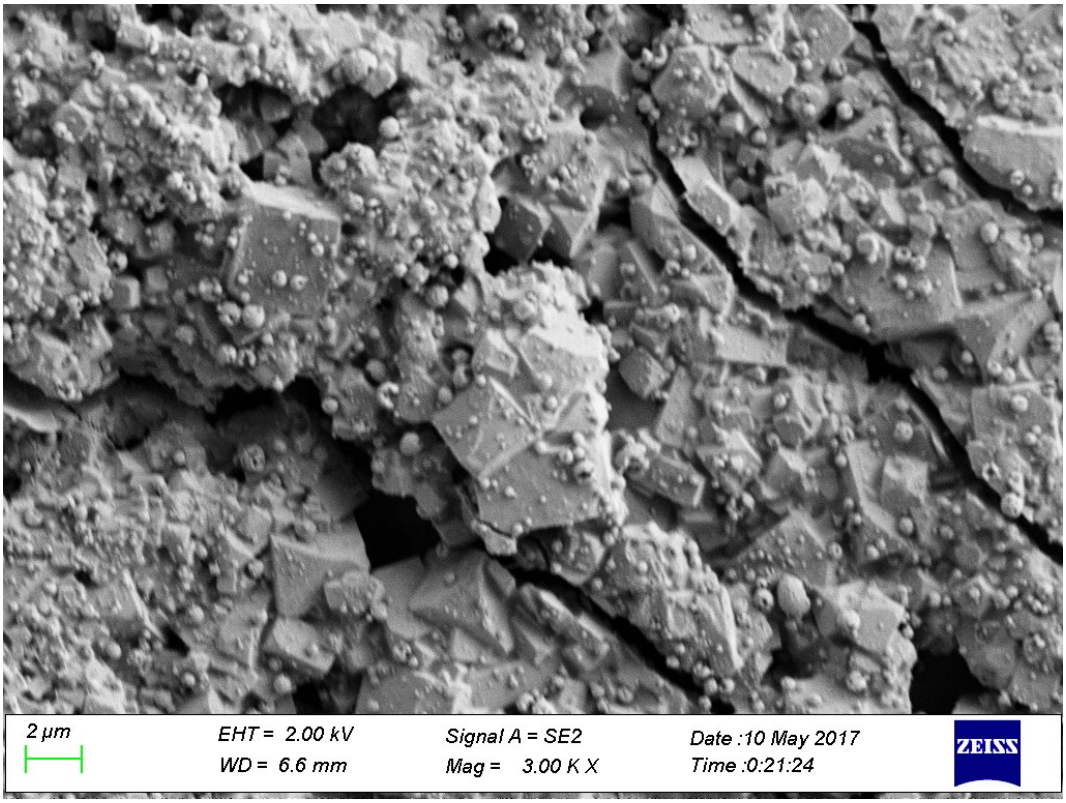

Figure 12. The accumulation of crystallized salts. Electrospun collagen fibers were not present as can be seen from this SEM image with a 3000X magnification.

4.2 Electrospun and cross-linked gelatin

Gelatin was successfully electrospun with 1:1 (v/v) 20X PBS and Etax A solvent. Table 1 on page 39 shows the optimal electrospinning conditions determined for gelatin and the varied electrospinning parameters. Gelatin was examined with an optical microscope and scanning electron microscope (SEM). Figures 13 and 14 show these results for the optimal middle point conditions with optical microscope and SEM, respectively. By varying just one of the electrospinning parameters at a time, drastic changes within the electrospun material were noticed as can be seen in Figure 15 (SEM). Appendix 1 shows a similar comparing figure with optical microscope images. Figure 16 shows a characteristic salt crystal deposition along electrospun gelatin fibers, which is caused by the high non-evaporating salt concentration in the solvent.

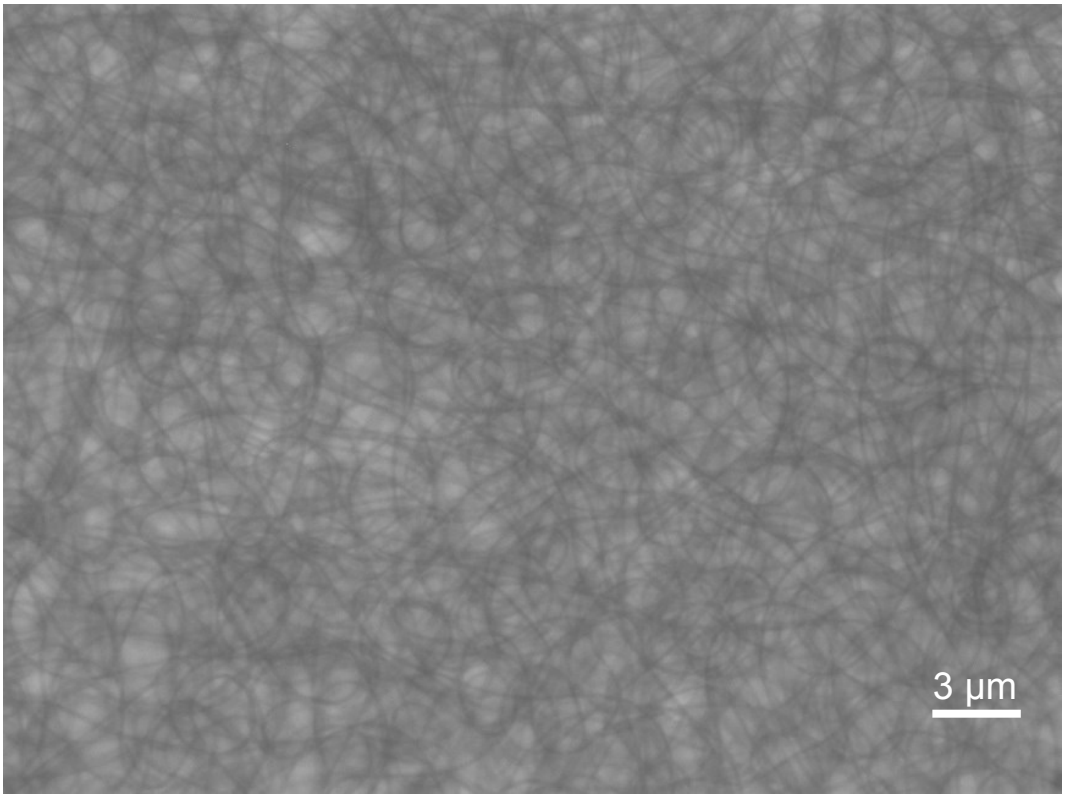

Figure 13. An optical microscope image of electrospun gelatin with 400X magnification. The gelatin was dissolved in 20X PBS and Etax A solvent and electrospun with the optimal middle point electrospinning conditions (voltage 17 kV, pumping speed 0,3 ml/h, collector distance 7,5 cm, gauge size 20, gelatin concentration 13% (w/v) and solvent ratio of 1:1 (v/v)). The sample was electrospun for 5 minutes at room temperature and moisture under atmospheric gas composition.

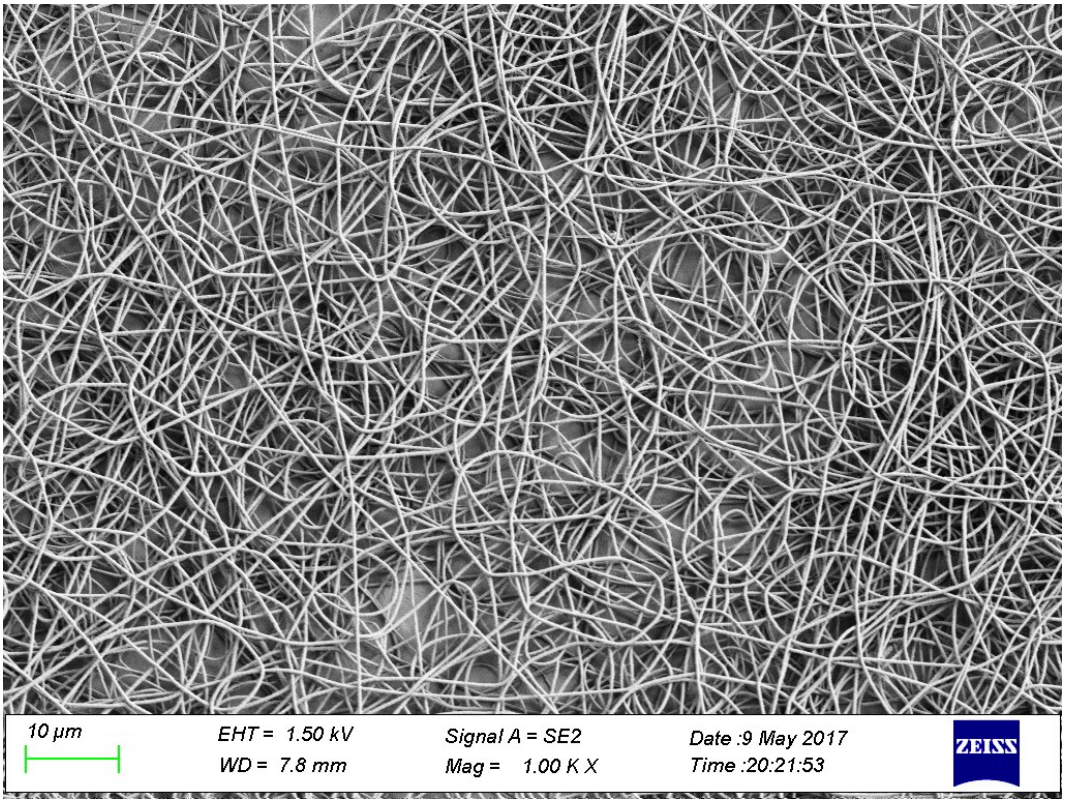

Figure 14. A scanning electron microscope (SEM) image of electrospun gelatin with 1000X magnification. The gelatin was dissolved in 20X PBS and Etax A solvent and electrospun with the optimal middle point electrospinning conditions (voltage 17 kV, pumping speed 0,3 ml/h, collector distance 7,5 cm, gauge size 20, gelatin concentration 13% (w/v) and solvent ratio of 1:1 (v/v)). The sample was electrospun for 5 minutes at room temperature and moisture under atmospheric gas composition.

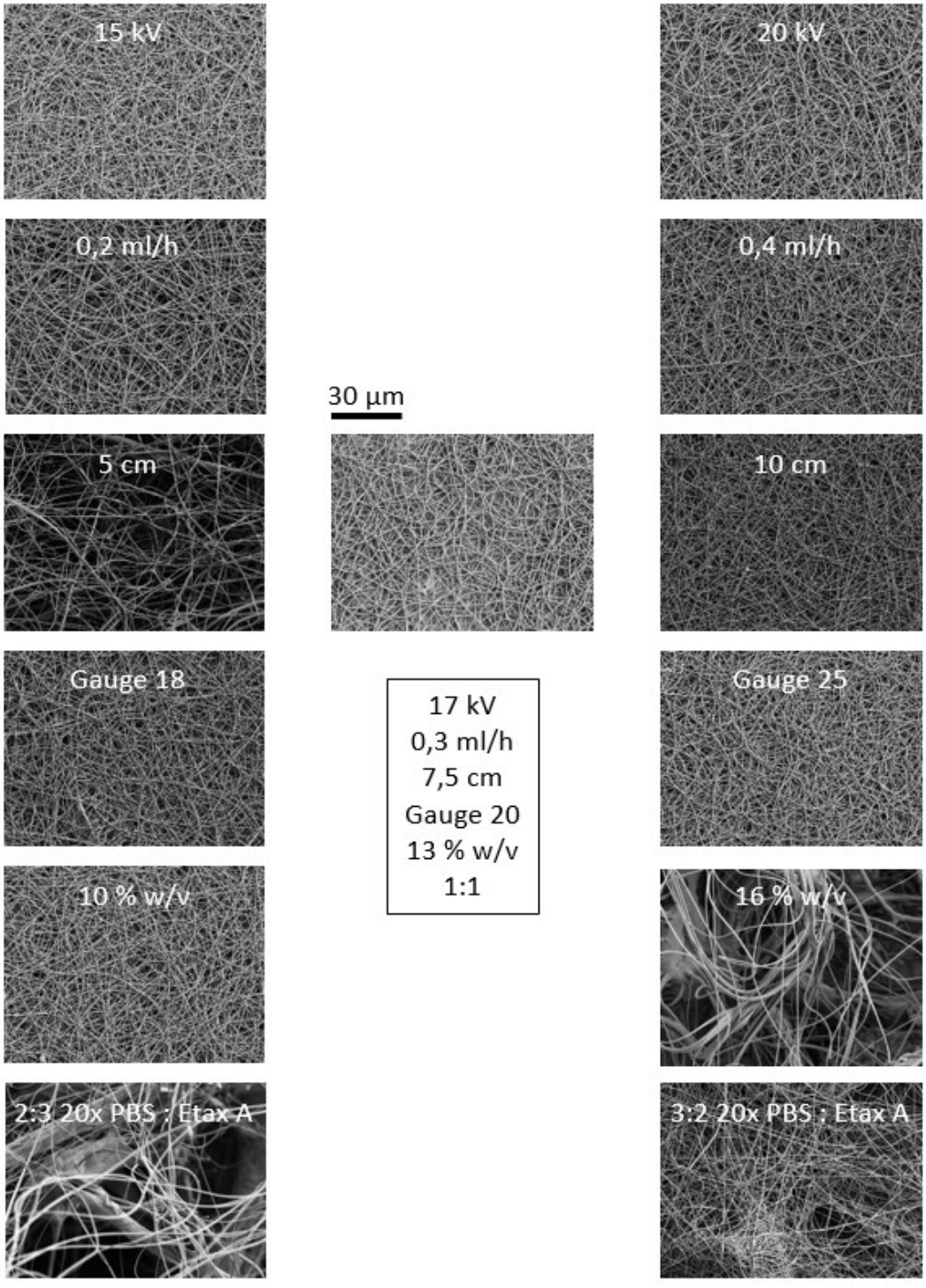

Figure 15. The effect of specific parameters on the electrospinning of gelatin. By varying one of the electrospinning parameters (voltage, pumping speed, distance, gauge size, concentration and solvent ratio) and keeping other parameters the same as in the middle point electrospinning (1000X SEM image and parameters presented in the middle) the effect of a specific

parameter could be observed in the electrospinning of gelatin. All of the images were taken with SEM with 1000X magnification as described in Chapter 3.2.3.

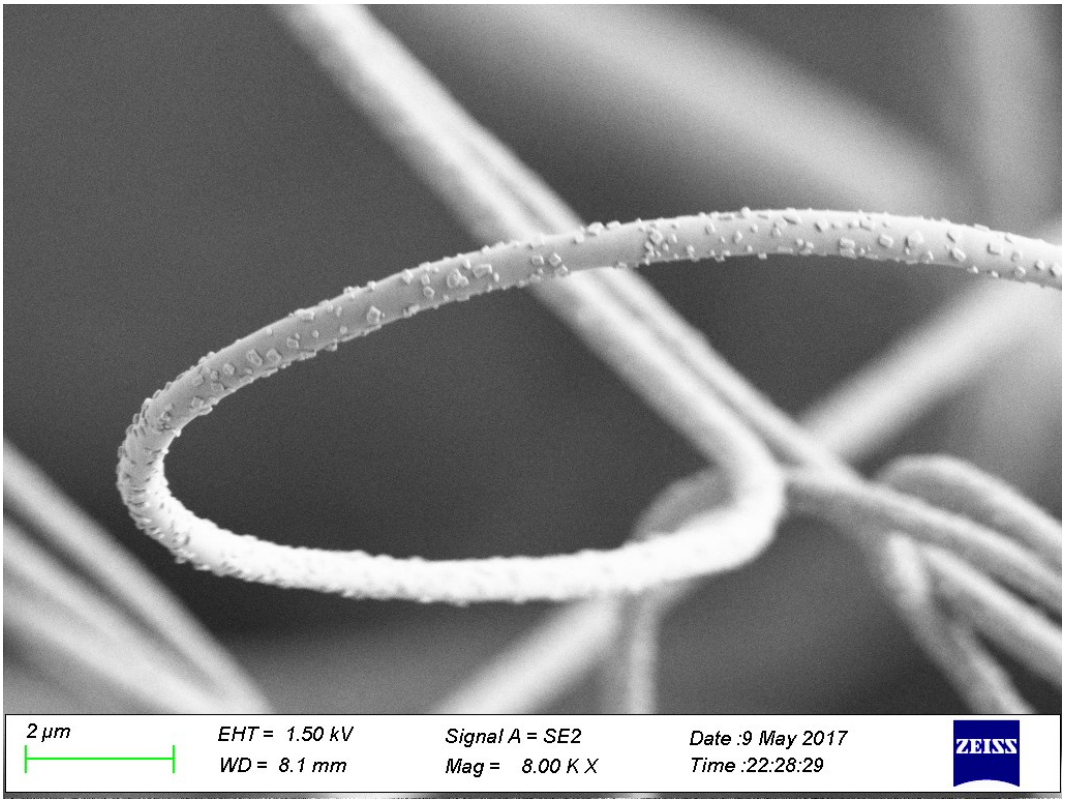

Figure 16. A scanning electron microscope (SEM) image of electrospun gelatin with 8000X magnification. The gelatin was dissolved in 1:1 (v/v) 20X PBS and Etax A solvent and electrospun with the following electrospinning conditions: voltage 17 kV, pumping speed 0,3 ml/h, collector distance 7,5 cm, gauge size 20 and gelatin concentration 16% (w/v). These electrospinning conditions differ from the optimal middle point conditions with regards to the increased concentration. However, these conditions were chosen as it was easier to obtain a clear high-resolution image out of a sample with sparse fiber distribution. Salt crystals caused by the 20X PBS are clearly visible along the fiber. These salt crystals were visible along all of the gelatin samples that were dissolved in the 1:1 (v/v) 20X PBS and Etax A solvent.

Cross-linked gelatin samples were also examined with the optical microscope and SEM. 1:1 (v/v) 20X PBS and Etax A dissolved 13% (w/v) gelatin was electrospun with the optimal middle conditions and cross-linked with glutaraldehyde (GTA) vapor for 72 hours as described in Chapter 3.1.1. Optical

microscope and SEM images are presented in Figures 17 and 18, respectively. Gelatin samples were cross-linked for either 24, 48 or 72 hours and the effect of cross-linking time on electrospun gelatin fibers is presented in Figure 19. A similar comparative figure may be found in Appendix 2.

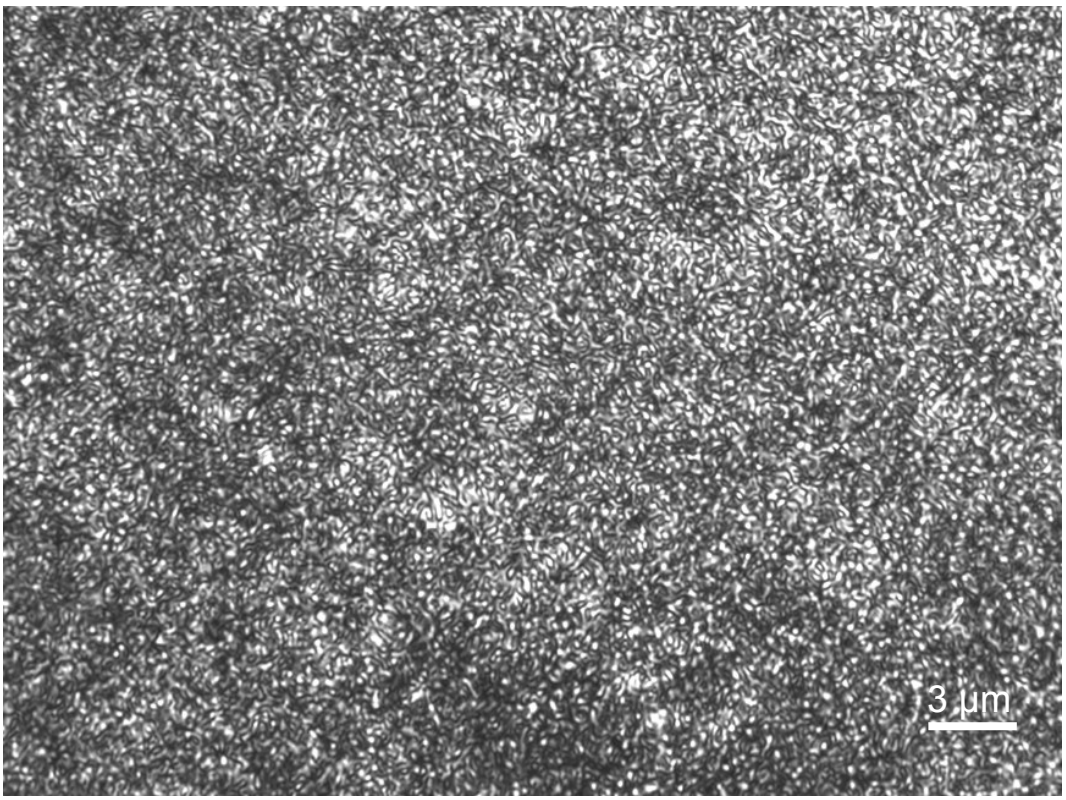

Figure 17. An optical microscope image of 13% (w/v) gelatin with 400X magnification. The gelatin was dissolved in 1:1 (v/v) 20X PBS and Etax A solvent, electrospun with the optimal middle point electrospinning conditions and cross-linked with glutaraldehyde (GTA) vapor for 72 hours.

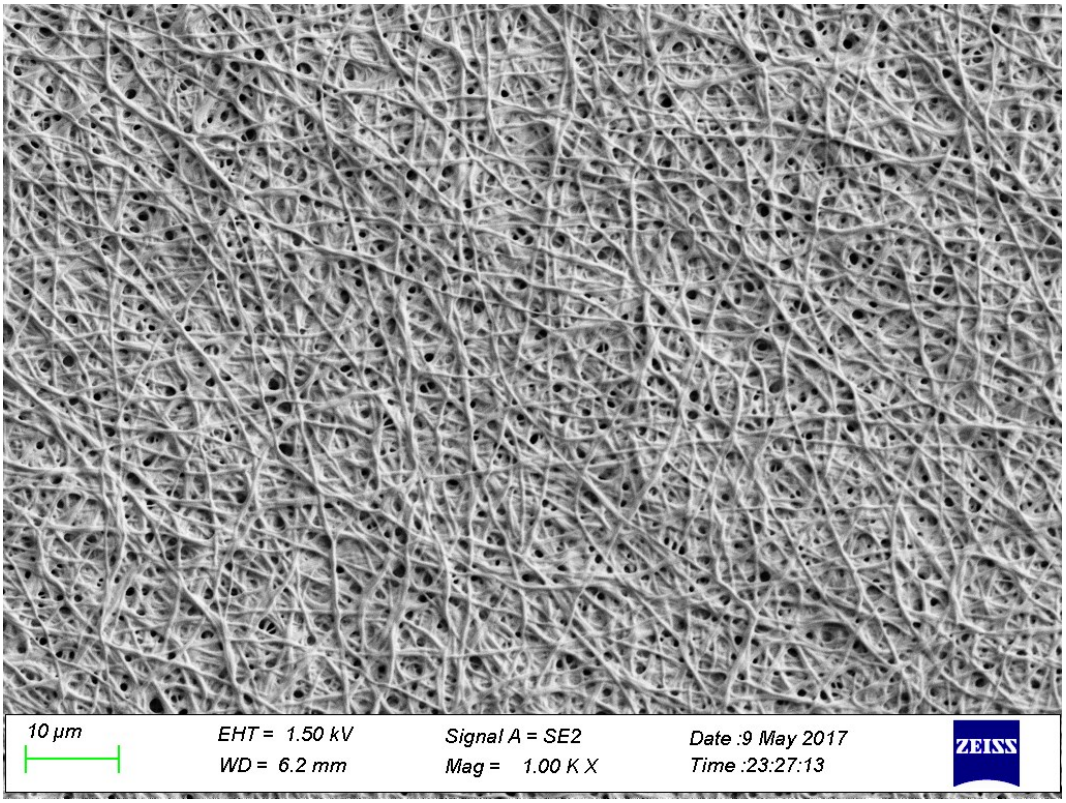

Figure 18. A scanning electron microscope (SEM) image of 13% (w/v) gelatin with 1000X magnification. The gelatin was dissolved in 1:1 (v/v) 20X PBS and Etax A solvent, electrospun with the optimal middle point electrospinning conditions and cross-linked with glutaraldehyde (GTA) vapor for 72 hours.

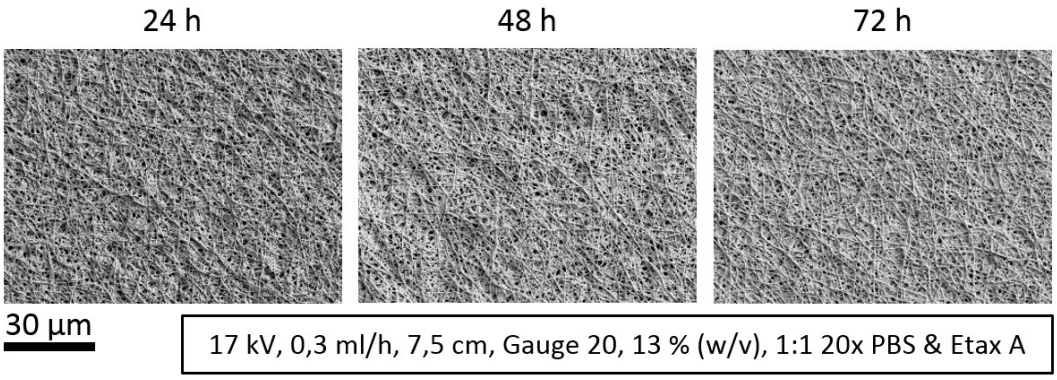

Figure 19. Scanning electron microscope (SEM) images of 13% (w/v) gelatin with 1000X magnification. The gelatin was dissolved in 1:1 (v/v) 20X PBS and Etax A solvent, electrospun with the optimal middle point electrospinning conditions and cross-linked with glutaraldehyde (GTA) vapor for 24, 48 and 72 hours.

4.3 Electrospun poly-ε-caprolactone (PCL)

Poly-ε-caprolactone (PCL) was successfully electrospun with acetone as a solvent. Table 1 on page 39 shows the optimal electrospinning conditions determined for PCL and the varied electrospinning parameters. PCL was examined with an optical microscope and scanning electron microscope (SEM). Figures 20 and 21 show these results for the optimal middle point conditions with optical microscope and SEM, respectively. By varying just one of the electrospinning parameters at a time, noticeable changes within the electrospun material were observed as seen in the Figure 22 (SEM). Appendix 3 shows a similar comparing figure with optical microscope images.

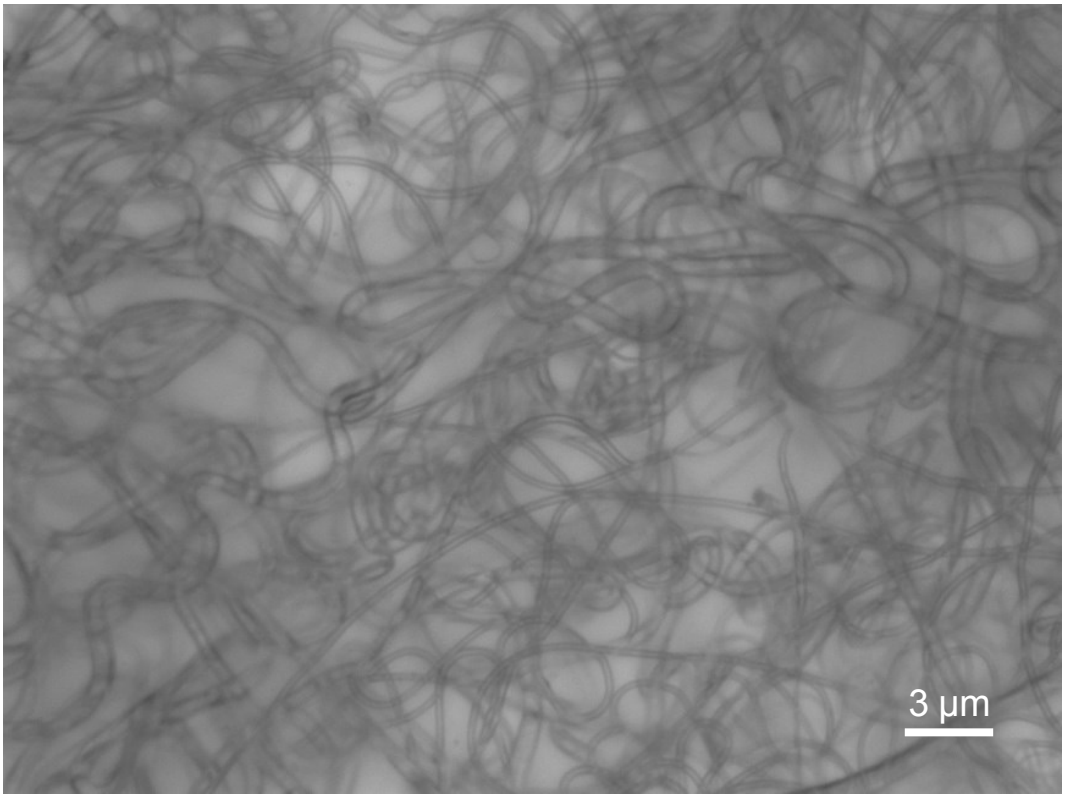

Figure 20. An optical microscope image of PCL with 400X magnification. The PCL was dissolved in acetone and electrospun with the optimal middle point electrospinning conditions (voltage 20 kV, pumping speed 3 ml/h, collector distance 15 cm, gauge size 18 and concentration of 15% (w/v)). The sample was electrospun for 5 minutes at room temperature and moisture under atmospheric gas composition.

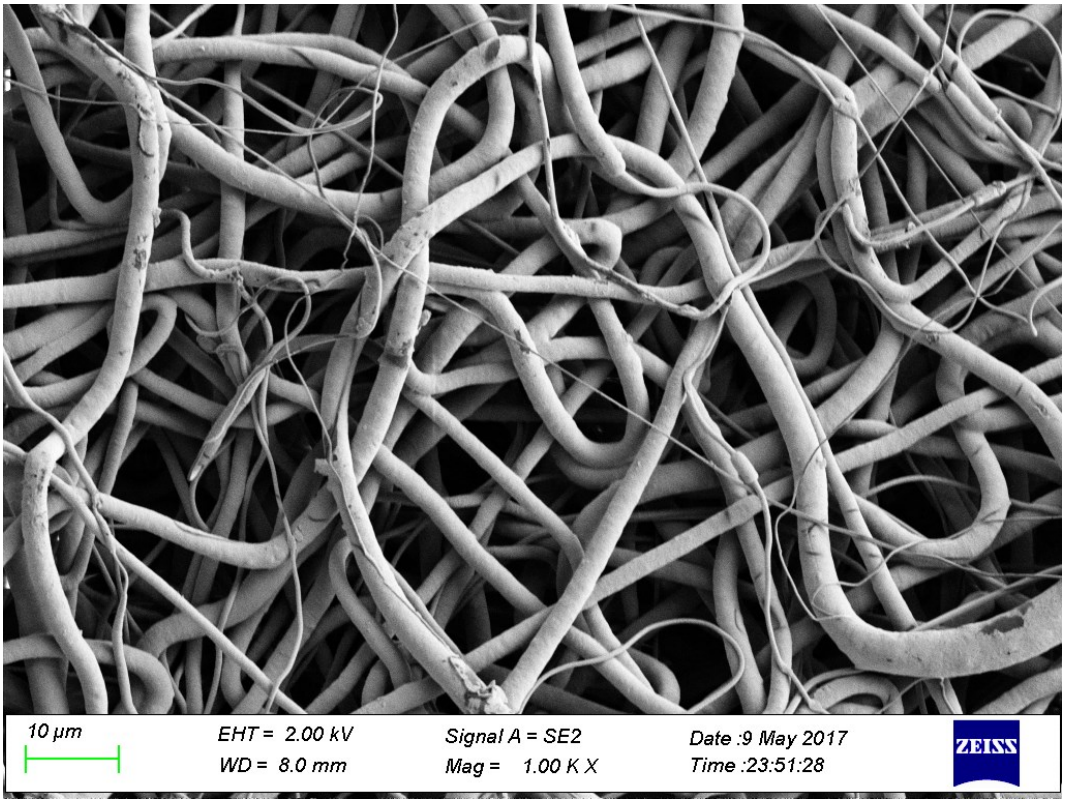

Figure 21. A scanning electron microscope (SEM) image of PCL with 1000X magnification. The PCL was dissolved in acetone and electrospun with the optimal middle point electrospinning conditions (voltage 20 kV, pumping speed 3 ml/h, collector distance 15 cm, gauge size 18 and concentration of 15% (w/v)). The sample was electrospun for 5 minutes at room temperature and moisture under atmospheric gas composition.

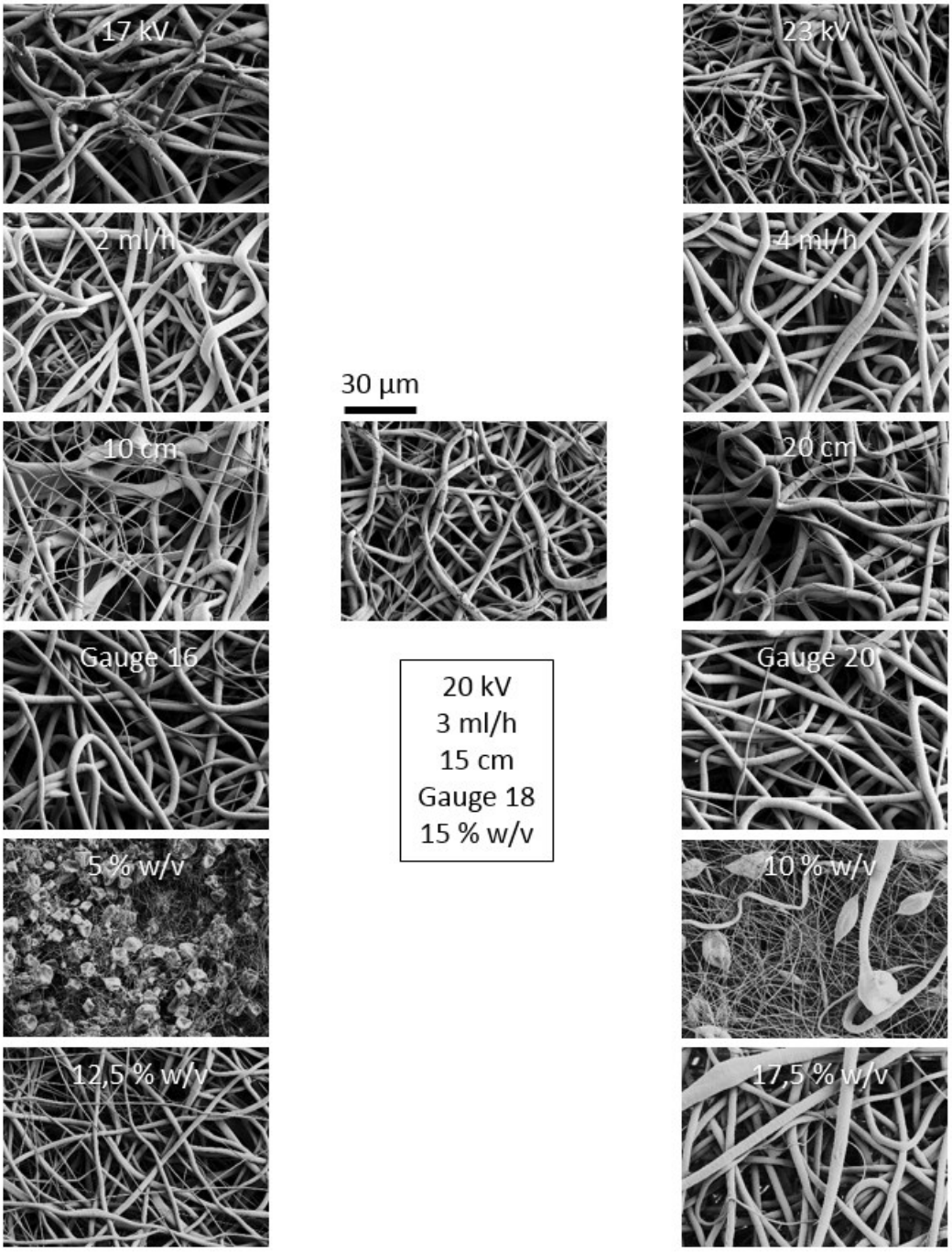

Figure 22. The effect of specific parameters on the electrospinning of PCL. By varying one of the electrospinning parameters (voltage, pumping speed, distance, gauge size, concentration and solvent ratio) and keeping other parameters the same as in the middle point electrospinning (1000X SEM image and parameters presented in the middle) the effect of a specific parameter could be observed in the PCL electrospinning. All of the images were taken with SEM with 1000X magnification as described in Chapter 3.2.3.

4.4 Electrospun poly(ethylene oxide) (PEO)

Poly(ethylene oxide) (PEO) was successfully electrospun with purified water as a solvent. Table 1 on page 39 shows the optimal electrospinning conditions determined for PEO and the varied electrospinning parameters. PEO was examined with an optical microscope and a scanning electron microscope (SEM). Figures 23 and 24 show these results for the optimal middle point conditions with optical microscope and SEM, respectively. By varying just one of the electrospinning parameters at a time, significant changes within the electrospun material were observed as seen in the Figure 25 (SEM). Appendix 4 shows a similar comparing figure with optical microscope images.

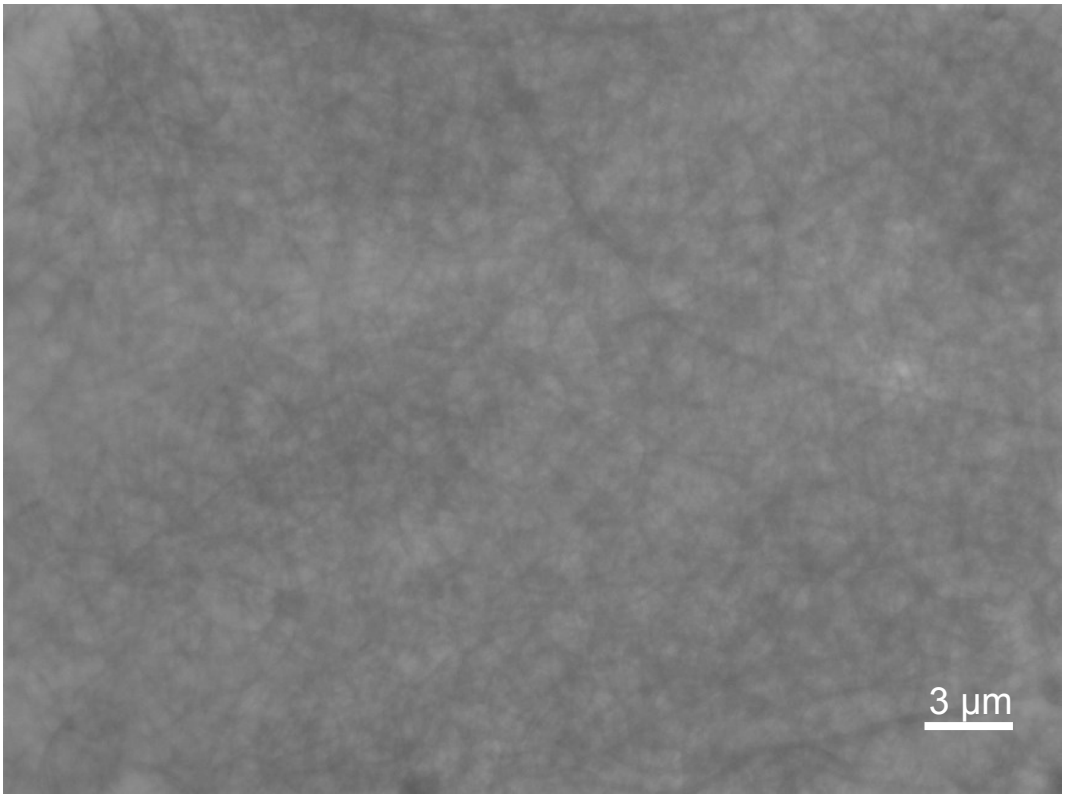

Figure 23. An optical microscope image of poly(ethylene oxide) (PEO) with 400X magnification. The PEO was dissolved in purified water and electrospun with the optimal middle point electrospinning conditions (voltage 25 kV, pumping speed 0,5 ml/h, collector distance 17,5 cm, gauge size 18 and concentration of 5% (w/v)). The sample was electrospun for 5 minutes at room temperature and moisture under atmospheric gas composition.

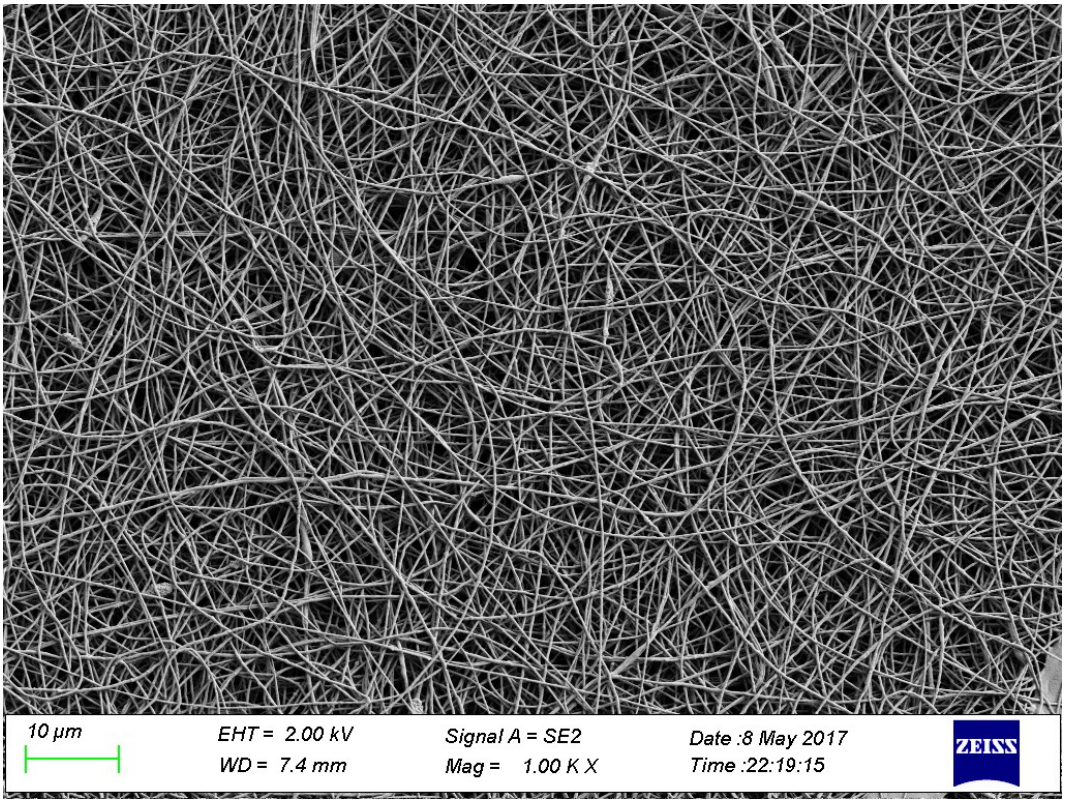

Figure 24. An optical microscope image of poly(ethylene oxide) (PEO) with 1000X magnification. The PEO was dissolved in purified water and electrospun with the optimal middle point electrospinning conditions (voltage 25 kV, pumping speed 0,5 ml/h, collector distance 17,5 cm, gauge size 18 and concentration of 5% (w/v)). The sample was electrospun for 5 minutes at room temperature and moisture under atmospheric gas composition.

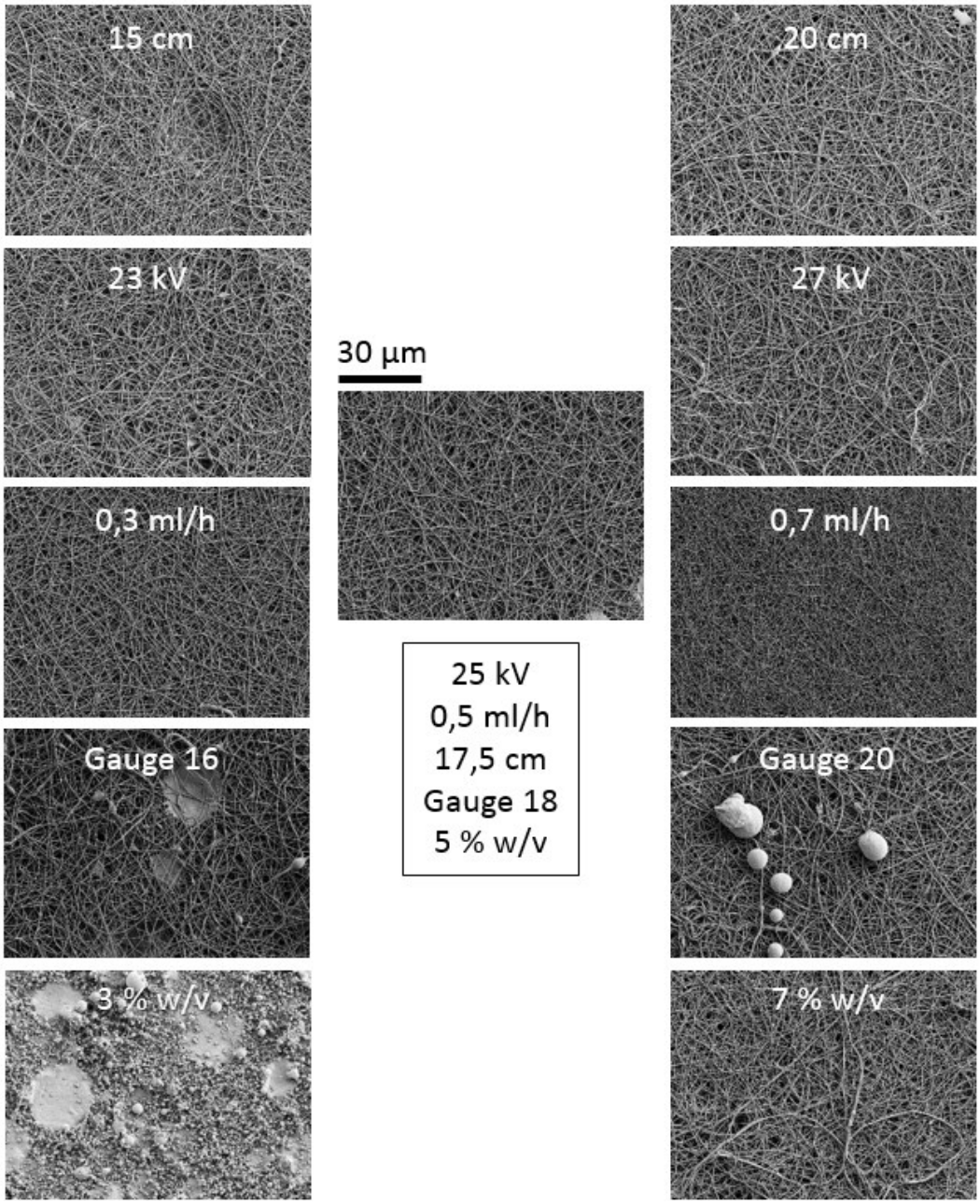

Figure 25. The effect of specific parameters on the electrospinning of PEO. By varying one of the electrospinning parameters (voltage, pumping speed, distance, gauge size, concentration and solvent ratio) and keeping other parameters the same as in the middle point electrospinning (1000X SEM image and electrospinning parameters presented in the middle) the effect of a specific parameter could be observed in the PEO electrospinning. All of the images were taken with SEM with 1000X magnification as described in Chapter 3.2.3.

4.5 Average fiber and pore diameters

Average fiber diameters were determined for electrospun gelatin, PCL and PEO and cross-linked gelatin. Fiber diameters were determined from samples that were electrospun with the optimal middle point electrospinning conditions (see Table 1 on page 39). Determinations were done by using Adobe Photoshop CC 2017 program's Ruler feature. As all of the SEM images had a size scale of 1 or 2 µm within the images, by measuring the length of these size scales in pixels and comparing this information to the fiber diameters in pixels the fiber diameters could be calculated in micrometers. Fibers were determined visually as shown in Figure 26 with the red lines that have been drawn across the fibers. Fiber diameters were measured from the SEM images with magnification of 3000X and 5000X (PCL, PEO, gelatin and cross-linked gelatin) and 10 000X (non-cross-linked gelatin). By averaging ten diameter measurements, the average fiber diameter per electrospun polymer could be calculated. Results between different magnifications with the same polymer were coherent and the average fiber diameter measured from the SEM images with magnification of 5000X are presented in Table 2. Appendix 5 shows the lengths of different size scales in pixels and a calculation example for fiber diameter.

Average pore diameters were determined in a similar manner to average fiber diameters but the pore diameters were measured only on electrospun PCL and electrospun and cross-linked gelatin as only these materials were used in the cultivation experiments. Pores were visually determined and two measurements perpendicular to each other were carried out per pore. These measurements are presented as yellow crosses in Figure 26. SEM images with a magnification of 1000X were used to determine the average pore size of PCL. SEM images with a magnification of 3000X and 5000X were used with cross-linked gelatin. Significant difference in average pore diameter was not observed between different magnifications. By averaging the two perpendicular measurements per pore and taking the average of ten similarly measured pores, a rough estimation on the pore diameter within the

electrospun scaffold could to be estimated. These values are presented in Table 3 and they are based on SEM images with 1000X (PCL) and 5000X (cross-linked gelatin) magnifications. Appendix 6 shows a calculation example for pore diameter. Fiber diameter measurements are presented in Appendix 7, cross-linked gelatin pore diameter measurements in Appendix 8 and PCL pore diameter measurements in Appendix 9.

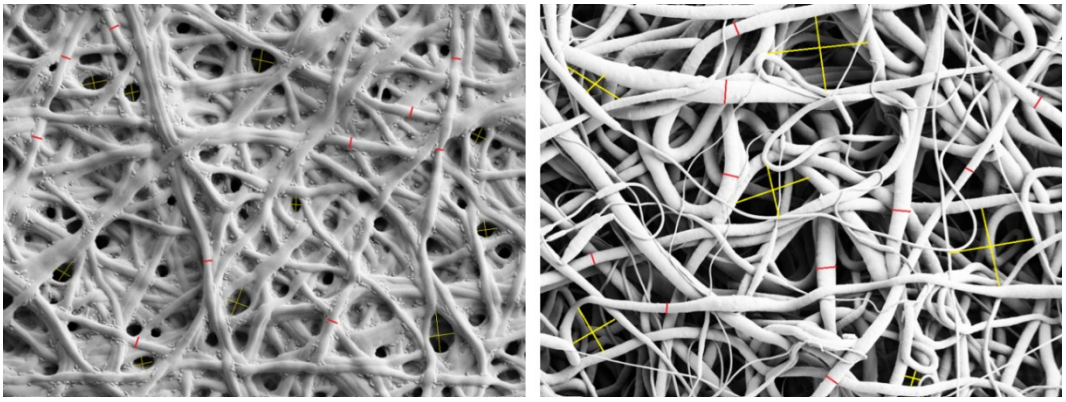

Figure 26. Scanning electron microscope (SEM) images of electrospun cross-linked (72 h) gelatin (magnification of 5000X) and PCL (magnification of 1000X). Red lines within both of the images represent the way fiber diameter was visually determined and measured with the Adobe Photoshop CC 2017 program's Ruler feature. Yellow crosses within both of the images represent the way pore diameters were visually determined and measured.

Table 2. Average fiber diameter in nanometers per electrospun polymer and cross-linking time.*

Polymer	Average fiber diameter (nm)
PCL	2200 ± 700
PEO	300 ± 100
Gelatin (non-cross-linked)	300 ± 0
Cross-linked gelatin (24 h)	400 ± 100
Cross-linked gelatin (48 h)	400 ± 100
Cross-linked gelatin (72 h)	500 ± 100

**Values gathered and averaged from the SEM images with a magnification of 5000X. Cross-linking was done only for gelatin samples; glutaraldehyde vapor exposure time in hours. All of the polymers were electrospun according to the optimal middle point electrospinning conditions listed in Table 1 on page 39.*

Table 3. Average pore diameter in nanometers per PCL and cross-linked gelatin (glutaraldehyde vapor exposure time in hours) samples.*

Polymer	Average pore diameter (nm)
PCL	13 900 ± 4600
Cross-linked gelatin (24 h)	1000 ± 300
Cross-linked gelatin (48 h)	900 ± 200
Cross-linked gelatin (72 h)	800 ± 300

**Values gathered and averaged from the SEM images with a magnification of 1000X (PCL) and 5000X (cross-linked gelatin). All of the polymers were electrospun according to the optimal middle point electrospinning conditions described in Table 1 on page 39.*

4.6 Cultivations

All of the fluorescence-stained cell-scaffold constructs both from static and RWV bioreactor cultivations were examined with confocal and widefield microscopes as described in Chapter 3.2.3. No images were taken from the images of the confocal microscope as only scaffold autofluorescence was seen. Figures 27 and 28 show the same scaffold autofluorescence seen with the widefield microscope. No cells were visible.

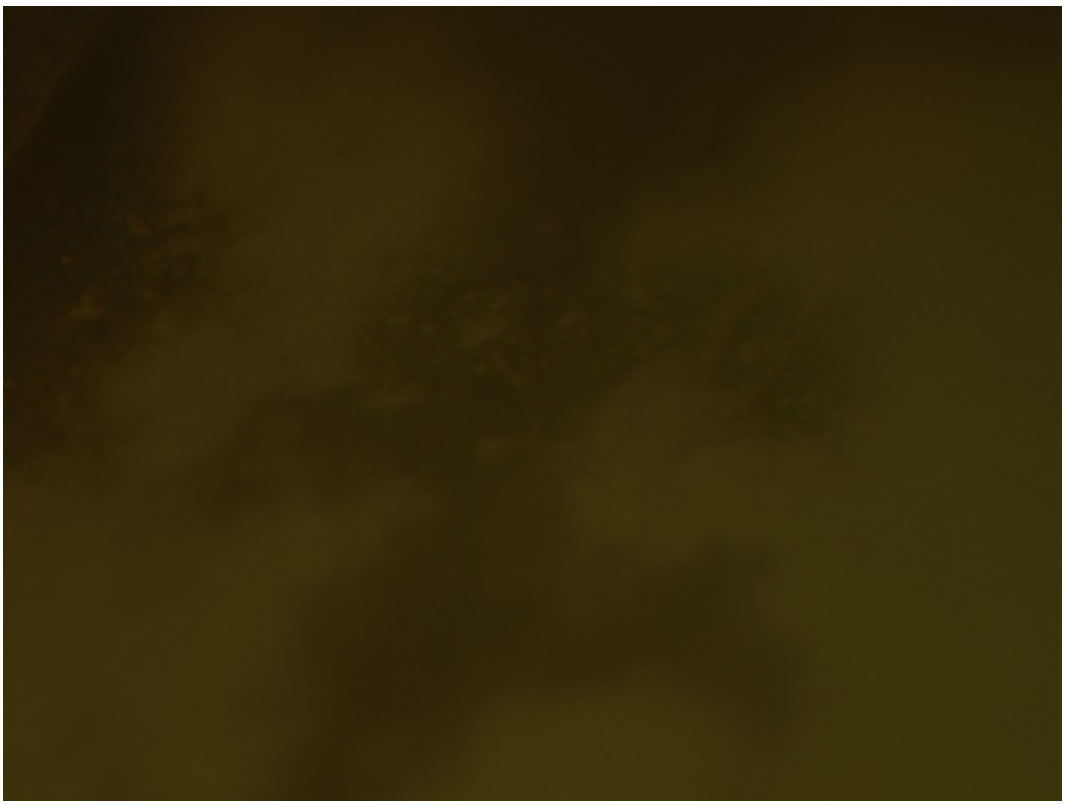

Figure 27. A widefield microscope (WFM) image of Alexa Fluor 568 fluorescent phalloidin stained poly-ε-caprolactone (PCL) scaffold. The scaffold was cultivated for three days under static conditions with A549 cells. 400X magnification, no cells were visible since the scaffold was autofluorescent.

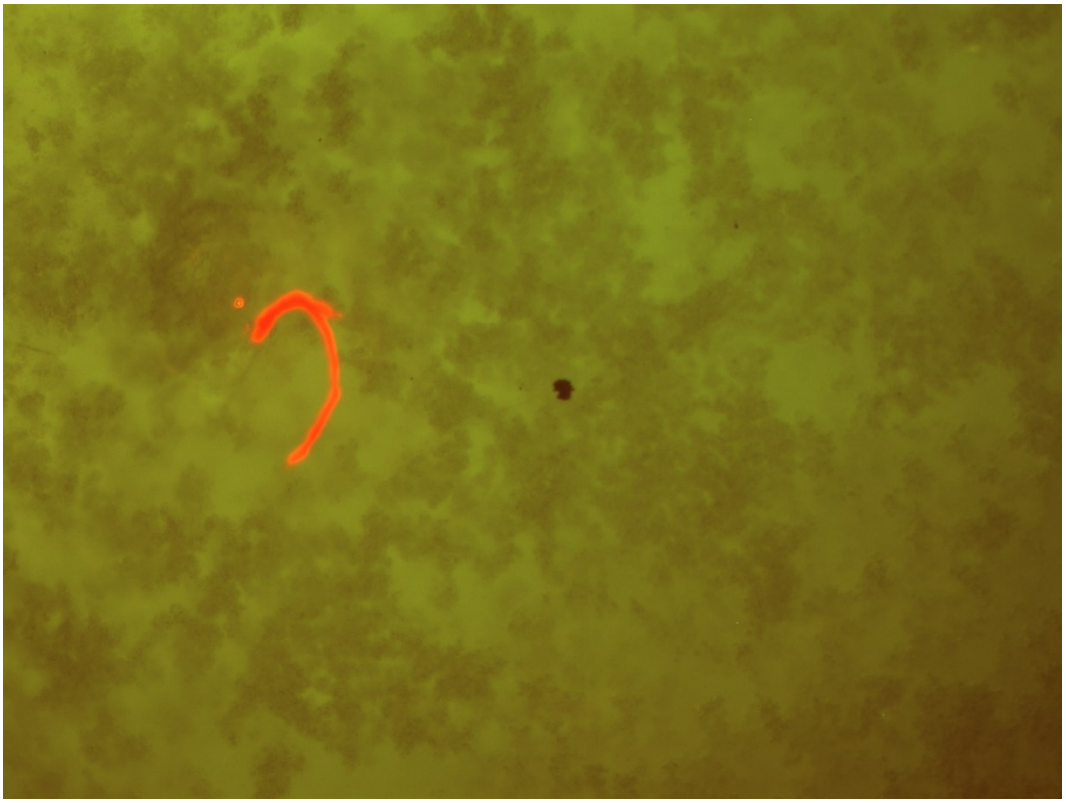

Figure 28. A widefield microscope (WFM) image of Alexa Fluor 568 fluorescent phalloidin stained 72-hours cross-linked gelatin scaffold. The scaffold was cultivated for three days under static conditions with A549 cells. 40X magnification, no cells were visible since the scaffold was autofluorescent. The orange fiber in the middle of the image is a hair.

Although all of the scaffolds showed only autofluorescence and no cells, cell spheroids were seen in the RWV bioreactor cultivation medium (Figure 29). It seems that the A549 cells did not attach to the scaffolds and preferred to grow as spheroids. However, this confirms that cells were able to grow at least some time inside the bioreactor although the cultivation conditions were not optimal. The optical microscope image in Figure 29 was taken with 400X magnification and shows A549 spheroid that was growing inside the cultivation vessel with the inner supportive structure.

Figure 29. Spheroids formed by A549 cells within the bioreactor cultivation. The image was taken at the end of the three-day cultivation with 400X magnification.

5. Discussion and suggestions for further research

The overall aim of the present work was to elucidate how a functional, natural-mimicking blood vessel could be created by using electrospun scaffolds and a student-assembled RWV bioreactor. Although a tissue-engineered blood vessel (TEBV) was not created within this thesis, the work to establish the methodology was successful enough to create the basis for future work that could lead to a TEBV. Thus, especially the functionality and versatility of the used methods is discussed in detail. In addition, as these methods were to be utilized on the CHEM-E3225 Cell and Tissue Engineering course at Aalto University, the work that was done will be also discussed in terms of being suitable for teaching. The discussion of the methods that were used will also be linked to future research possibilities as both the RWV bioreactor and the electrospinning set-up have significant development potential.

The following discussion is divided into two subchapters. Subchapter 5.1 Electrospinning gathers together results concerning the electrospinning set-up itself and how well the electrospinning of different polymers succeeded. Subchapter 5.2 Cultivations summarizes the work that was done in order to elucidate whether cells start to grow along the electrospun scaffolds and if the RWV bioreactor outperforms traditional static cultivations in tissue culturing.

5.1 Electrospinning

Electrospinning results were satisfactory in general. Although collagen was not successfully electrospun, electrospinning of gelatin as an alternative natural polymer was achieved. In addition, PCL and PEO were successfully electrospun and an electrospinning set-up was assembled.

5.1.1 Collagen and gelatin

The attempts to electrospin collagen were not successful, most likely due to the different properties of the origin of the Kensey Nash semed S collagen used in the protocol by Dong et al. (2009) and that of the Sigma-Aldrich collagen (Gallop and Seifter, 1963) used for the present study as argued in Chapter 4.1. Namely, the Sigma-Aldrich collagen has been extracted from calf

skin by acidic treatment and it has the chemical structure of tropocollagen, whereas the enzymatically extracted collagen used by Dong et al. (2009) lacks the telopeptide regions that allow tropocollagen chains to form intermolecular cross-links and thus collagen fibrils. Therefore, the enzymatically extracted collagen is more soluble as it lacks these cross-linking regions. One option in the present study would have been to confirm the hypothesis that the problem with collagen was due to the method used to extract collagen by the manufacturer. This could have been done by testing also enzymatically derived collagen in addition to the collagen derived from acidic extraction. However, due to delivery problems within the timeframe of the work, this was not possible. Accordingly, enzymatically isolated or otherwise telopeptide-free collagen (atelocollagen) should be experimented in the future to test if it can be successfully electrospun, and to confirm if the difference in the original collagen extraction method was actually at the root of the problem of the present experiments.

Whereas collagen did not dissolve into the 1:1 (v/v) 20X PBS and Etax A solvent and only “electrospun” PBS salts were accumulated on the collector plate (Figures 11 and 12), a homogenous nonwoven sheet of fine fibers was produced when gelatin was dissolved into and electrospun with the same solvent (Figure 14). Moreover, the screening for the optimal electrospinning conditions for gelatin was successful and a correct mixture of parameters was identified. It is apparent that especially a smaller electrospinning distance, a higher concentration and an unbalanced solvent ratio cause drastic changes in the homogeneity of produced fibers. However, although the other parameters do not seem to disturb the uniformity of produced fiber sheets within the SEM images (Figure 15), changes in the overall electrospinning process did affect the final outcome. For example, a higher voltage or pumping speed caused spider-web-like formations along the hollow protective cylinder or disturbances in the Taylor cone, respectively. Thus, the optimal middle point conditions are recommended for successful electrospinning of gelatin and further screening of electrospinning conditions is not necessary. However,

because easily-dissolving electrospun gelatin needs to be cross-linked prior cell seeding, the cross-linking process should be further studied.

The effect of glutaraldehyde (GTA) vapor cross-linking was evident as shown by comparison of the non-cross-linked gelatin and the 72-hours cross-linked gelatin (Figures 14 and 18, respectively). Individual fibers were swollen and the mesh of fibers was tighter with smaller, about 1 µm in diameter pores. Average fiber diameter for the non-cross-linked gelatin and the 72-hours cross-linked gelatin was 300 ± 0 nm and 500 ± 100 nm, respectively (Table 2). These values are in line with the average fiber diameter for non-cross-linked gelatin by Erencia et al. (2016) (304 ± 37 nm; 10 % (w/v) gelatin (type A porcine skin) in a 1:1 (v/v) solution of 10X PBS and ethanol; 0,75 ml/h; 18 kV) and by Zha et al. (2012) (276 ± 37 nm; 11,5 % (w/v) gelatin (type A porcine skin) in a 1:1 solution of 20X PBS and ethanol; 0,25 ml/h; 12 kV). Although the desired attribute of water-endurance was gained by cross-linking, the desired porous meshness of non-cross-linked gelatin was lost. Cross-linked gelatin forms a structure, which resembles a unified membrane. The membrane most likely does not allow cells to infiltrate into the scaffold as the initial intention was. However, this type of a membrane could be utilized for example as a scaffold for the basal lamina (Chapter 2.1.3) within a TEBV.

As gelatin was not the original choice of polymer, the cross-linking process and different cross-linking agents were not examined in sufficient detail prior choosing glutaraldehyde vapor. Moreover, it should be noted that the reference method by Zhang et al. (2006) focused on a somewhat different goal than did the present study. As the attention of the present work was in line with the work of Zhang et al. (2006) focusing solely on aiming to cross-link electrospun gelatin so that it does not dissolve even during long incubations, the concept of cell infiltration was neglected. Already after 24 hours, the electrospun gelatin was thoroughly cross-linked into a membrane-like texture and further cross-linking did not change the texture dramatically (Figure 19). Thus a shorter (<24h) cross-linking time should be tested if more porous but still water-resistant gelatin scaffold is desired. In addition, different cross-linking agents

such as genipin should be tested to see how they affect the gelatin scaffold and cell infiltration.

To conclude the discussion on collagen and gelatin, the latter which was used as the substitute for collagen, future research should not only include the testing of collagen but also selecting and testing an appropriate cross-linking method if it is required. On the other hand, for teaching purposes gelatin is a more economical choice than collagen, whereas the properties of collagen for biological systems is rather unique. For example, depending on the blood vessel *tunica,* different attributes of scaffolds may be desired, and thus both collagen and gelatin, and all the different cross-linking methods should be extensively tested in the future studies on TEBV.

5.1.2 Poly-ε-caprolactone and poly(ethylene oxide)

Poly-ε-caprolactone (PCL) was successfully electrospun with acetone as a solvent. Bead-free mesh of nonwoven fibers was produced even though it was diameter-heterogeneous (Figure 21). PCL fibers were significantly larger than gelatin fibers with an average diameter of 2200 ± 700 nm and an average pore size of 13 900 ± 4600 nm (Table 2). Bassi et al. (2011) reported a smaller average fiber diameter (269 ± 102 nm; 10 % (w/v); 20 kV; 3 ml/h), however, the PCL concentration was significantly smaller than in the present thesis (15 % (w/v)) and the fibers were treated with poly(vinyl phosphonic acid-co-acrylic acid) (PVPA). Electrospinning with a 10 % (w/v) solution and a gauge size 18 needle resulted in beaded fibers in the present thesis (Figure 22) but because Bassi et al. (2011) did not report their needle size, it is not possible to evaluate whether beads were caused by a different gauge size or by some other non-reported factor.

The heterogeneity of PCL fibers was most likely due to slight problems in the electrospinning process. Acetone is highly volatile and it started to evaporate already from the Taylor cone. This caused PCL to clump and the Taylor cone was transformed into a half-solid lump that after a while clogged the syringe needle. Manually this was overcome by removing the lump and continuing electrospinning. Unfortunately, this needed to be repeated every two to three

minutes thus the process should be improved in the future. One solution could be a coaxial needle with a gas jacket as suggested by Larsen, Spretz and Velarde-Ortiz (2004). By pumping the PCL-acetone solution into the inner tube and a solvent-saturated inert gas (for example N_2 gas saturated with acetone) into the outer tube, the acetone within the PCL solution would not evaporate too quickly and a more homogeneous fiber diameter could be achieved. However, the fiber diameter heterogeneity is not as a significant problem when PCL is utilized as a scaffold in tissue engineering. In addition, the large pore size suits tissue engineering applications as cells may move through the PCL scaffold.

The lower PCL concentrations caused the formation of beads or beaded fibers (PCL concentrations of 5 or 10% (w/v), respectively) (Figure 22). Other parameters did not seem to disrupt the fiber smoothness or the mesh structure of the produced PCL as observed by SEM, however, the overall process of electrospinning did not succeed as well in the absence of the optimal middle point conditions. For example, a higher voltage and a shorter electrospinning distance caused noticeable spider-web-like formations along the hollow protective cylinder, and a higher pumping speed, a smaller needle diameter and a higher concentration caused uneven, “horizontal-Eiffel-tower” formations on the collector plate. Thus, the middle point conditions are recommended to be used with the current electrospinning set-up.

Electrospinning of poly(ethylene oxide) (PEO) succeeded and a nonwoven sheet of homogeneous fibers was produced (Figure 24). PEO fibers have the same average diameter (300 ± 100 nm) as the electrospun gelatin fibers. Similar results were obtained for example by Son et al. (2004) (360 nm; 7 % (w/v) PEO in water; M_v = 300 000 g/mol). Also, the overall unified mesh structure resembled the electrospun and non-cross-linked gelatin. Especially a lower concentration and different gauge sizes affected the electrospinning of PEO (Figure 25). A lower concentration (3% (w/v)) did not result as a mesh of fibers, which was also seen when lower PCL concentrations were electrospun. The gauge size did not affect the microstructure of gelatin or PCL whereas with PEO either beads (gauge 20) or flattened droplets (gauge 16) were clearly

visible. These were most likely caused by how well the needle diameter worked with the water-PEO droplet. With a smaller diameter (gauge 20) there is most likely a shortage of polymer within the needle tip droplet, which causes the same type of bead-like structures as seen with lower concentrations. With a larger diameter (gauge 16) the surface tension between droplet and needle walls is not strong enough and smaller droplets are drawn towards the collector plate. The same effect is also seen with lower concentrations in which the lower viscosity causes the syringe-needle-droplet to lose its shape due to lower surface tension. Although the other electrospinning parameters did not seem to have an effect on the electrospun sheet of PEO fibers, the overall process was ideal only with the middle point conditions. For example, a lower voltage or a smaller pumping speed causes changes in the Taylor cone or a non-homogeneous accumulation on the collector plate, respectively.

As PEO dissolves into purified water, the electrospun fibers do not maintain their shape when in contact with water. Although electrospun PEO could be cross-linked, it is more useful as a sacrificial component. With an improved electrospinning set-up, PEO could be for example co-spun with gelatin so that the fibers are thoroughly mixed. Once gelatin fibers are cross-linked, PEO could simply be rinsed off. This would increase the pore size of cross-linked gelatin. For example, Zander et al. (2013) used a similar approach with PCL and PEO to increase the pore size.

5.1.3 The LEVIOSA! electrospinning set-up

The LEVIOSA! electrospinning set-up functioned well. The strongest proof of this was the successful electrospinning of three different polymers. In general, LEVIOSA! was safe and easy to use. The transparent electrospinning cabinet and the collector panel made it easy to observe the electrospinning process. The collector panel with a hollow protective cylinder and a metallic collector stick served well. Although the collector panel assembly was especially designed to collect small and expensive samples such as collagen, it also proved to be convenient when elucidating the optimal electrospinning conditions and electrospinning multiple samples consecutively. On the other

hand, LEVIOSA! is a rather basic set-up and more development work should be done. Fortunately, all parts inside the cabinet are movable and the large size of the cabinet allows fitting multiple new assemblies inside it.

The literature offers an array of possible improvement ideas for the electrospinning set-up. The ones that would be easily included to the LEVIOSA! set-up and help to produce a TEBV include a coaxial needle, a rotating collector mandrel, electrospinning with multiple syringes and pumps, and the aforementioned coaxial gas jacket needle. Moreover, future research should focus on the effect of ambient conditions (mostly temperature and air moisture) on the electrospinning process and possible modifications should accordingly be carried out on the LEVIOSA! set-up.

A coaxial needle could be useful even without the gas jacket. It could be used for example to pump PCL into the inner tube and gelatin or collagen into the outer one and consequently, protein-coated PCL fibers could be electrospun. This would combine the resilience of PCL and the cell-recognition sites of collagen. The coaxial needle could also be utilized when scaffolds with drug delivery properties are electrospun. Namely, by pumping the drug substance into the inner tube, hollow drug-filled fibers with medicinal properties could be created. In addition, the maturing of a TEBV could be accelerated with the right mixture of growth factors. (Lu et al., 2016)

Although the current syringe pump of LEVIOSA! fits two syringes, a second pump would allow more possibilities for the electrospinning process. Currently, if two syringes and hence two different polymers are electrospun simultaneously, the pumping speed cannot be accordingly adjusted to be optimal for both polymers. By placing the two pumps on opposite sides of a rotating mandrel, not only the pumping speed and electrospinning distance could be optimized, but also the evaporating solvents would not interfere with one another – for example, the hydrophobic PCL easily clumps when exposed to water vapor. This type of a 180° pumping technique has also been discussed in the literature (Zander et al., 2013).

A rotating mandrel (Figure 3) was intended to be utilized also within this thesis instead of the wrapping technique, but due to unexpected delays, the rotating mandrel equipment was not finished on time. By electrospinning on a rotating mandrel, a tubular scaffold could be easily created. In addition, the directionality of fibers could be controlled by rotating the mandrel faster, and with unidirectional fibers, the scaffold properties could be improved. A rotating mandrel is also a necessity if multiple pumps are used. In conclusion, the process of production of tubular scaffolds by LEVIOSA! should be improved, as in the current set-up polymer-mixed scaffolds cannot be created.

5.2 Cultivations

The results of cell cultivation experiments were partially satisfactory. The student-built BIOHOVER bioreactor had a good design, however, some major problems occurred during experiments. In addition, the static cultivation experiments, the sample staining protocols and the microscopy did not yield information on the cell-scaffold relations.

5.2.1 Scaffolds

Before reviewing the current challenges of static and RWV bioreactor cultivations, properties of scaffolds that were used in this thesis are discussed as their composition should be improved in order to facilitate TEBV production. With the LEVIOSA! electrospinning set-up, different polymer fibers cannot be efficiently mixed as neither a coaxial needle nor a rotating mandrel are a part of the set-up. For now, layers of different polymers may be electrospun on top of each other but this does not create a scaffold that would have the required qualities as PCL and gelatin layers do not stick to each other if the fibers are not entangled. For example, the pore size could be controlled better and borders of different layers could be faded if PCL, PEO and gelatin were electrospun simultaneously in the future. Moreover, a rotating mandrel would allow seamless tubular scaffolds. As the current electrospinning set-up lacks these parts, only monopolymeric scaffolds of PCL and gelatin were electrospun and cultivated in this thesis. Monopolymeric scaffolds did not have

all of the desired properties, which resulted in some problems in the cultivations.

As PCL is highly hydrophobic, it floated on top of the medium when cultivated. Using a grid in the static cultivations slightly helped with the floating but as there was a gap between the grid and the bottom of the well, cells easily floated off of the scaffold. The tubular PCL scaffolds never completely submerged into the medium in the bioreactor cultivations and this caused the PCL scaffolds to hit the cultivation vessel's wall. This most likely caused significant cell stress. The gelatin scaffolds had the same problem with the gap in the static cultivations and although they could have been grown without the grid, the gelatin scaffolds easily folded and bundled into non-ideal clumps without the grid. The same lack of holding the shape was also seen in the bioreactor cultivations and even though the gelatin scaffolds hovered within the medium as they were supposed to, the tubular shape collapsed. Once attached to the inner protective structure both PCL and gelatin scaffolds were submerged (Figure 10). The inner structure, however, most likely caused disturbance in the laminar flow inside the cultivation vessel and thus caused shear stress. In addition, the insides of the scaffolds were in contact with the nylon threads that held them in place. It is likely that this also caused cell stress. On the other hand, however, A549 cells formed spheroids during the cultivation thus confirming that BIOHOVER supports the cultivation of mammalian cells (Figure 29). Nevertheless, this also means that rather than attaching to the scaffolds, the cells have been floating freely in the medium long enough to form spheroids. It is possible that the cells never attached to the scaffolds and this partially explains why no cells were seen on the cell-scaffold constructs (Figure 27 and 28).

5.2.2 Bioreactor cultivations

In addition to the scaffolds, there were also other challenges with the bioreactor cultivations and it is recommended that the whole concept of a RWV bioreactor is reviewed and possible re-engineered for future cultivation purposes. The main issues were problems with the temperature control, the

cultivation vessels and one of the stepper motors. The easiest to fix is the malfunctioning stepper motor, which can simply be replaced with a new one as there was no design fault with the stepper motor concept itself. Also, the temperature control is probably easily fixed by adjusting the control limits of the heating element and scaling down the metallic heating board. Currently heating stops when 37,1°C is reached, but because the heating board stores efficiently heat energy, the temperature keeps on rising even without active heating. However, if these two issues can be resolved, the malfunctioning cultivation vessel causes major problems. Namely, as the bubbles are being removed from the vessel, the pressure inside increases. This leads to leaking through the screw threads between the lid and the vessel, and unsuccessful removal of the bubbles. The air space within the cultivation vessel prevents the desired laminar flow, causes shear stress on the cultivated cells and the loss of microgravity. In addition, there is not currently a gas exchange within the vessel, although this is only beneficial in the present set-up, because the air space inside the cultivation chamber is not controlled. Thus, a completely new cultivation vessel should be designed before more experiments are done. Although the bioreactor cultivations did not succeed as planned, the design of the RWV bioreactor itself was successful.

5.2.3 The BIOHOVER RWV bioreactor

A RWV bioreactor called BIOHOVER was designed and built by four students from the School of Engineering at Aalto University. BIOHOVER was easy to use and keep clean with 70% ethanol. It had the basic controls of temperature and rotating speed, and the transparent cultivation chamber allowed visually monitoring the cultivation. Especially the attachment and the removal of the cultivation vessels was user-friendly and the slider-attached turned steel tailstock was easily tightened when the cultivation vessels were secured on place. Another aspect that made BIOHOVER easy to use was the combination of a joystick and a LED display that allowed the controlling of rotating speed and temperature. Although BIOHOVER did not work ideally for the cell cultivation experiments that were carried out in this thesis, the basic design is

a flexible platform for future development. Especially impressive is that it was built by students who did not have any previous biological background. Hence, BIOHOVER is an excellent proof that the collaboration between the School of Chemical Engineering (CHEM) and the School of Engineering (ENG) was fruitful and resulted in a concrete piece of equipment that can be utilized both in teaching and in research.

This was a pioneering initiative between CHEM and ENG and BIOHOVER was the first RWV bioreactor ever built at Aalto University. Collaboration will be continued and BIOHOVER will be further developed. Development ideas include the fixing of the current problems but also including monitoring to the bioreactor. Online monitoring of the CO_2 and O_2 levels, the cultivation pH or the cell amount could allow a more efficient control over the cell growth and adjusting of the conditions accordingly. As the pH value and the cell amount should be monitored directly from the cultivation vessel, some of the already-on-market non-invasive monitoring probes could also be utilized with BIOHOVER (Rolfe, 2012).

Once BIOHOVER is further developed into a functional bioreactor and the LEVIOSA! electrospinning set-up is upgraded, the development work towards a TEBV could actually start. By studying different scaffold combinations and using appropriate cells such as endothelial cells, smooth muscle cells and fibroblasts a close resemblance to a TEBV could be produced. In addition, the method by which the cells are inoculated into the RWV bioreactor should be further elucidated as in the present study the cells were injected straight into the culturing medium but for example endothelial cells should only grow along the lumen. Thus, for example direct seeding into the lumen should be carried out as has been discussed by Boland et al. (2004). With reference to teaching, the A549 cells are most likely still a good choice in the future as even if the equipment would work flawlessly, a resilient cell line is easier for unexperienced students to work with.

5.2.4 Microscopy

The next step after successful formation and cultivation of a tubular cell-scaffold construct is to find out how well cells have infiltrated into the scaffold and started to form their own ECM. Scanning electron microscopy (SEM) of the electrospun scaffolds proved to be an excellent method for comparing different electrospinning conditions, for visualizing the mesh structure and for estimating the average pore and fiber diameters. Surprisingly, also the optical microscope proved to be useful. A comparison of non-cross-linked gelatin, cross-linked gelatin, PCL and PEO showed a clear resemblance between the optical and the scanning electron microscope images.

Widefield and confocal microscopes were used to determine whether cells had attached to the scaffolds. However, in the present experiments, only scaffold autofluorescence was detected and no cell-scaffold-interactions information was gained. The fluorescent phalloidin staining was intended to stain the actin filaments inside the cells whereas no fluorescence was thought to be caused by the scaffold materials. If the scaffolds were autofluorescence-free, the spreading and morphology of the cells could have easily been examined. As this was not the case, conclusive comparisons between different cultivation methods (bioreactor versus static cultivation) or different polymers (PCL versus gelatin) cannot be made. As the A549 cells formed spheroids, and both the cultivation methods and the scaffolds had their problems, it is likely that the cell attachment was not ideal, and should be researched further. In addition, the microscopy of cell-scaffold constructs should be elaborated on in more detail. Moreover, the microscopy of cell-scaffold constructs should be studied further in order to determine if the scaffold autofluorescence could be decreased or if other staining protocols would give better results. Scanning electron microscope could be used to examine the cell-scaffold constructs as it worked well with the electrospun materials alone. However, SEM shows only the surface of a sample and other methods should be implemented to study the cell infiltration. The cell-scaffold constructs should also be sliced into thinner fragments to ease the microscopy studies.

As a summary of the above discussion, in the present thesis, a basic electrospinning set-up and a RWV bioreactor were built, and three different polymers were successfully electrospun. In addition, some first-stage cell experiments were performed although there were challenges with respect to the equipment, scaffolds and microscopy. The work forms a strong platform for future research and teaching as well as for further development of the many parameters involved with the electrospinning process, cell cultivation and the RWV bioreactors.

6. Conclusions

Three different polymer-solvent pairs (gelatin with 1:1 (v/v) 20X PBS and Etax A, poly-ε-caprolactone with acetone and poly(ethylene oxide) with purified water) were successfully electrospun and homogeneous meshes of nonwoven fibers were produced. Gelatin was also successfully cross-linked with glutaraldehyde vapor. Fiber diameters for gelatin, 72-hours cross-linked gelatin, PCL and PEO were 300 ± 0, 500 ± 100, 2200 ± 700 and 300 ± 100 nm, respectively. The optimal electrospinning conditions were identified by varying the electrospinning parameters, including voltage, distance, pumping speed, gauge size and polymer concentration. The used electrospinning set-up LEVIOSA! was self-assembled and it worked satisfyingly as a basic electrospinning equipment. Future work with LEVIOSA! should include the introduction of a rotating mandrel, a coaxial needle and another syringe pump so that tubular tissue-engineered blood vessel (TEBV) scaffolds could be created more efficiently. In addition, the effect of ambient conditions on the electrospinning process should be investigated.

The TEBV scaffolds were produced by wrapping either 72-hours cross-linked gelatin or PCL to form tubular constructs. The average pore sizes of these scaffolds were 800 ± 300 and 13 900 ± 4600 nm, respectively. However, the small pore size of the cross-linked gelatin most likely did not allow cells to infiltrate into the scaffold although this was not confirmed with microscopy. PCL scaffolds were highly hydrophobic and the cell cultivation on them was challenging. Due to the basic structure of the LEVIOSA! electrospinning set-up, it was not possible to mix PCL and gelatin together, which could have been advantageous for the cell cultivations.

A Rotary Wall Vessel (RWV) bioreactor called BIOHOVER was student-built, and the work was supervised as part of this thesis. A549 lung carcinoma cells were successfully cultivated in BIOHOVER although there were some problems with the leaking cultivation vessel, the temperature control and the vessel rotation. Thus, the cell cultivation along the PCL and gelatin scaffolds did not succeed as planned. This might also be due to problems with the

scaffolds as also the static cultivation tests had problems. However, BIOHOVER worked as a basic cultivation equipment and future development work should be continued to overcome the current problems. In addition, monitoring probes should be incorporated into the BIOHOVER bioreactor chamber or the cultivation vessels. Moreover, the fluorescence microscopy protocols and techniques should be further studied as, in the present thesis, the scaffold-autofluorescence posed a problem.

The present thesis has met the original goals set for the work, and has built a strong platform of methods, approaches and equipment for the future production of a TEBV. Once the LEVIOSA! electrospinning set-up and the BIOHOVER RWV bioreactor work properly and reliantly in the future, TEBV research may continue towards the ultimate goal of drug delivery system research. In addition to research, an equally important aim of this thesis, the introduction of electrospinning and the RWV bioreactor to the core of the methodology of the course CHEM-E3225 Cell and Tissue Engineering, was successfully achieved.

7. References

Alberts, B., Johnson, A., Lewis, J., Raff, M., Roberts, K. and Walter P. (2008). *Molecular Biology of the Cell.* 5th ed. New York: Garland Science, pp. 1131-1204.

Aleshcheva, G., Bauer, J., Hemmersbach, R., Slumstrup, L., Wehland, M., Infanger, M. and Grimm, D. (2016). Scaffold-free Tissue Formation under Real and Simulated Microgravity Conditions. *Basic & Clinical Pharmacology & Toxicology,* 119(S3), pp. 26-33.

Arnoult, O. (2010). *A Novel Benign Solution for Collagen Processing.* PhD. Case Western Reserve University.

Ayyaswamy, P. and Mukundakrishnan, K. (2007). Optimal Conditions for Simulating Microgravity Employing NASA Designed Rotating Wall Vessels. *Acta Astronautica,* 60(4-7), pp. 397-405.

Bak, S., Yoon, G., Lee, S. and Kim, H. (2016). Effect of Humidity and Benign Solvent Composition on Electrospinning of Collagen Nanofibrous Sheets. *Materials Letters,* 181(1), pp. 136-139.

Bassi, A., Gough, J., Zakikhani, M. and Downes, S. (2011). The Chemical and Physical Properties of Poly(ε-caprolactone) Scaffolds Functionalised with Poly(vinyl phosphonic acid-co-acrylic acid). *Journal of Tissue Engineering,* 2011(615328), pp. 1-9.

Beutel, S. and Henkel, S. (2011). *In Situ* Sensor Techniques in Modern Bioprocess Monitoring. *Applied Microbiology and Biotechnology,* 91(6), pp. 1493-1505.

Bhardwaj, N. and Kundu S. (2010). Electrospinning: A Fascinating Fiber Fabrication Technique. *Biotechnology Advances,* 28(3), pp. 325-347.

Blakemore, C. and Jennett, S. (2001). The Oxford Companion to the Body. 1st ed. Oxford: Oxford University Press, pp. 694-747.

Boland, E., Matthews, J., Pawlowski, K., Simpson, D., Wnek, G. and Bowlin, G. (2004). Electrospinning Collagen and Elastin: Preliminary Vascular Tissue Engineering. *Frontiers in Bioscience,* 9(1-2), pp. 1422-1432.

Buttafoco, L. (2005). *Collagen-based Scaffolds for Tissue Engineering of Small-diameter Blood Vessels.* PhD. University of Twente.

Carlton, R. (2011). *Pharmaceutical Microscopy.* New York: Springer, pp. 85-130, 157-159.

Cipitria, A., Skelton, A., Dargaville, T., Dalton, P. and Hutmacher, D. (2011). Design, Fabrication and Characterization of PCL electrospun Scaffolds – A Review. *Journal of Materials Chemistry,* 21(1), pp. 9419-9453.

Chang, Y., Yang, S., Liu, J., Dong, E., Wang, Y., Cao, A., Liu, Y. and Wang, H. (2011). In Vitro Toxicity Evaluation of Graphene Oxide on A549 Cells. *Toxicology Letters,* 200(2011), pp. 201-210.

Chen, H. and Hu, Y. Bioreactors for Tissue Engineering. (2006). *Biotechnology Letters,* 28(18), pp. 1415-1423.

Chiu, B., Wan, J., Abley, D. and Akabutu, J. (2005). Induction of Vascular Endothelial Phenotype and Cellular Proliferation from Human Cord Blood Stem Cells Cultured in Simulated Microgravity. *Acta Astronautica,* 56(9-12), pp. 918-922.

Cooley, J. (1902). Apparatus for Electrically Dispersing Fluids. 692,631.

Dippold, D., Cai, A., Hardt, M., Boccaccini, A., Horch, R., Beire, J. and Schubert, D. (2017). Novel Approach Towards Aligned PCL-collagen Nanofibrous Constructs From a Benign Solvent System. *Materials Science and Engineering: C, Materials for Biological Applications,* 72(1), pp. 278-283.

Dong, B., Arnoult, O., Smith, M. and Wnek, G. (2009). Electrospinning of Collagen Nanofiber Scaffolds from Benign Solvents. *Macromolecular Rapid Communications,* 30(7), pp. 539-542.

Duan, N., Geng, X., Ye, L., Zhang, A., Feng, Z., Guo, L. and Gu, Y. (2016). A Vascular Tissue Engineering Scaffold with Core-shell Structured Nano-fibers Formed by Coaxial Electrospinning and Its Biocompatibility Evaluation. *Biomedical Materials,* 11(3), pp. 1-10.

El Haj, A. and Cartmell, S. (2010). Bioreactors for Bone Tissue Engineering. *Proceedings of the Institution Mechanical Engineers, Part H: Journal of Engineering in Medicine,* 224(12), Pp. 1523-1532.

Ercolani, E., Del Gaudio, C. and Bianco A. (2015). Vascular Tissue Engineering of Small-diameter Blood Vessels: Reviewing the Electrospinning Approach. *Journal of Tissue Engineering and Regenerative Medicine,* 9(8), pp. 861-888.

Erencia, M., Cano, F., Tornero, J., Macanás, J. and Carrillo, F. (2016). Preparation of Electrospun Nanofibers from Soltuions of Different Gelatin Types Using a Benign Solvent Mixture Composed of Water/PBS/ethanol. *Polymers Advanced Technologies,* 27(3), pp. 382-392.

Formhals, A. (1934). Process and Apparatus for Preparing Artificial Threads. 1,975,504.

Fullana, M. (2015). *Practical Applications of Collagen-based Scaffolds for Use in Tissue Engineering and Regeneration.* PhD. Case Western Reserve University.

Gallop, P. and Seifter, S. (1963). Preparation and Properties of Soluble Collagens. *Methods in Enzymology*, 6(1), pp. 635-641.

Geiger, B. and Yamada K. (2011). Molecular Architecture and Function of Matrix Adhesions. *Cold Spring Harbor Perpectives in Biology,* 3(5), pp. 1-21.

Giard, D., Aaronson, S., Todaro, G., Arnstein, P., Kersey, J., Dosik, H. and Parks, W. (1973). In Vitro Cultivation of Human Tumors: Establishment of Cell Lines Derived from a Series of Solid Tumors. *Journal of the National Cancer Institute,* 51(5), pp. 1417-1423.

Gibco. (2015). *Cell Culture Basics Handbook.* 1st ed. [pdf] Waltham: Thermo Fisher Scientific, pp. 1-110. Available at: https://www.thermofisher.com/content/dam/LifeTech/global/promotions/global/images/aai-2015/aai-pdfs/GibcoCellCultureBasicsHandbook.pdf [Accessed 27 May 2017].

Grimm, D., Wehland, M., Pietsch, J., Aleshcheva, G., Wise, P., van Loon, J., Ulbrich, C., Magnusson, N., Infanger, M. and Bauer, J. (2014). Growing Tissues in Real and Simulated Microgravity: New Methods for Tissue Engineering. *Tissue Engineering: Part B,* 20(6), pp. 555-566.

Hasan, A., Nurunnabi, M., Morshed, M., Paul, A., Polini, A., Kuila, T., Al Hariri, M., Lee, Y. and Jaffa, A. (2014). Recent Advanced in Application of Biosensors in Tissue Engineering. *BioMed Research International,* 2014(307519), pp. 1-18.

He, W., Yong, T., Teo, W., Ma, Z. and Ramakrishna, S. (2005). Fabrication and Endothelialization of Collagen-blended Biodegradable Polymer Nanofibers: Potential Vascular Graft for Blood Vessel Tissue Engineering. *Tissue Engineering,* 11(9-10), pp. 1574-1588.

Heydarkhan-Hagvall, S., Schenke-Laylan, K., Dhanasopon, A., Rofall, F., Smith, H., Wu, B., Shemin, R., Beygui, R. and MacLellan, W. (2008). Three-dimensional Electrospun ECM-based Hybrid Scaffolds for Cardiovascular Tissue Engineering. *Biomaterials,* 29(19), pp. 2907-2914.

Hoch, E., Tovar, G. and Borchers, K. (2014). Bioprinting of Artificial Blood Vessels: Current Approaches Towards a Demanding Goal. *European Journal of Cardio-Thoracic Surgery,* 46(5), pp. 767-778.

Hynes, R. (2009). The Extracellular Matrix: Not Just Pretty Fibrils. *Science,* 326(5957), pp. 1216-1219.

Hynes, R. and Naba, A. (2012). Overview of the Matriosome – An Inevntory of Extracellular Matric Constituents and Functions. *Cold Spring Harbor Perpectives in Biology,* 4(1), pp. 1-16.

Inoguchi, H., Kwon, I., Inoue, E., Takamizawa, K., Maehara, Y. and Matsuda, T. (2006). Mechanical Responses of a Compliant Electrospun Poly(L-lactide-co-ε-caprolactone) Small-diameter Vascular Graft. *Biomaterials,* 27(8), pp. 1470-1478.

Jiang, Q., Reddy, N., Zhang, S., Roscioli, N. and Yang Y. (2013). Water-stable Electrospun Collagen Fibers from a Non-toxic Solvent and Crosslinking System. *Journal of Biomedical Materials Research Part A,* 101(5), pp. 1237-1247.

Jiang, Y., Jiang, L., Huang, A., Wang, X., Li, Q. and Turng, L. (2017). Electrospun Polycaprolactone/gelatin Composites with Enhanced Cell-matrix Interactions as Blood Vessel Endothelial Layer Scaffolds. *Materials Science and Engineering: C, Materials for Biological Applications,* 71(1), pp. 901-908.

Ju, Y., Choi, J., Atala, A., Yoo, J. and Lee, S. (2010). Bilayered Scaffold for Engineering Cellularized Blood Vessels. *Biomaterials,* 31(15), pp. 4313-4321.

Jung, Y., Ji, H., Chen, A., Chan, H., Atchison, L., Klitzman, B., Truskey, G. and Leong, K. (2015). Scaffold-free, Human Mesenchymal Stem Cell-Based Tissue Engineered Blood Vessels. *Nature Scientific Reports,* 5(15116), pp. 1-9.

Khorshidi, S., Solouk, A., Mirzadeh, H., Mazinani, S., Lagaron, J., Sharifi, S. and Ramakrishna, S. (2016). A Review of Key Challenges of Electrospun Scaffolds for Tissue-engineering Applications. *Journal of Tissue Engineering and Regenerative Medicine,* 10(9), pp. 715-738.

Klaus, D. (2001). Clinostats and Bioreactors. *Gravitational and Space Biology,* 14(2), pp. 55-64.

Korossis, S., Bolland, F., Kearney, J., Fisher, J. and Ingham, E. (2005). Bioreactors in Tissue Engineering. In: N. Ashammakhi and R. Reis, ed., *Topics in Tissue Engineering, Vol. 2*. [ebook] Helsinki: Expertissues, pp. 1-23. Available at: http://www.oulu.fi/spareparts/ebook_topics_in_t_e_vol2/abstracts/korossis_0102.pdf [Accessed 27 May 2017].

Kumar, A. and Starly B. (2015). Large Scale Industrialized Cell Expansion: Producing the Critical Raw Material for Biofabrication Processes. *Biofabrication,* 7(4), pp. 1-14.

Larsen, G., Spretz, R. and Velarde-Ortiz, R. (2004). Use of Coaxial Gas Jackets to Stablize Taylor Cones of Volatile Solutions and to Induce Particle-to-fiber Transitions. *Advanced Materials,* 16(2), pp. 166-169.

Lee, J., Tae, G., Kim, Y., Park, I., Kim, S. and Kim S. (2008a). The Effect of Gelatin Incorporation into Electrospun Poly(L-lactide-co-ε-caprolactone) Fibers on Mechanical Properties and Cytocompatibility. *Biomaterials,* 29(12), pp. 1872-1879.

Lee, S., Liu, J., Oh, S., Soker, S., Atala, A. and Yoo, J. (2008b). Development of a Composite Vascular Scaffolding System That Withstands Physiological Vascular Conditions. *Biomaterials,* 29(19), pp. 2891-2898.

Liu, N., Zang, R., Yang, S. and Li, Y. (2014). Stem Cell Engineering in Bioreactors for Large-scale Bioprocessing. *Engineering in Life Sciences,* 14(1), 4-15.

Lu, Y., Huang, J., Yu, G., Cardenas, R., Wei, S., Wujcik, E. and Guo, Z. (2016). Coaxial Electrospun Fibers: Applications in Drug Delivery and Tissue Engineering. *WIREs Nanomedicine and Nanobiotechnology,* 8(5), pp. 654-677.

L'Heureux, N., Dusserre N., Konig, G., Victor, B., Keire, P., Wight, T., Chronos, N., Kyles, A., Gregory, C., Hoyt, G., Robbins, R. and McAllister T. (2006).

Human Tissue-engineered Blood Vessels for Adult Arterial Revascularization. *Nature Medicine,* 12(3), pp. 361-365.

L'Heureux, N., Pâquet, S., Labbé, R., Germain, L. and Auger, F. (1998). A Completely Biological Tissue-enigneered Human Blood Vessel. *The FASEB Journal,* 12(1), pp. 47-56.

Marrero, B., Messina, J. and Heller, R. (2009) Generation of a Tumor Spheroid in a Microgravity Environment as a 3D Model of Melanoma. *In Vitro Cellular & Developmental Biology - Animal,* 45(9), pp. 523-534.

Martin, I., Wendt, D. and Heberer M. (2004). The Role of Bioreactors in Tissue Engineering. *Trends in Biotechnology,* 22(2), pp. 80-86.

Martin, Y. and Vermette P. (2005). Bioreactors for Tissue Mass Culture: Design, Characterization, and Recent Advances. *Biomaterials,* 26(35), pp. 7481-7503.

Mazzoleni, G., Boukhechba, F., Steimber, N., Boniotti, J., Bouler, J. and Rochet, N. (2011). Impact of Dynamic Culture in the RCCS Bioreactor on a Three-dimensional Model of Bone Matrix Formation. *Procedia Engineering,* 10(1), pp. 3662-3667.

McClure, M. Sell, S., Simpson, D. Walpoth, B. and Bowlin, B. (2010). A Three Layered Electrospun Matrix to Mimic Native Arterial Architecture Using Polycaprolactone, Elastin, and Collagen: A Preliminary Study. *Acta Biomaterialia,* 6(7), pp. 2422-2433.

Mihailova, M., Trenev, V., Genova, P. and Konstantinov, S. (2006). Process Simulation in a Mechatronic Bioreactor Device with Speed-regulated Motors for Growing of Three-dimensional Cell Cultures. *Annals of the New York Academy of Sciences,* 1091(4), pp. 470-489.

Moffat, K., Rebekah, N., Freed, L. and Guilak F. (2014). Engineering Functional Tissues: *In Vitro* Culture Parameters. In: R. Lanza, R. Langer and

J. Vacanti, ed., *Principles of Tissue Engineering,* 4th ed. London: Elsevier Inc., pp. 237-259.

Morton, W. (1902). Method for Dispersing Fluids. 705,691.

Muerza-Cascante, M., Haylock, D., Hutmacher, D. and Dalton, P. (2015). Melt Electrospinning and Its Technologization in Tissue Engineering. *Tissue Engineering: Part B,* 21(2), pp. 187-202.

Mun, C., Jung, Y., Kim, S., Lee, S., Kim, H., Kwon, I. and Kim, S. (2012). Three-dimensional Electrospun Poly(Lactide-co-ε-caprolactone) for Small-diameter Vascular Grafts. *Tissue Engineering: Part A,* 18(15-16), pp. 1608-1616.

OpenStax. (2016). Arteries and veins share the same general features, but the walls of arteries are much thicker because of the higher pressure of the blood that flows through them. [image]. Available at: https://cnx.org/contents/FPtK1zmh@8.25:WNsszrPZ@4/Structure-and-Function-of-Bloo [Accessed 27 May 2017].

Partap, S., Plunkett, N. and O'Brien F. (2010). Bioreactors in Tissue Engineering. In: D. Eberli, ed., *Tissue Engineering,* 1st ed. [ebook] Rijeka: InTech, pp. 323-336. Available at: https://www.intechopen.com/books/tissue-engineering [Accessed 27 May 2017].

Pham, Q., Sharma, U. and Mikos, A. (2006). Electrospinning of Polymeric Nanofibers for Tissue Engineering Applications: A Review. *Tissue Engineering,* 12(5), pp. 1197-1211.

Punnoose, A., Elamparithi, A. and Kuruvilla, S. (2016). Electrospun Type 1 Collagen Matrices using a Novel Benign Solvent for Cardiac Tissue Engineering. *Artificial Cells, Nanomedicine, and Biotechnology,* 44(5), pp. 1318-1325.

Reddy, N., Reddy, R. and Jiang Q. (2015). Crosslinking Biopolymers for Biomedical Applications. *Trends in Biotechnology,* 33(6), pp. 362-369.

Ricard-Blum, S. (2011). The Collagen Family. *Cold Spring Harbor Perspectives in Biology.* 3(1), pp. 1-19.

Richardson, D. (2003). *NASA's Bioreactor: Growing Cells in a Microgravity Environment. Educational Brief.* [pdf] Huntsville: National Aeronautics and Space Administration, pp. 1-20. Available at: https://er.jsc.nasa.gov/seh/cell_growth_in_zero_g.pdf [Accessed 27 May 2017].

Riemschneider, R. and Abedin, M. (1979). Pepsin-solubilized Collagen from Cow Placenta. *Die Angewandte Makromolekulare Chemie,* 82(1276), pp. 171-186.

Rodrigues, C. Fernandes, T., Diogo, M., da Silva, C. and Cabral, J. (2011). Stem Cell Cultivation in Bioreactors. *Biotechnology Advances,* 29(6), pp. 815-829.

Rolfe, P. (2012). Micro- and Nanosensors for Medical and Biological Measurement. *Sensor and Materials,* 24(6), pp. 275-302.

Ruoslahti, E. (1991). Integrins. *Journal of Clinical Investigation,* 87(1), pp. 1-5.

Saleh, F., Frith, J., Lee, J. and Genever, P. (2012). Three-dimensional *in Vitro* Culture Techniques for Mesenchymal Stem Cells. In: K. Mace and K. Braun, ed., *Progenitor Cells, Methods and Protocols,* 1st ed. Berlin: Springer, pp. 31-45. In series: J. Walker, ed., *Methods in Molecular Biology*, Vol 916. Berlin: Springer.

Salehi-Nik, N., Amoabediny, G., Pouran, B., Tabesh, H., Shokrgozar, M., Haghighipour, N., Khatibi, N., Anisi, F., Mottaghy, K. and Zandieh-Doulabi, Z. (2013). Engineering Parameters in Bioreactor's Design: A Critical Aspect in Tissue Engineering. *BioMed Research International,* 2013(762132), pp. 1-15.

Sigma-Aldrich. (2017). *Schematic of various components of the ECM.* [image]. Available at: http://www.sigmaaldrich.com/technical-

documents/articles/biology/3d-biomatrix-white-paper-3d-cell-culture-101.html [Accessed 27 May 2017].

Sell, S., Wolfe, P., Garg, K., McCool, J., Rodriguez, I. and Bowlin, G. (2010). The Use of Natural Polymers in Tissue Engineering: A Focus on Electrospun Extracellular Matrix Analogues. *Polymers,* 2(4), pp. 522-553.

Sill, T. and von Recum, H. (2008). Electrospinning Applications in Drug Delivery and Tissue Engineering. *Biomaterials,* 29(13), pp. 1989-2006.

Soffer, L., Wang, X., Zhang, X., Kluge, J., Dorfmann, L., Kaplan, D. and Leisk, G. (2008). Silk-based Electrospun Tubular Scaffolds for Tissue-engineered Vascular Grafts. *Journal of Biomaterials Science, Polymer Edition,* 19(5), pp. 653-664.

Son, W., Youk, J., Lee, T. and Park, W. (2004). The Effects of Solution Properties and Polyelectrolyte on Electrospinning of Ultrafine Poly(ethylene oxide) Fibers. *Polymer,* 45(9), pp. 2959-2966.

Stizel, J., Liu, J., Lee, S., Komura, M., Berry, J., Soker, S., Lim, G., Van Dyke, M., Czerw, R., Yoo, J. and Atala, A. (2006). Controlled Fabrication of a Biological Vascular Substitute. *Biomaterials,* 27(7), pp. 1088-1094.

Strobel, H., Calamari, E., Beliveau, A., Jain, A. and Rolle, M. (2017). Fabrication and Characterization of Electrospun Polycaprolactone and Gelatin Composite Cuffs for Tissue Engineered Blood Vessels. *Journal of Biomedical Materials Research Part B: Applied Biomaterials,* (Accepted, Unpublished).

Unsworth, B. and Lelkes, P. (1998). Growing Tissues in Microgravity. *Nature Medicine,* 4(8), pp. 901-907.

Weinberg, C. and Bell, E. (1986). A Blood Vessel Model Constructed From Collagen and Cultured Vascular Cells. *Science,* 231(4736), pp. 397-400.

Yokoyama, U., Tonooka, Y., Koretake, R., Akimoto, T., Gonda, Y., Saito, J., Umemura, M., Fujita, T., Sakuma, S., Arai, F., Kaneko, M. and Ishikawa, Y.

(2017). Arterial Graft with Elastic Layer Structure Grown From Cells. *Scientific Reports,* 7(140), pp. 1-16.

Zander, N., Orlicki, J., Rawlett, A. and Beebe, T. (2013). Electrospun Polycaprolactone Scaffolds with Tailored Porosity Using Two Approaches for Enhanced Cellular Infiltration. *Journal of Materials Science: Materials in Medicine*, 24(1), pp. 179-187.

Zeugolis, D., Khew, S., Yew, E., Ekaputra, A., Tong, Y., Yung, L., Hutmacher, D., Sheppard, C. and Raghunath M. (2008). Electro-spinning of pure collagen nano-fibers – Just an expensive way to make gelatin? *Biomaterials,* 29(15), pp. 2293-2305.

Zha, Z., Teng, W., Markle, V., Dai, Z. and Wu, X. (2012). Fabrication of Gelatin Nanofibrous Scaffolds Using Ethanol/Phosphate Buffer Saline as a Benign Solvent. *Biopolymers,* 97(12), pp. 1026-1036.

Zhang, Y., Venugopal, J., Huang, Z., Lim, C. and Ramakrishna, S. (2006). Crosslinking of the Electrospun Gelatin Nanofibers. *Polymer,* 47(8), pp. 2911-2917.

Zhao, J., Griffin, M., Cai, J., Shaoxue, L., Bulter, P. and Kalaskar, D. (2016). Bioreactors for Tissue Engineering: An Update. *Biochemical Engineering Journal,* 109(1), pp. 268-281.

8. Appendices

LIGHT MICROSCOPE IMAGES OF ELECTROSPUN GELATIN **APPENDIX 1**

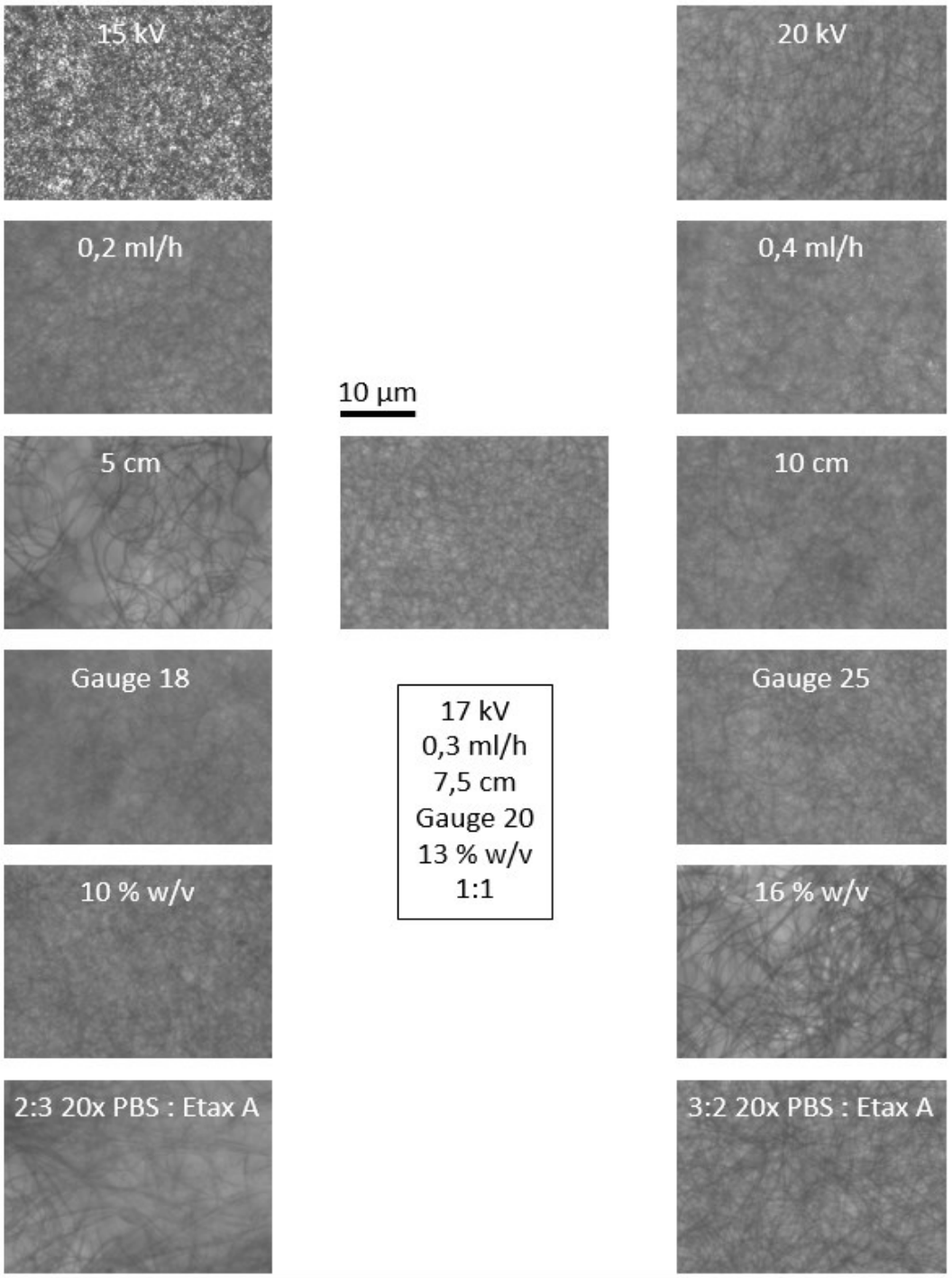

Figure 1. Optical microscope images with 400X magnification of electrospun gelatin. By varying one of the electrospinning parameters (voltage, pumping speed, distance, gauge size, concentration and solvent ratio) and keeping other parameters, the same as in the optimal middle point electrospinning the effect of a specific parameter was being able to be observed within the gelatin electrospinning.

LIGHT MICROSCOPE IMAGES OF ELECTROSPUN AND CROSS-LINKED GELATIN **APPENDIX 2**

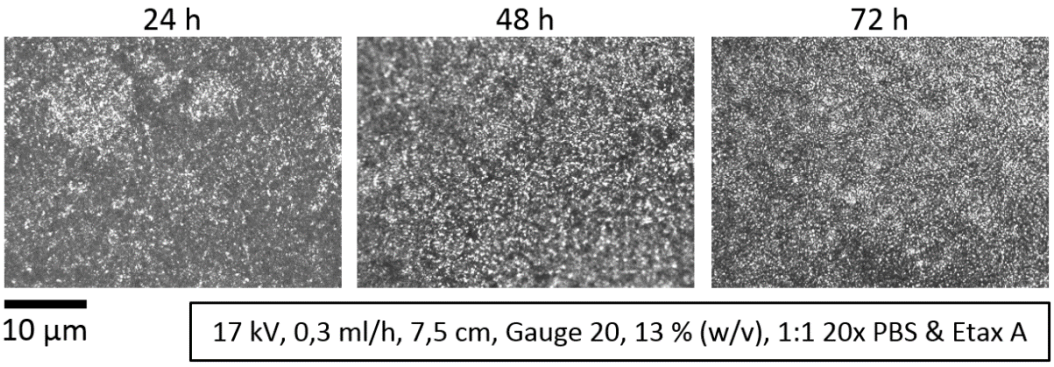

Figure 1. Optical microscope images of gelatin with 400X magnification. The gelatin was electrospun with the optimal middle point electrospinning conditions and cross-linked with glutaraldehyde (GTA) vapor for 24, 48 and 72 hours.

LIGHT MICROSCOPE IMAGES OF ELECTROSPUN POLY-E-CAPROLACTONE (PCL) **APPENDIX 3**

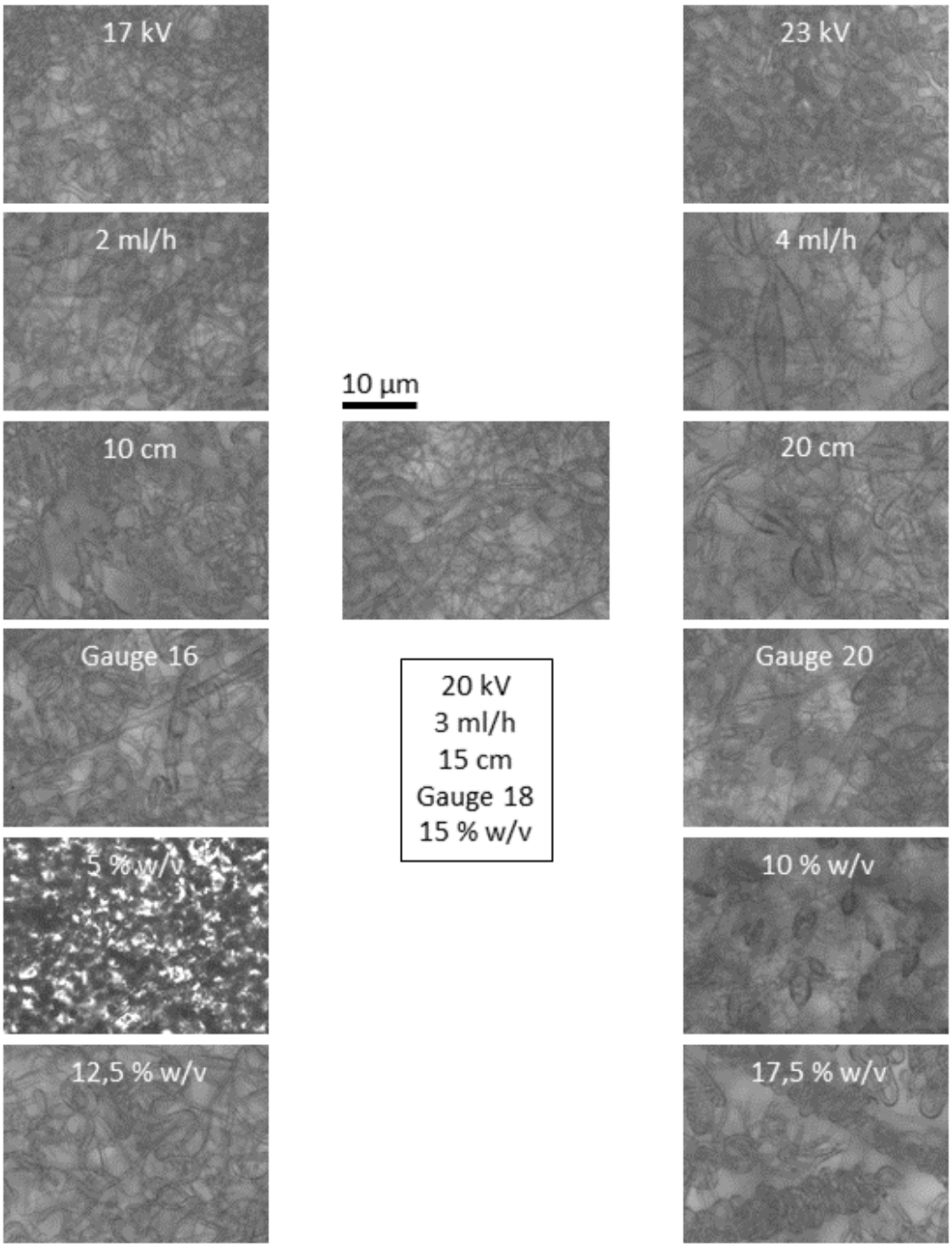

Figure 1. Optical microscope images of electrospun poly-ε-caprolactone (PCL) with 400X magnification. By varying one of the electrospinning parameters (voltage, pumping speed, distance, gauge size, concentration and solvent ratio) and keeping other parameters, the same as in the optimal middle point electrospinning the effect of a specific parameter was being able to be observed within the PCL electrospinning.

LIGHT MICROSCOPE IMAGES OF ELECTROSPUN POLY(ETHYLENE OXIDE) (PEO) **APPENDIX 4**

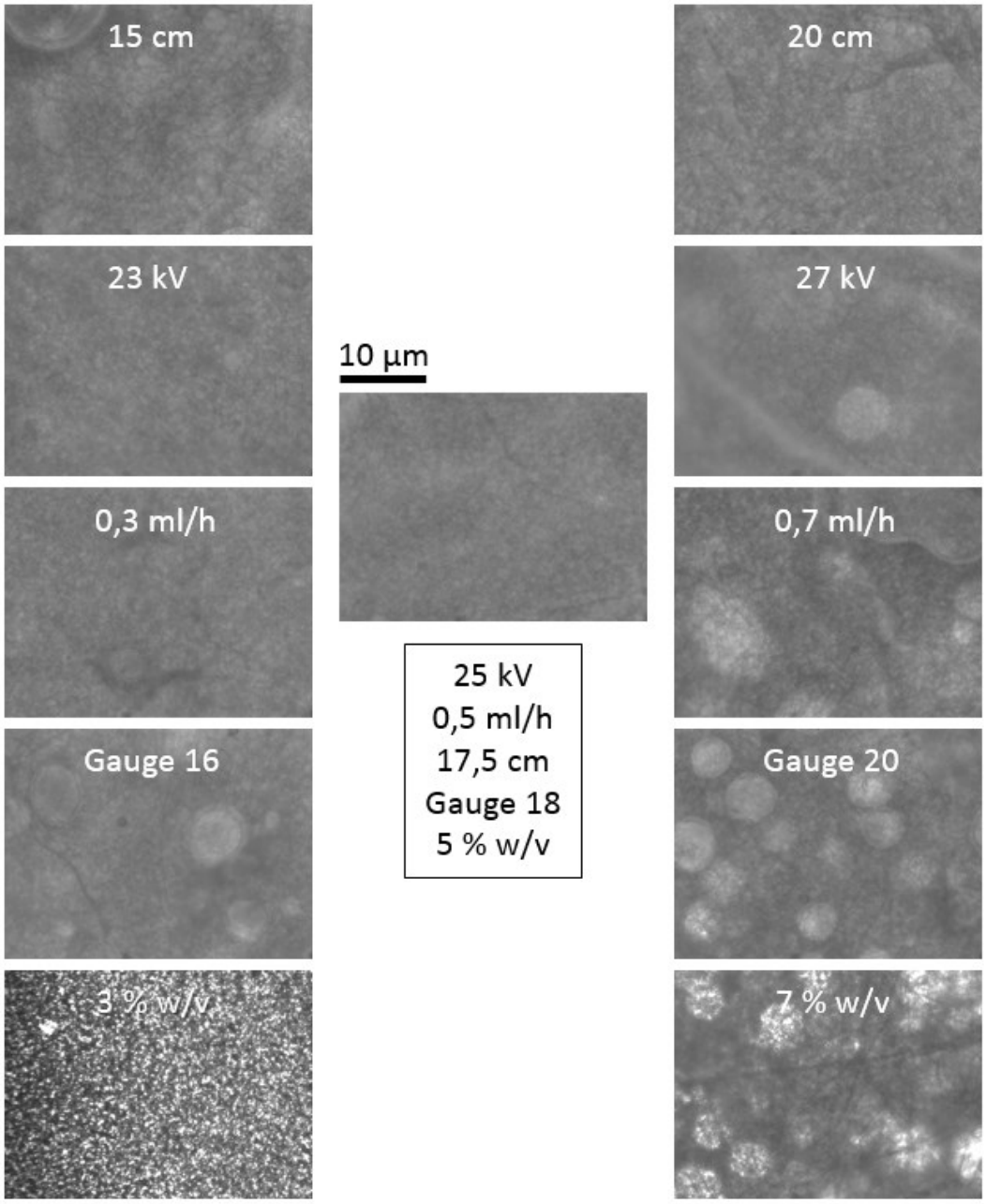

Figure 1. Optical microscope images of electrospun poly(ethylene oxide) (PEO) with 400X magnification. By varying one of the electrospinning parameters (voltage, pumping speed, distance, gauge size, concentration and solvent ratio) and keeping other parameters, the same as in the optimal middle point electrospinning the effect of a specific parameter was being able to be observed within the PEO electrospinning.

AVERAGE FIBER DIAMETER CALCULATION EXAMPLE APPENDIX 5

Table 1. Pixels-to-micrometers information that was measured from the SEM images by using the image-attached measuring scale and Adobe Photoshop CC 2017 program's Ruler function.

	µm	Pixels
1000X	10	90
3000X	2	54
5000X	1	44
10 000X	1	90

Calculations for a gelatin fiber diameter from a SEM image with a 5000X magnification

---

Measurements in pixels (10 measurements):

$$14, 10, 11, 10, 16, 14, 12, 12, 13 \text{ and } 14 \text{ pixels}$$

Calculating pixels into micrometers:

$$\frac{1\ \mu m \times (\text{measurement})}{44 \text{ pixels}}, \text{ for example } 14 \text{ pixels} \rightarrow \frac{1\ \mu m \times 14 \text{ pixels}}{44 \text{ pixels}} = 0{,}3\ \mu m$$

Thus measurements in micrometers:

$$0{,}3;\ 0{,}2;\ 0{,}3;\ 0{,}2;\ 0{,}4;\ 0{,}3;\ 0{,}3;\ 0{,}3;\ 0{,}3 \text{ and } 0{,}3\ \mu m$$

Average diameter in pixels (10 measurements):

$$\frac{14+10+11+10+16+14+12+12+13+14}{10} = 13 \text{ pixels}$$

Standard deviation (in pixels) = $\sqrt{Variance}$

$$\frac{(14-13)^2+(10-13)^2+(11-13)^2+(10-13)^2+(16-13)^2+(14-13)^2+(12-13)^2+(12-13)^2+(13-13)^2+(14-13)^2}{10} \approx 3{,}6$$

$$\sqrt{3{,}6} \approx \pm 2$$

Average diameter in micrometers (10 measurements):

$$\frac{0{,}3+0{,}2+0{,}3+0{,}2+0{,}4+0{,}3+0{,}3+0{,}3+0{,}3+0{,}3}{10} = 0{,}3\ \mu m$$

Standard deviation (in micrometers) = $\sqrt{Variance}$

$$\frac{(0{,}3-0{,}3)^2+(0{,}2-0{,}3)^2+(0{,}3-0{,}3)^2+(0{,}2-0{,}3)^2+(0{,}4-0{,}3)^2+(0{,}3-0{,}3)^2+(0{,}3-0{,}3)^2+(0{,}3-0{,}3)^2+(0{,}3-0{,}3)^2+(0{,}3-0{,}3)^2}{10} \approx 0{,}002$$

$$\sqrt{0{,}002} \approx \pm 0{,}04$$

AVERAGE PORE DIAMETER CALCULATION EXAMPLE APPENDIX 6

Table 1. Pixels-to-micrometers information that was measured from the SEM images.

	µm	Pixels
1000X	10	90
3000X	2	54
5000X	1	44
10 000X	1	90

Calculations for a cross-linked gelatin pore diameter (cross-linking for 72 hours) from a SEM image with a 5000X magnification

---

Measurements in pixels (10 pores, 2 measurements per ach pore):

30x20, 71x67, 18x18, 56x47, 41x37, 26x49, 22x45 27x37, 31x35 and 18x19 pixels

Pore diameter averages (per pore in pixels; 10 pores):

For example: $\frac{30+20}{2} = 25$; other pores $= 69, 18, 52, 39, 38, 34, 32, 33$ and 19

Calculating pixels into micrometers:

$\frac{1\ \mu m\ x\ (measurement)}{44\ pixels}$, for example 25 pixels → $\frac{1\ \mu m\ x\ 25\ pixels}{44\ pixels} = 0{,}6\ \mu m$

Thus measurements in micrometers:

0,6; 1,6; 0,4; 1,2; 0,9; 0,9; 0,8; 0,7; 0,8 and 0,4 µm

Average diameter in pixels (10 measurements):

$$\frac{25+69+18+52+39+38+34+32+33+19}{10} = 36\ pixels$$

Standard deviation (in pixels) = $\sqrt{Variance}$

$$\frac{(25-36)^2+(69-36)^2+(18-36)^2+(52-36)^2+(39-36)^2+(38-36)^2+(34-36)^2+(32-36)^2+(33-36)^2+(19-36)^2}{10} \approx 212$$

$$\sqrt{212} \approx \pm 15$$

Average diameter in micrometers (10 measurements):

$$\frac{0{,}6+1{,}6+0{,}4+1{,}2+0{,}9+0{,}9+0{,}9+0{,}7+0{,}8+0{,}4}{10} = 0{,}8\ \mu m$$

Standard deviation (in micrometers) = $\sqrt{Variance}$

$$\frac{(0{,}6-0{,}8)^2+(1{,}6-0{,}8)^2+(0{,}4-0{,}8)^2+(1{,}2-0{,}8)^2+(0{,}9-0{,}8)^2+(0{,}9-0{,}8)^2+(0{,}0{,}8-0{,}8)^2+(0{,}0{,}7-0{,}8)^2+(0{,}8-0{,}8)^2+(0{,}4-0{,}8)^2}{10} \approx 0{,}1$$

$$\sqrt{0{,}1} \approx \pm 0{,}3$$

FIBER DIAMETER MEASUREMENTS APPENDIX 7

Table 1. Fiber diameter measurements for PCL, gelatin and PEO. Measurements were taken from SEM images with magnifications of 3000X, 5000X and 10 000X. M1, M2, etc. stand for Measurement 1, Measurement 2, etc. Average fiber diameters and standard deviations in micrometers per polymer and per magnification are highlighted in grey.

	PCL / Fiber diameters				**Gelatin / Fiber diameters**						**PEO / Fiber diameters**			
	3000X		5000X		3000X		5000X		10 000X		3000X		5000X	
	Pixels	µm	Pixels	µm	Pixels	µm	Pixels	µm	Pixels	µm	Pixels	µm	Pixels	µm
M1	66	2,4	87	2,0	7	0,3	14	0,3	24	0,3	6	0,2	12	0,3
M2	49	1,8	65	1,5	6	0,2	10	0,2	26	0,3	6	0,2	20	0,5
M3	121	0,8	110	2,5	6	0,2	11	0,3	25	0,3	7	0,3	12	0,3
M4	63	2,3	136	3,1	9	0,3	10	0,2	27	0,3	7	0,3	12	0,3
M5	65	2,4	70	1,6	9	0,3	16	0,4	24	0,3	7	0,3	14	0,3
M6	47	1,7	157	3,6	9	0,3	14	0,3	19	0,2	4	0,1	16	0,4
M7	115	4,3	82	1,9	9	0,3	12	0,3	28	0,3	9	0,3	10	0,2
M8	64	2,4	61	1,4	5	0,2	12	0,3	30	0,3	9	0,3	11	0,3
M9	66	2,4	57	1,3	8	0,3	13	0,3	20	0,2	9	0,3	11	0,3
M10	24	0,9	121	2,8	18	0,7	14	0,3	26	0,3	4	0,1	11	0,3
Average	58	**2,1**	95	**2,2**	9	**0,3**	13	**0,3**	25	**0,3**	7	**0,3**	13	**0,3**
σ	25	**0,9**	33	**0,7**	3	**0,1**	2	**0,0**	3	**0,0**	2	**0,1**	3	**0,1**

Table 2. Fiber diameter measurements for cross-linked gelatin. Measurements were taken from SEM images with magnifications of 3000X and 5000X. M1, M2, etc. stand for Measurement 1, Measurement 2, etc. Average fiber diameters and standard deviations in micrometers per cross-linking time and per magnification are highlighted in grey.

	Cross-linked gelatin / Fiber diameters											
	24 h				48 h				72 h			
	3000X		5000X		3000X		5000X		3000X		5000X	
	Pixels	µm	Pixels	µm	Pixels	µm	Pixels	µm	Pixels	µm	Pixels	µm
M1	9	0,3	16	0,4	11	0,4	24	0,5	11	0,4	22	0,5
M2	6	0,2	17	0,4	14	0,5	14	0,3	13	0,5	19	0,4
M3	11	0,4	18	0,4	11	0,4	20	0,5	11	0,4	21	0,5
M4	10	0,4	22	0,5	14	0,5	22	0,5	8	0,3	15	0,3
M5	12	0,4	18	0,4	12	0,4	20	0,5	12	0,4	18	0,4
M6	11	0,4	17	0,4	19	0,7	20	0,5	10	0,4	21	0,5
M7	10	0,4	17	0,4	10	0,4	16	0,4	12	0,4	16	0,4
M8	9	0,3	16	0,4	12	0,4	13	0,3	11	0,4	23	0,5
M9	11	0,4	20	0,5	12	0,4	17	0,4	10	0,4	22	0,5
M10	10	0,4	14	0,3	9	0,3	17	0,4	11	0,4	23	0,5
Average	9,9	**0,4**	17,5	**0,4**	12,4	**0,5**	18,3	**0,4**	10,9	**0,4**	20,0	**0,5**
σ	1,6	**0,1**	2,1	**0,1**	2,7	**0,1**	3,3	**0,1**	1,3	**0,1**	2,7	**0,1**

PORE DIAMETER MEASUREMENTS FOR ELECTROSPUN AND CROSS-LINKED GELATIN

APPENDIX 8

Table 1. Pore diameter measurements for cross-linked gelatin samples. Measurements were taken from SEM images with magnifications of 3000X and 5000X. M1, M2, etc. stand for Measurement 1, Measurement 2, etc., L1 and L2 stand for Length 1 and Length 2 (two measurements per pore), A stands for Average and D stands for Diameter. Average pore diameters and standard deviations in micrometers per cross-linking time and per magnification are highlighted in grey.

		Cross-linked gelatin / Pores											
		24 h				48 h				72 h			
		3000X		5000X		3000X		5000X		3000X		5000X	
		Pixels	D (µm)	Pixels	D (µm)	Pixels	D (µm)	Pixels	D (µm)	Pixels	D (µm)	Pixels	D (µm)
M1	L1	48		49		28		59		25		30	
	L2	38		42		28		26		46		20	
	A	43	1,6	46	1,0	28	1,0	43	1,0	36	1,3	25	0,6
M2	L1	43		26		18		41		27		71	
	L2	46		39		29		41		35		67	
	A	45	1,7	33	0,7	24	0,9	41	0,9	31	1,2	69	1,6
M3	L1	37		60		39		50		30		18	
	L2	57		35		20		48		18		18	
	A	47	1,7	48	1,1	30	1,1	49	1,1	24	0,9	18	0,4
M4	L1	32		23		22		37		28		56	
	L2	31		31		31		27		28		47	
	A	32	1,2	27	0,6	27	1,0	32	0,7	28	1,0	52	1,2
M5	L1	16		65		24		29		15		41	
	L2	20		68		29		43		13		37	
	A	18	0,7	67	1,5	27	1,0	36	0,8	14	0,5	39	0,9
M6	L1	19		69		20		30		12		26	
	L2	17		53		25		39		14		49	
	A	18	0,7	61	1,4	23	0,8	35	0,8	13	0,5	38	0,9
M7	L1	29		60		30		58		20		22	
	L2	23		44		43		35		17		45	
	A	26	1,0	52	1,2	37	1,4	47	1,1	19	0,7	34	0,8
M8	L1	30		22		26		19		47		27	
	L2	35		29		18		21		41		37	
	A	33	1,2	26	0,6	22	0,8	20	0,5	44	1,6	32	0,7
M9	L1	43		55		24		37		46		31	
	L2	39		43		21		59		34		35	
	A	41	1,5	49	1,1	23	0,8	48	1,1	40	1,5	33	0,8
M10	L1	24		32		41		59		43		18	
	L2	24		48		21		35		30		19	
	A	24	0,9	40	0,9	31	1,2	47	1,1	37	1,4	19	0,4
Average			**1,2**		**1,0**		**1,0**		**0,9**		**1,1**		**0,8**
σ			**0,4**		**0,3**		**0,2**		**0,2**		**0,4**		**0,3**

PORE DIAMETER MEASUREMENTS FOR ELECTROSPUN POLY-E-CAPROLACTONE (PCL)

APPENDIX 9

Table 1. Pore diameter measurements for PCL samples. Measurements were taken from SEM images with magnifications of 1000X. M1, M2, etc. stand for Measurement 1, Measurement 2, etc., L1 and L2 stand for Length 1 and Length 2 (two measurements per pore) and D stands for Diameter. Average pore diameter and standard deviation in micrometers is highlighted in grey.

	PCL / Pores			
	1000X			
	L1 (Pixels)	L2 (Pixels)	Average (Pixels)	D (µm)
M1	162	72	117	13,0
M2	168	191	179,5	19,9
M3	110	180	145	16,1
M4	150	80	115	12,8
M5	54	57	55,5	6,2
M6	156	61	108,5	12,1
M7	176	191	183,5	20,4
M8	43	98	70,5	7,8
M9	109	102	105,5	11,7
M10	42	96	69	7,7
M11	104	166	135	15,0
M12	142	187	164,5	18,3
M13	109	233	171	19,0
M14	52	121	86,5	9,6
M15	159	169	164	18,2
			Average	**13,9**
			σ	**4,6**